STAT

TRANSLATION

PHOTOPLASTICITY

By S. I. Gubkin, S. I. Dobrovol'sky, B. B. Boyko

August 1959, 194 pages

USSR

STAT

PREPARED BY
LIAISON OFFICE
TECHNICAL INFORMATION CENTER
HCLTD
WRIGHT-PATTERSON AIR FORCE BASE, OHIO

STAT

STAT

Akademiya Nauk BSSR

Fiziko-Tekhnicheskiy Institut

S. I. Gubkin

S. I. Dobrovol'sky, B. B. Boyko

FOTOPLASTICHNOST'

Izdatel'stvo Akademii Nauk Belorusskoy SSR

Minsk 1957

167 pages

SUMMARY

This monograph presents the basic principles of a new experimental method for studying the processes of plastic deformation and stresses by translucence in polarized light optically sensitive materials which are subjected to a permanent deformation. This is known as the method of photo-plasticity.

The initial presentation of the new method is given in the present monograph in terms of viscous flow.

The results of this work may be used in studying models of the various processes of plastic deformation.

This book is intended for use by engineers and scientific personnel.

STAT

INTRODUCTION

One of the authors of this monograph, S. I. Gubkin, organized in 1949, at the Physical-Technical Institute of the Academy of Sciences of BSSR, a laboratory for the purpose of developing the method of photoplasticity.

The initial investigations in this laboratory were conducted by S. I. Gubkin and S. I. Dobrovol'sky. Some results of these investigations were published in Doklady AN USSR [10, 11]. In 1952, the staff in the laboratory was joined by B. B. Boyko.

By the end of 1954, it was possible to conclude that as a result of the laboratory investigations one of the basic problems of photoplasticity was resolved in its basic form — determining the stress state by methods of photoplasticity under viscous flow conditions. The solution of this problem which depicts the basic characteristics of this method permits us to consider that the problem of photoplasticity has been solved in principle and established as an independent method of investigation.

In order to permit the most rapid possible development and application of this useful method, the Scientific Council of the Physical-Technical Institute of AN BSSR recommended that the laboratory publish this monograph.

The present monograph summarizes the material obtained in the investigations conducted during the development of the method of photoplasticity at the PTI [Physical-Technical Institute] AN BSSR under the direction and with participation of the Member of

STAT

AN BSSR, S. I. Gubkin.

The work of preparing the monograph for publication was divided among the authors as follows: S. I. Gubkin prepared an outline of the work and prepared the first and sixth chapters and also edited the manuscript; B. B. Boyko prepared the fourth chapter and the second section of the fifth chapter, and S. I. Dobrovol'sky prepared the second and third chapters and the first and third sections of the fifth chapter.

This monograph was designed for readers who are familiar with the method of photoelasticity.

STAT

CHAPTER I

METHOD OF PHOTOPLASTICITY

1. Photoelasticity

At the present time there is no field of technology in which one does not have to deal with stresses and strains, both elastic and plastic. The study of distribution of stresses in an elastically deformed body and the determination of these stresses is one of the most important problems of modern mechanics. An analytical solution of these problems based on theory of elasticity is usually associated with a solution of partial differential equations with partial derivatives and with difficulties in finding boundary conditions. The difficulties are particularly troublesome in problems involving irregular outlines and a complex distribution of applied loads. The solution of problems which are of the greatest practical interest are those associated for instance with stress concentratons in machine parts subjected to repetitive loads of alternating sign, and in a number of cases problems of this kind present the greatest difficulties.

The theory of double refraction which appeared in the forties of the last century in regard to "compressed and nonuniformly heated noncrystalline bodies" which was derived by F. Neuman from the conditions of static equilibrium and which was subsequently developed by Maxwell, lay the basis for the creation of an experimental method of measurement of stresses in an elastic medium.

The French scientist Leger conducted at the end of the last century

STAT

extensive investigations leading to the initial development of the experimental method of measurement in an elastic medium which subsequently was named the method of photoelasticity (i.e., a method for obtaining a pictorial representation of the state of stress for an elastically deformed medium). This work was highly praised by our compatriot, the founder of metallography, D. K. Chernov, in his communication of 10 March 1884 on the topic, "Some Generalizations on New Observations in the Working of Steel" /1/.

In 1912, under the direction of Prof. V. L. Kirpichev, there was constructed and established by A. K. Zaytsev the first Russian laboratory for studying stresses in transparent models by the method of photoelasticity. This installation was constructed for the laboratory of applied mechanics of the present Leningrad Polytechnic Institute. A detailed historical review of this method is given in "Proceedings of the Conference on the Optical Method of Measuring Stresses" /2/.

The essence of the method of photoelasticity consists of the following. An optically isotropic plate prepared from an optically sensitive transparent material having been placed in a state of nonuniform elastic strain becomes optically anisotropic as long as the applied load causing the elastic deformation is maintained. Therefore, polarized white or monochromatic light displays double refraction in passing through the loaded plate. This effect consists in the splitting of a light ray into two rays which vibrate in two mutually perpendicular planes and which propagate in the medium with different velocities. Because of the difference in the velocities, we observe a difference between the propagations of the two rays defined by the formula

$$R = cd(\sigma_1 - \sigma_2), \qquad (1)$$

where R is the difference in the paths;

d is the thickness of the plate;

c is a constant known as the optical coefficient of stress which depends

on the properties of the material;

σ_1 and σ_2 are the principal stresses at a given point.

It must be noted that the maximum shearing stress is given by

$$\tau_{max} = \frac{\sigma_1 - \sigma_2}{2}.$$

In the case of circularly polarized monochromatic light subjected to double refraction in passing through a loaded place in the field of the polariscope, we obtain on the photographic plate a system of dark fringes which are called isochromatics (Fig. 1). Each of these fringes represents the locus of the points in which the shearing stress has the same value. In this instance, the magnitude of the shearing stress is determined by the value assigned to a fringe and to its order. The order n of the fringe is determined by the difference in the path expressed in wavelengths of light. The value of a fringe is given by the expression

$$\tau_0 = \frac{\tau_{max} \cdot d}{n}. \qquad (2)$$

In order to determine the fringe value there are appropriate methods.

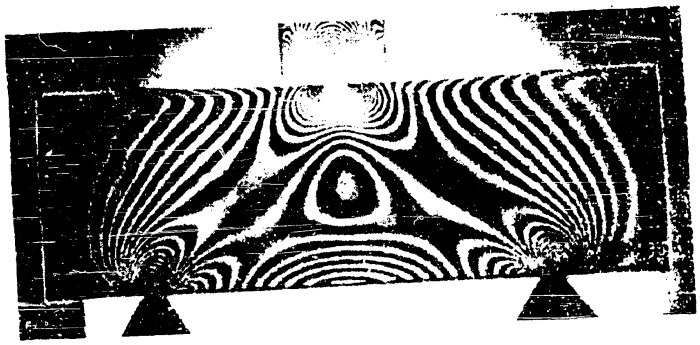

Figure 1. A system of dark fringes (isochromatics) produced by polarized light in elastic optically sensitive materials.

In the case where white light is used, the fringes corresponding to equal shearing stresses have different colors which depend upon the value of the maximum shearing stress (Figure 2, see insert between pages 46 - 47).

STAT

Experience has shown that for quantitative studies it is more convenient to use monochromatic light, while white light which gives a color picture of the distribution of stresses is more useful for graphical demonstration.

When we use plane polarized light, we observe on the general fringe pattern certain supplementary dark lines or regions which are called isoclinics. Isoclinics represent the locus of the points in which the principal stresses have the same direction, one of which coincides with the orientation of the plane of polarization of light. Having the isoclinics, we can construct a grid of trajectories of the principal stresses.

Knowing at each point the magnitude of the maximum shearing stress and the directions of the principal stresses as well as the boundary conditions, it is possible to determine the tensor of the stresses at each point of the elastically deformed body using the methods of the theory of elasticity.

The photoelastic method has undergone extensive development during the recent years. The work done over a period of many years in a number of scientific schools in the development of this method has led to greater perfection of this method. Improvement in the experimental technique has enabled us to obtain an undistorted picture of the stresses along the edges of the model. This has presented great possibilities for studying the concentration of stresses. The considerable material accumulated in recent years on the coefficients of stress concentrations has clarified the causes of fatigue failures and has shown the way in a number of cases to eliminating these failures. These data were obtained primarily as a result of investigations carried out by means of the photoelastic method.

At the present time there is no other method which permits us to determine so completely the state of stress with considerable precision and with relatively small expenditure of time and effort.

The recent developments in three-dimensional photoelasticity offer even more promising perspectives.

STAT

Of particular significance in the development of this method are the works of the Soviet physicist A. V. Stepanov with the following results.

(a) The peculiarities of stress distribution in elastic anisotropic media compared with isotropic media under the same conditions have been determined /3/. An analysis of these peculiarities leads to the conclusion that even in so-called quasi-isotropic media, among which all polycrystalline metals may be included, the distribution of stresses may sometimes differ significantly from the distribution in isotropic media. Therefore, when we determine the distribution of stresses in metal parts by means of models of isotropic material, we do not always obtain a precise picture of the actual distribution of stresses in these parts;

(b) A group of anisotropic crystalline substances was discovered whose mechanical properties and crystalline structure are similar to the mechanical properties and structure of metallic crystals /4/. Among these substances are haloid salts of silver and thallium and their various alloys. These substances were discovered by A. V. Stepanov about 1935, and, at the July session of the Academy of Sciences of USSR in 1944, he reported a new optical method of determining stresses in an elastic medium, differing from the usual photoelastic method, in which models prepared from a transparent material of crystalline structure were utilized. A. V. Stepanov proposed that the "transparent metals" be used as materials for such models. Among these he named chloric silver* and other haloid salts of silver and thallium and their various alloys.

A. V. Stepanov's proposal permits us to determine by means of elastically loaded models of "transparent metals" a much more precise picture of the distribution of stresses than by means of models made of similarly loaded isotropic material. Acceptance of this proposal will lead to considerable further development of the existing method of photoelasticity.

* A. V. Stepanov, Author's certificate No 47829, 30 June 1936.

STAT

At the present time, the engineering profession is already aware of the fact that the photoelastic method is a reliable and perfected tool in the hands of investigators and designers which yields in many cases a rapid and accurate solution of very difficult practical problems and which at the same time offers the means of confirming solutions by mathematical theory of elasticity, thus increasing the value of the theory itself. Therefore, during the recent years, there have appeared many important papers on the subject of photoelasticity, many new laboratories have been established for experimental determination of states of stress by the photoelastic method, and numerous studies are in progress to perfect still further this visual method of stress analysis which in the words of A. K. Zaytsev "makes the invisible visible" /5/.

2. <u>The Need for Development of an Experimental Method of Studying the State of Stress with Plastic Deformations</u>.

When we determine the state of stress in plastically deformed bodies by analytical methods, we must use the mathematical tools which are now available to us in the mathematical theory of plasticity and those data on the mechanical behavior of bodies which we can obtain by modern laboratory experimental techniques. The solution of problems in the theory of plasticity as well as in the theory of elasticity involve the use of very difficult differential equations with partial derivatives and the difficulties associated with formulation of boundary conditions.

However, the difficulties which arise in solving problems in the theory of plasticity, taking into account the present state of the science of deformations, are infinitely more difficult than the difficulties arising in the problems of the theory of elasticity.

This can be explained by the following circumstances:

1. The mathematical theory of plasticity is not nearly as well developed as the mathematical theory of elasticity. This is explained first of all by the considerably greater scientific maturity of the theory of elasticity as

STAT

compared with the theory of plasticity, which is a relatively recent offshoot of science, and also by the inadequate study of the physical nature of the plastic process.

2. In the general case considerably greater difficulties arise in formulating the boundary conditions for problems in plasticity than for those in elasticity.

Particularly great difficulties arise in the solution of problems in which plastic deformation is accompanied by surface friction /6/. The latter has exceptionally great effect both on the character of stress distribution in the deformed body and on the magnitude of the deforming forces. In a number of cases this magnitude is affected not so much by the mechanical properties of metal (which determine its resistance to plastic deformation) as the conditions of contact friction. As is shown by experiments, the deforming force may be reduced by a factor of more than five in certain cases by changing the conditions of contact friction.

In spite of the great significance of the conditions of contact, we do not as yet know the laws governing the contact friction during plastic deformation. In many practical cases of deformation the specific frictional force is given by the complex function:

$$\tau_m = F(N, \tau_{sn}, W, t_n^\circ), \qquad (3)$$

where τ_m is a specific frictional force;

N is the normal pressure;

τ_{sn} is the yield point in shear of the surface layer situated near the contact surface;

W is the velocity of slip of the particles of the material in the surface layer;

t_n° is the temperature of the contact layer (it may differ from the temperature of the body being deformed).

STAT

Experimental determination of function (3) is at times extremely difficult.

3. Considerably greater difficulties arise in describing the mechanical behavior of a plastically deformed body than in describing the behavior of an elastic body.

The description of the mechanical behavior of an isotropic elastic body is completely determined by two constants -- Young's modulus and Poisson's ratio. However, the mechanical behavior of a plastically deformed body may be described in the general case only by a complex function of the following type:

$$\sigma_{sq} = \varphi(t^\circ, q, v, \sigma, x, c). \qquad (4)$$

Here σ_{sq} is the resistance of the material to deformation;

t° is the temperature, $^\circ C$;

q is the degree of deformation;

v is the rate of deformation;

σ is the average stress;

x is the chemical composition;

c is the structure of the material being deformed which as a rule changes during the process of deformation.

Thus, instead of completely determined constants which describe the elastic behavior of the body, in describing the plastic behavior of the same body we must deal with a complex function which considerably complicates the solution of the problem. At the same time, the laboratory procedure by means of which we can determine precisely the constants describing the behavior of an elastic body is not yet sufficiently developed for a precise determination of the functions of type (4).

4. The nature of the plastic process has not yet been adequately studied. This makes it impossible to take into account certain phenomena which accompany

STAT

the process of plastic deformation and affect the distribution of stresses, thus lessening the precision.

Therefore, the science of plasticity needs the creation of an experimental method of measuring the stresses by a method similar to the photoelastic method even to a greater degree than the science of elasticity. This is necessary to conserve equipment and time in solving many important problems in plasticity as well as to assure further progress of the science of plasticity and its mathematical theory. The development of the experimental method of measuring stresses in plastically deformed bodies will permit us to verify the existing methods of mathematical theory of plasticity, as well as to perfect and develop them. Such a method in addition will broaden our concept of the nature of plastic deformation itself.

The basis of the method of photoelasticity is the effect of double refraction caused by elastic deformation of the medium. However, plastic deformation can occur and develop only in an elastically deformed medium. This postulate is a most important law of plastic deformation. From it we can draw a corollary regarding the possibility of observing the effect of double refraction in a plastically deformed body. Thus, there arises the possibility of creating an experimental method of measuring stresses caused by plastic deformation. The basis of the proposed method, just as in the photoelastic method, is the effect of double refraction caused by elastic deformation, i.e., by a reversible displacement of kinetic units of a substance (atoms, molecules, macromolecules), which also accompany every process of plastic change in form. Therefore, the given method may be called the method of photoplasticity as being analogous with the method of photoelasticity (the method of obtaining a pictorial representation of the states of stress for a plastically deformed medium).

The method of photoplasticity, while based on the same physical phenomenon as the method of photoelasticity, differs from it in certain principles,

STAT

and, therefore, may be considered quite independent. We shall discuss this more fully below.

The method of photoelasticity utilizes the process of elastic deformation and solves the problem of stress distribution by supposing that the stresses in the model do not exceed the elastic limit. Therefore, the mechanical behavior of models of isotropic material is described by Hooke's law with only two constants being involved -- Young's modulus and Poisson's ratio.

The method of photoplasticity is the model analysis of the process of plastic deformation and solves the problem of states of stress by supposing that the stresses in the model exceed the elastic limit. The mechanical behavior of the models in this case is described by the laws of plasticity, which have a variable form depending upon the nature of the material being deformed and the conditions of deformation. Thus, the mechanical behavior of the models in the case of the method of photoplasticity may be different. Therefore, every method must be developed by solving typical problems corresponding to the classification of the rheological behavior of solid bodies.

3. Classification of the Rheological Behavior of Solid Bodies.

The character of the relationship between resistance to shear and such parameters as rate of deformation, the degree of deformation and average stress, as well as the nature of failure of the substance yield an adequate picture of the rheological behavior of the substance at a given temperature. In this instance all solid substances may be distinguished by their characteristic deformations and they may be represented by several rheological bodies among which are:

1. Brittle Body. An ideal brittle body fails at elastic deformations of negligible value without indicating any yielding whatsoever. By deformations of negligible value we mean deformations less than 0.001% (one of the specified values of the elastic limit). In the case of presence of any symptoms of yielding or failure at small elastic deformations of the order of

STAT

0.001-1%, the body is brittle if the residual deformations are of the same magnitude as the elastic ones.

2. Elastic Body. An ideal elastic body permits unlimited elastic deformations without any indications of yielding or failure. The body which fails without any symptoms of plastic deformation, but at large values of elastic deformations is an elastic body. By large elastic deformations we mean deformations which have minimum values measured in tens of percent. The relationship between the stresses and deformations may be either linear or nonlinear. An elastic body may be combined with a brittle one. Thus, we may have elastic-brittle bodies. However, if the failure takes place as a result of large elastic deformations, then such a failure cannot be defined as a brittle failure. This, then, becomes a special type of failure which we associate with elastic bodies.

3. Viscous Body. The basic characteristics of a viscous body are the following:

(a) The resistance of a viscous body to shear depends upon the rate of deformation and does not depend upon its magnitude;

(b) during the flow process of a viscous body there is an absence of residual changes in its structure and properties;

(c) before a certain rate of deformation determined by the nature of the given viscous body and temperature is attained, this body shows infinitely large plastic deformations without any symptoms of discontinuities.

In his well-known work P. P. Kobeko cites a description of interesting experiments by Kornfeld and Ryvkin in which they subjected a stream of liquid to rapid impact applied at right angles to the direction of its flow and photographed the stream at the moment of impact /7/. For an impact applied at 19 m/sec the stream was deflected plastically as a unit, while for an impact applied at 23 m/sec the stream is shattered as brittle glass and is fragmented in the manner shown clearly in Figure 3.

STAT

A. Nadai shows that one of the compounds of silica (silicone) prepared in the form of a sphere flows under its own weight, but when this sphere is permitted to fall 1-2 m, it rebounds as an ideally elastic material /8/. However, the elastic state is apparently only a transitional one and if the rate of deformation is increased, the sphere becomes a brittle body. According to the observations of the authors, certain gels behave in precisely the same manner for very slow rates as elasto-viscous bodies, and at rates of deformation exceeding certain values they behave as elastic ones.

The resistance to shear of a viscous body for a given rate of deformation depends notably upon the hydrostatic pressure. This relationship may be expressed by the formula

$$\tau_\sigma = \tau_n \cdot e^{-\alpha\sigma}, \qquad (5)$$

where σ is the average stress;

τ_n is the resistance to shear for $\sigma = 0$;

τ_σ is the resistance to shear at a mean stress equal to σ;

α is a function dependent upon the molecular weight.

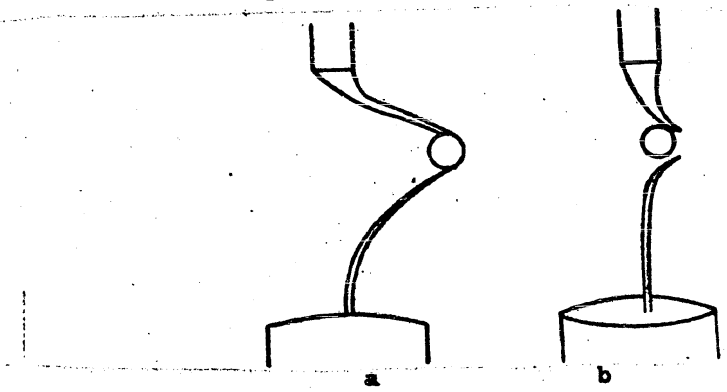

Figure 3. a -- the form of a stream of liquid with a viscosity of 5000 poises subjected to lateral impact at a velocity of 19 m/sec; b -- the same for an impact with a velocity of 23 m/sec (from Kornfeld and Ryvkin).

Formula (5) is analogous to the well-known formula which gives the relationship between the coefficient of viscosity and the hydrostatic pressure.

It is useful to consider two types of viscous bodies: a liquid viscous

body and a solid one. The liquid viscous body has a low yield point and as a result assumes under its own weight after a certain length of time the shape of its container. A solid viscous body has such a yield point that under the influence of its own weight it cannot assume the form of its container.

The rheological curves of a viscous body are shown in Figure 4.

4. Plastic Body. A plastic body possesses the following characteristics:

(a) its resistance to shear does not depend upon the rate of deformation but may depend upon its magnitude;

(b) during the process of plastic deformation there occurs a change in the structure and properties of the body.

It is necessary to distinguish between a nonfailing plastic body and a failing one. A nonfailing plastic body produces infinitely large plastic deformation without any symptoms of discontinuities, while a failing body becomes embrittled by plastic deformation and fails when the deformation attains a certain value. A plastically embrittled body (nonplastic body) must be differentiated from a brittle one. The former may fail at very small elastic deformations without any noticeable geometric symptons of plastic deformation just as a brittle body, but it differs from a brittle body in that failure may occur in it only as a result of a preliminary plastic deformation, while a brittle body fails without it. An embrittled body and a brittle one also differ in the character of their failures. The failure of an embrittled body is usually termed a viscous failure while that of a brittle body is called a brittle failure.

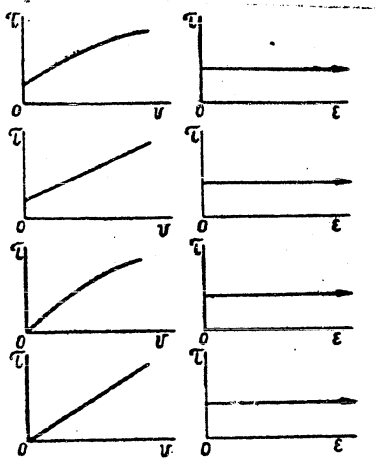

Figure 4. Rheological curves of a viscous body: τ is the stress; V is the rate of deformation; ϵ is the extent of deformation; ⟶ indicates an infinitely large plastic deformation.

STAT

The mean value of the stress has practically no effect on the resistance of the plastic nonfailing body to shear. In the case of a plastic failing body, the effect of the mean stress becomes more pronounced as the body becomes more embrittled in the process of plastic deformation.

Figure 5 shows rheological curves characteristic of a plastic body.

Figure 5a shows the rheological curve of a nonfailing body. In the initial stage we observe the greatest increase in the strength of the material. As the value of deformation increases, the strength gain decreases and finally ceases entirely, as a result of which the rheological curve becomes a straight line parallel to the axis of abscissa. The straight line in Figure 5b is characteristic either for a material already strengthened by means of preliminary plastic deformation or for the very first stage of deformation of certain materials having a sharply defined yield point and which are undergoing cold working. A material with such a rheological behavior is often called an ideal plastic body /8/. The curve in Figure 5c is typical of plastic materials which fail as a result of embrittlement in the process of plastic deformation. The straight line in Figure 5d may in certain cases represent with sufficient accuracy that portion of the actual rheological curve corresponding to a given stage of deformation. The curve in Figure 5e is characteristic for materials with a sharply defined embrittlement occurring during the process of deformation. In most cases, this curve indicates that under given conditions of change of form the predominant mechanism of flow is an intercrystalline deformation which takes place with progressive breakdown of the bonds between crystals.

It is quite obvious that there are in nature combinations of different rheological bodies. Therefore, it is proper to describe the behavior of the following combined bodies: (1) plastic-viscous; (2) plastic-brittle; (3) elastic-plastic; (4) elastic-viscous; (5) elastic-brittle; (6) viscous-plastic-elastic; (7) elastic-viscous-plastic; (8) elastic-plastic-brittle; (9) elastic-viscous-plastic-brittle.

STAT

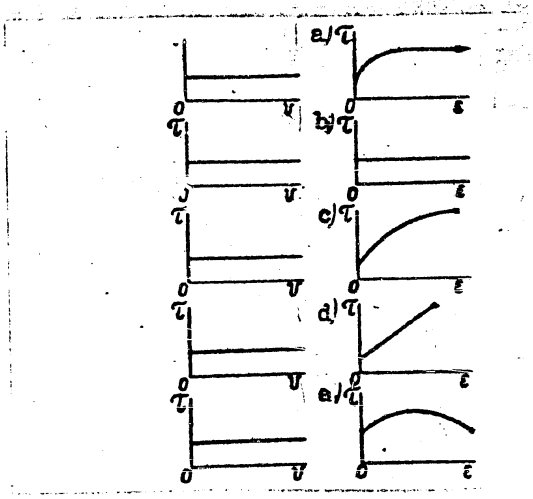

Figure 5. Rheological curves of a plastic body: ⟹ indicates infinitely large plastic deformation; X indicates failure.

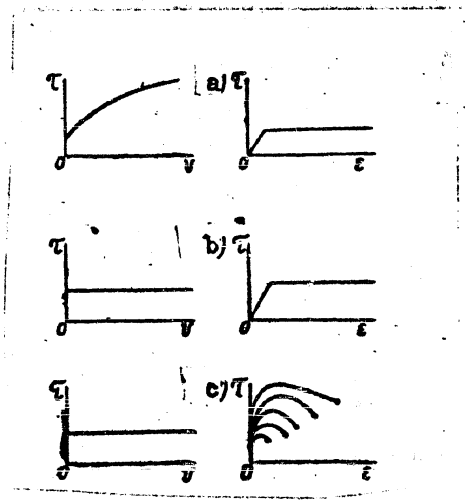

Figure 6. Rheological curves for combined bodies.

The combined bodies possess respectively the combination of characteristics of the basic rheological bodies which form the combination. The rheological curves of the combined bodies also reflect the combinations of the curves of the basic bodies (see Figure 6).

It must be noted that elasticity to some degree is present in all natural bodies. In addition to that, the process of flow can only occur in an elastically deformed body. However, in many cases it is expedient to neglect the elasticity to simplify the calculations and the description of the behavior of the bodies. For instance, it may be neglected in describing the behavior of a large number of viscous bodies. Whether or not the elasticity of a viscous body may be neglected is even considered one of the most important criteria for deciding whether a body is solid or liquid. For instance, in the experiments of Kornfeld and Ryvkin mentioned above, the experimenters investigated the behavior of a stream of solution of rosin in mineral oil. This substance having a viscosity $\eta = 5 \cdot 10^3$ poises may be considered only as a liquid body as judged by the aggregate of its properties. The authors also dealt with a rosin plasticized with a rosin oil but in different proportions than

those used in the above experiments. The viscosity of this substance was $\eta = 2.5 \cdot 10^8$; it was not possible to determine the yield point by ordinary means because of its extremely small value. The rheological behavior of this body corresponds to the graph shown in Figure 38. At the same time, according to external characteristics, this solid body which can be deformed plastically with ease under a slow action of applied forces, under impact shatters into small fragments as a brittle body. By means of pressure this body may acquire any form, which changes only after a considerable period measured in months. Thus, according to all symptoms this body approaches a solid viscous body. A body possessing elastic properties to such an extent that they cannot be neglected must be classified as a solid body, and in this instance we must describe its rheological behavior by the combined rheological characteristic shown in Figure 6a. Even a body whose elastic deformation can be neglected but which has a yield point which cannot be neglected must be classified as a solid body.

In considering large plastic deformations of a plastic body we can neglect elastic deformations, but in the case of plastic deformations which are commensurate with elastic ones we must consider that we are dealing with an elastic-plastic body whose description has great practical significance. Rheological characteristics of this body are shown in Figure 6b.

Rheological characteristics determined by the relationship between resistance to shear and the magnitude of deformation are the same for both the plastic-brittle body and the plastic body which fails in the process of deformation (an embrittled body). However, these bodies are distinguished by somewhat different rheological behavior because of the completely different character of failure. In addition to that, the average stress has a considerably greater effect on the resistance to shear of a plastic-brittle body than on the resistance to shear of a plastic failing body. Figure 6c shows the rheological characteristic of a plastic-brittle body with average stress taken into

account, and in this instance this characteristic is given not by a single curve, but by a family of curves. Red sandstone and marble (Figure 7) indicate a behavior analogous to that described in Figure 6c. The average stress exerts so great effect on the behavior of the body that by increasing the absolute value of the negative mean stress it is possible in a number of cases to transform a body from a brittle-plastic state into a plastic one and even to obtain a plastic nonfailing body in some cases.

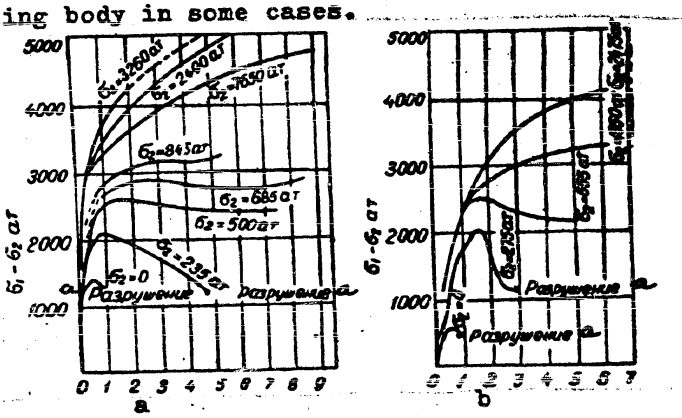

Figure 7. Rheological curves for marble (a) and sandstone (b) under triaxial compression (from Karman).
Legend: a) failure

Plastic-viscous bodies which are widespread in nature present considerable interest to us. Among them we can consider first of all the great majority of polycrystalline metallic alloys. The metallic substance in a temperature range below the temperature of recrystallization shows symptoms of a plastic body to the greatest degree, particularly for the lower temperatures. The lower the temperature of deformation, the greater the increase in strength and the less the effect of the rate of deformation on the resistance to shear. However, the behavior of metallic alloys becomes different at temperatures exceeding the temperature of recrystallization. Then we begin to notice symptoms of a viscous body and these symptoms are more pronounced at higher temperatures.

Thus, if at the low temperatures symptoms of a plastic body predominate, then at temperatures approaching the temperature of fusion symptoms of a

STAT

viscous body predominate in many cases. At high temperatures we may observe that the extent of deformation has no effect on resistance to shear in spite of the presence of structural transformations occurring during the process of deformation, and the rheological behavior is described by characteristics associated with a viscous body (Figure 4). However, the physical significance of the rheological characteristic in this case is quite different from the characteristic shown in Figure 4. In the case of a plastic-viscous body the characteristic indicates that the gain in strength occurring in the process of plastic deformation is completely eliminated by the weakening process which accompanies the deformation, while in the case of a viscous body the deformation proceeds without gain in strength and residual structural changes.

The mechanical properties of the substance reflect the nature of the intermolecular forces. We can draw certain conclusions regarding the structure of the substance in a series of cases from the values of the mechanical properties.

A study of the rheological behavior of the substance along with an analysis of the mechanical properties and mechanism of flow improves our understanding of the structure of the substance and the structural changes caused by its flow. Conversely, the study of the structure and the structural changes of a substance aids us in gaining a better understanding of its rheological behavior. It is known that the character of the changes of many mechanical properties of an alloy depends upon its chemical composition and the type of its composition diagram. Besides that, many mechanical properties and the rheological behavior of bodies depend on the peculiarities of their structure and molecular weight. Thus, the viscosity and rheological behavior of bodies cannot be considered as being unrelated to their molecular weight. In the case of a small molecular weight we are dealing with mobile liquids. As the molecular weight of polymers increases, the mobile fluid is transformed successively into a viscous, then an elastic-viscous body, and, finally, into

STAT

an elastic (highly elastic) body. Mechanisms of plasticity also depend on the peculiarities of structure. Viscous bodies are associated with unordered mechanisms of plasticity. In such bodies the predominant mechanism is a simple amorphous mechanism of plasticity. In plastic bodies we observe orderly mechanisms of plasticity such as intercrystalline slip and twinning. When we consider not only the orderliness of the structure itself but the actual order as is shown well by a diagram taken from P. P. Kobeko /7/ (see Figure 8), then we may derive considerable useful material for clarifying the rheological peculiarities of a substance which depend upon the degree of orderliness of its structure.

The deformation characteristics of rheological bodies described above (based on generalizations of materials derived from physical and physical-chemical investigations) permit us to pose the question of classifying the rheological behavior of solid bodies with respect to its chemical and structural peculiarities. The creation of such a classification would aid in obtaining a solution of a series of most important problems in various fields of science involving the questions of deformations and chemical compositions.

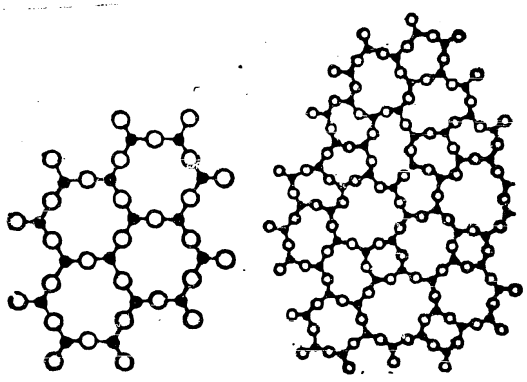

Figure 8. A schematic two-dimensional diagram of crystalline structure (left) and amorphous structure (right) of quartz.

The deformation characteristics which describe the behavior of basic rheological bodies as proposed here are not yet sufficiently developed for

STAT

the proposed classification. Both the deformation characteristics and the terminology need to be defined more accurately. At the same time our concept of the symptoms of rheological behavior must be broadened in order to establish a more intimate relationship with chemical and structural properties of the substance.

However, in order to solve the particular problem related to the typical problems of photoplasticity, the classification of rheological behavior of solid bodies proposed here may be utilized successfully in its present form. On the basis of this classification we may draw the conclusion that the basic typical problems of the method of photoplasticity are: (1) viscous, (2) plastic, and (3) viscous-plastic. For each of these problems there is a characteristic experimental procedure as well as an analytical method of attack.

In the present monograph there is given a solution of the problem of viscous photoplasticity, and methods for solutions of other problems in photoplasticity are indicated. The problem is posed in this fashion since the viscous problem is the simplest one both with respect to experimental technique and theoretical treatment. In the process of solving this problem a series of important questions of methods of attack which have a great significance for all problems of photoplasticity will be clarified; this solution will facilitate the solution of more complex problems among which are the problems of plastic and viscous-plastic behavior.

4. Basic Problems of Photoplasticity.

A. V. Stepanov showed that the transparent crystals which he discovered behave under pressure in a manner analagous to metals: they become stronger, acquire a metallic texture, accumulate potential energy in the form of residual stresses and indicate the possibility of a large plastic deformation by means of the very same mechanisms which operate in producing plastic deformation in a metallic substance. Basing his reasoning on the indicated

properties of transparent crystals, he considers it possible to apply an optical method for studying the states of stress which arise as a result of plastic deformation in specimens having a grainy structure while they undergo a change in crystalline structure. In A. V. Stepanov's opinion, investigations of this kind may have great significance in the study of various problems in metallurgy, geology and the theory of elasticity of a homogeneous and quasi-isotropic body, the interaction between discrete particles of a semi-crystal, the behavior of an individual grain and its boundaries, which will aid in the development of our concepts of such phenomena as elastic hysteresis, creep, fatigue and relaxation. Similar investigations may also be undertaken for the study of the process of cutting of metals and the forming of metal by pressure. By studying the stresses present in transparent crystalline substances in polarized light, it is possible to reproduce in a model the complex technological process of a combination of mechanical and thermal treatment. A. V. Stepanov showed experimentally that in plastic tensioning of a flat specimen of polycrystalline chloric silver the grains being deformed become outlined fairly clearly (see Figure 9). In addition to that, he indicated the possibility of studying the nature of residual stresses by means of "transparent metals" investigated in polarized light.

S. O. Tsobkallo and B. A. Kuznetzov have shown that it is possible to study the nature of fatigue [19] by means of "transparent metals" under polarized light. D. B. Gogoberidze and I. D. Kirvalidze drew the same conclusion having studied by means of an optical method various fatigue phenomena in monocrystals of rock salt /9/.

S. I. Gubkin and S. I. Dobrovol'sky suggested in their work (devoted to the application of transparent models to the study of forming of parts by means of pressure) that during the plastic deformation of certain slowly deformed gels the observed pattern of isochromatics indicates the geometric locus of maximum shearing stresses of the same magnitude [10]. The same

authors have established in another work that the very same well-defined pattern of isochromatics may be observed in plastic deformations of certain transparent resins [11]. They also established that during plastic deformation of transparent optically sensitive materials it is possible to observe both an ordered and disordered isochromatic pattern.

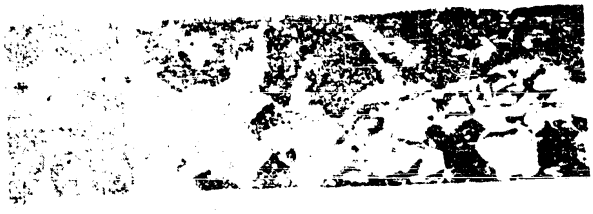

Figure 9. View of a specimen of chloric silver in tension observed in the field of a plane polariscope (from Stepanov).

An isochromatic grid is called an ordered one when it reveals a certain isochromatic pattern characteristic for the given type of loading (Figure 10a). A disordered isochromatic grid is one which reveals a field of variously colored polygons with a real or apparent absence of any system of coloring of these polygons (Figure 10b).

Figure 10. Isochromatic pattern: a -- an ordered one; b -- a disordered one.

An ordered pattern of isochromatics is observed in homogeneous media such as certain plastic polymers (certain synthetic and natural resins) and also in semi-crystals whose grains are so fine that they approach in their

STAT

behavior a homogeneous substance. A disordered pattern of isochromatics is observed in nonhomogeneous media such as in polycrystals whose grains have a different coloring. The finer the grain structure, the greater the likelihood that the disordered isochromatic pattern will become an ordered one.

In Figure 10b there is shown a polycrystal of chloric silver with a surface plastically deformed with a die. In view of the fact that the grain structure is coarse, we have a disordered isochromatic pattern consisting of variously colored polygons.

Figure 11. A distorted view of isochromatics (a die forced into a specimen of chloric silver).

As the grain structure becomes finer, the isochromatic pattern becomes ordered although the fringe pattern is distorted (Figure 11).

Both an ordered and a disordered isochromatic pattern may find its special application. For a quantitative determination of distribution of stresses an ordered fringe pattern is necessary. For the study of various phenomena which accompany the process of plastic formation, in many cases a disordered isochromatic pattern has a predominant significance since it permits us to study the mechanisms of these phenomena and to observe their kinetics. A disordered isochromatic pattern may be called a structural isochromatic pattern inasmuch as it reveals the structure of the model undergoing deformation. An ordered isochromatic pattern which reveals the distribution of forces in the volume of the model undergoing deformation may be called an isochromatic pattern of macroforces.

S. I. Gubkin and S. I. Dobrovol'sky established that in addition to an isochromatic pattern it is possible to obtain a pattern of isoclinics from transparent optically sensitive material undergoing plastic deformation. The latter makes it possible to obtain a grid of normal principal stresses and

STAT

maximum shearing stresses (stress grids). Such grids (Figures 112-113) present a qualitative picture of the distribution of stresses. If, however, we succeed in evaluating the value of a fringe of a transparent optically sensitive material subjected to plastic deformation, we shall obtain all the necessary information for a quantitative solution of the problem of distribution of stresses in a plastically deformed material analagous to the problem which is solved by the method of photoelasticity [12].

Thus, along with the method of photoelasticity there arises the method of photoplasticity which is based on the same phenomenon of double refraction as the method of photoelasticity, but which differs from the latter in a whole series of specific peculiarities which put the method of photoplasticity into a category of completely independent methods having considerably greater range of applicability than the method of photoelasticity.

At the present time, the theory of elasticity serves a great variety of sciences and areas of technology. As a result, this method is applicable to a large variety of problems which can be solved by this theory. The theory of plasticity is called upon in solving extremely complex problems in the field of geology, geophysics and mechanics of mineralogy; it serves as a basis for development of the theory of shaping metals by means of pressure and cutting processes, the formation of cermets and welding; it acquires an increasing significance in the development of the theory of both metallic and nonmetallic alloys; it assists in advancing the calculation of strength of structures and in the various areas of applied mechanics; it has great significance in the development of branches of chemical technology (for instance, that concerned with pressure molding of plastics, and the production of synthetic fibers and paints). Even certain medical sciences have recently shown an interest in the various applications of the theory of plasticity.

Hence, photoplasticity as a method of model analysis of plastic deformation processes observed in various natural phenomena and encountered in various

fields of technology is called upon to solve a great variety of problems. All the problems of modelling the processes of plastic deformation may be classified as problems having the following objectives:

(1) an analysis of stress distributions in plastically deformed bodies;

(2) a study of physical phenomena accompanying plastic flow.

The first group of problems in its turn may be divided into two subgroups. In the analysis of stress distributions in plastically deformed bodies the problems may be divided into qualitative and quantitative ones the same as in a chemical analysis. In this instance the question is not one of precision of measurements but of the requirements of the problem. In case of many problems concerning geological and geophysical phenomena and also for certain processes of shaping metals by means of pressure and cutting, the basic requirement is that of establishing the general picture of distribution of stresses for the purpose of revealing the peculiarities of the phenomenon or process and of establishing the character of its development. In such cases, it is not necessary to obtain the absolute values of the stresses. The isochromatic pattern of the stress distributions without any quantitative analysis of this pattern is quite sufficient for establishing the peculiarities of the phenomenon or process under study. Thus, the establishment of the isochromatic pattern of distribution of stresses in the last instant of the filling of the mold in a stamping process reveals the characteristic features of the process being studied without any quantitative analysis of the fringe pattern. The photograph in Figure 73 shows that during the last instant of the stamping process there occurs throughout the casting a uniform state of stress and that only in the vicinity of the slit do we observe any nonuniform distribution of stresses. This conclusion assists us in forming a correct concept of the mechanism of the stamping process.

In solving problems similar to this our attention must be directed primarily to realizing those conditions of similarity which have a decisive

influence on the peculiarities under investigation and the character of the process being studied by means of the model.

The second subgroup of problems which are analagous to the problem of photoelasticity are of entirely different nature, since the basic requirement in this case is the determination of the values of stresses at each point of the body being deformed. In solving these problems the basic requirement is that of determining the precise value of a fringe and determination of the directions of principal stresses by means of deciphering of the isoclinics. Particular attention must be directed to the possibility of realizing the conditions of a plane state of stress.

The second group of problems of photoplasticity has as its objective the study of physical phenomena which accompany plastic deformation. Many of these phenomena have great practical significance. Among the basic problems in this group may be enumerated the study by means of models of processes of plastic deformation designed to increase our knowledge of:

(1) the mechanism of flow and fractures;

(2) the nature of residual stresses;

(3) the nature of fatigue, relaxation, creep, elastic aftereffect and contact friction.

In solving this group of problems, as in the first group, we may deal with both qualitative and quantitative problems.

5. Basic Characteristics of the Method of Photoplasticity.

In spite of the fact that the same principle forms the basis of both the photoelastic and photoplastic methods, these methods differ from each other in substance.

Among the characteristic peculiarities of the method of photoplasticity we may enumerate the following:

1. By means of the method of photoplasticity we may study in models not only the distribution of stresses in plastically deformed bodies but also

the structural changes occurring during plastic deformation, using for this purpose optically sensitive models of crystalline materials (haloid salts of silver, thallium and their alloys).

The discovery by A. V. Stepanov of optically sensitive crystalline materials permits us on the one hand to significantly improve the method of photoelasticity, and on the other hand to create a new area of studies by means of a method of photoplasticity, since there is a possibility of utilizing the structural isochromatic pattern for the study of mechanisms of plasticity and failure and also to study the nature of the phenomena accompanying plastic deformation.

Thus, the range of problems which can be solved by the method of photoplasticity is considerably greater than the range of problems which can be solved by the method of photoelasticity. While the method of photoelasticity solves the problems of distribution of stresses in elastically deformed bodies, the method of photoplasticity in addition to these problems also solves problems concerned with the nature of plastic deformation.

2. The area of qualitative problems on distribution of stresses which can be solved by the method of photoplasticity is considerably wider than the area of similar problems solved by the method of photoelasticity. At the same time, certain of the qualitative problems of the method of photoplasticity may be utilized in studying by means of models the geological and geophysical phenomena of nature involving plastic deformation.

3. The requirements imposed on the materials used for models in the methods of photoelasticity and photoplasticity are different, hence the model materials themselves are different.

4. The behavior of materials in the models being studied by the methods of photoelasticity and photoplasticity is different. Therefore, the mechanical properties of the model materials which must be determined are also different. In the method of photoelasticity we must know such properties of the

model material as Young's modulus and Poisson's ratio, while in the method of photoplasticity we must know the relationship between the shearing stresses and either the degree or the rate of deformation. Sometimes it is necessary to know both of these relationships and also the relationship between the shearing stress and the average applied stress.

5. The experimental procedures in the methods of photoelasticity and photoplasticity are basically different. In the method of photoplasticity, deformation in the direction of incident light must be avoided, otherwise the surface being illuminated becomes uneven and the pattern of isochromatics becomes sharply distorted. Deformation in the direction of the incident light is avoided by means of glass plates of required thickness which restrain this deformation by exerting the necessary forces. This leads to formation of certain frictional forces on the surface of the glass. Sometimes these forces may be neglected. This is possible in those cases where the frictional forces are considerably reduced by applying a lubricant. The effect of the frictional forces is noticeable only at a slight distance from the surface of the model. Therefore, as is shown by experiment the frictional forces exerted by the glass may be neglected if the thickness of the model in the direction of light is taken sufficiently large so that the isochromatic pattern being observed is essentially in a state of plane strain. The avoidance of deformation in the direction of incident light, reduction of the frictional forces at the surface of restraining glass plates and the use of proper thickness of the model are specific features of the experimental procedure in the method of photoplasticity.

6. The procedure for determination of the fringe value for the model material in the method of photoplasticity has distinctive features which differ from the procedure used in the method of photoelasticity.

Thus, the methods of photoelasticity and photoplasticity are essentially different methods both with respect to the experimental procedures and with

STAT

respect to the materials used for the models, as well as the behavior of these materials in models and the determination of the properties which describe their behavior.

STAT

CHAPTER II

MATERIALS UTILIZED IN THE METHOD OF PHOTOPLASTICITY

1. Specifications for Materials Used in the Photoelastic Method.

The materials used in the method of photoelasticity must have certain optical and mechanical properties. Among these properties are the following:

1. An adequate transparency.
2. Mechanical and optical homogeneity.
3. Sufficient hardness.
4. Ease of machining.
5. A high value of piezo-optical constants characterizing the ability of the substance to become doubly refractive under the action of mechanical forces.
6. A linear relationship between the stresses and strains, and also between stresses and the difference between the paths of the rays.
7. Absence of initial refraction of light.
8. Adequate constancy of optical and mechanical properties for small changes in temperature.
9. Absence of "edge effect" following machining.
10. Absence of noticeable optical and mechanical creep and also absence of elastic aftereffect and plastic flow.

We must add still other special requirements to those enumerated for the study of the stressed state in three-dimensional models. Thus, for the study of distribution of stresses in three-dimensional models by the method

of "freezing," the material must have the ability of "freezing" the stress pattern. In utilizing the method of scattering of light the model being deformed must have the required "turbidity."

At the present time we still do not have materials which would satisfy completely all the indicated requirements. The majority of optically sensitive materials utilized successfully in the photoelastic method both in our country and abroad satisfy only the most basic of the requirements.

2. Specifications for Materials Used in the Method of Photoplasticity.

The materials utilized in the method of photoplasticity must meet essentially the same requirements as in the method of photoelasticity (except for the requirements given under 6 and 10), and in addition to that, they must meet special requirements which may be reduced to the following:

(a) the material must produce large plastic deformations;

(b) the rheological behavior of the material must correspond to the rheological behavior of the prototype.

For the purpose of photoplasticity we may use both amorphous and crystalline materials.

In certain cases the materials must be capable of serving as model materials for fatigue processes, creep and elastic aftereffect, while in other cases it must permit measuring the residual stresses of the first, second and third kind indicated, as well as the effect of the structure on the plastic behavior of crystalline bodies.

Amorphous bodies are substances with a disordered disposition of kinetic units (atoms, molecules and macromolecules). These bodies may be classified into two basic groups. The first group consists of simple amorphous substances containing molecules of small dimensions (small molecular weight); the second group includes compounds consisting of macromolecules. Each macromolecule is a complex of chemically combined simple molecules. Such amorphous bodies (polymers) have a distinctive characteristic of relatively

STAT

high strength.

Up to the present time, the method of photoelasticity has utilized materials which belong primarily to the second group of amorphous bodies.

Recently, the work of the authors has indicated that among simple amorphous substances there are transparent optically sensitive materials which are quite plastic at the same time, and that these may be successfully utilized for the purposes of photoplasticity.

These materials are characterized by the following peculiarities: mechanical and optical homogeneity; linear relationship between the difference in the optical paths and the magnitude of the maximum shearing stresses (see formula (2)); absence of an initial double refraction following processing and machining; absence of any irreversible changes of structure and properties during the process of flow; very large plastic deformations without any symptoms of failure at definite rates of deformation and temperature; dependence of the resistance to shear upon the rate of deformation and the average stress (hydrostatic pressure) and independence of the resistance to shear on the extent of deformation; noticeable effect of temperature changes on the optical sensitivity and viscosity, and reduction in the fringe value of the material with an increase in temperature. In addition to that, the rheological behavior of these materials corresponds to the behavior of a viscous solid body (see Chapter I, Section 3). Therefore, such materials may be successfully applied in studying states of stress under conditions of viscous flow.

As was already indicated, the problem of studying processes of plastic deformation by means of models is an analysis of the state of stress in the body undergoing deformation and the study of phenomena accompanying plastic flow. The solution of these problems is associated with crystalline materials such as metals and alloys. Naturally, more complete solution of the indicated problems by the method of photoplasticity may be attained by using models of

STAT

materials which either completely or to a large extent simulate the properties of metals and alloys.

The materials utilized in the photoplastic method must also have the following distinctive characteristics in addition to such properties as a high optical sensitivity and transparency:

1. Plasticity. Resistance of such materials to shear must depend upon the degree of deformation and be independent of its rate. In the process of plastic deformation there must occur a change in structure and properties. We must be able to vary the grain size and obtain the proper structure in the material by combining deformation and thermal treatment.

2. Absence of an initial double refraction. When double refraction is present, we must be able to select such thermal treatment as will assure complete removal of residual stresses or reduce them to an acceptable magnitude.

3. Similarity of rheological curves to the corresponding curves of the material in the prototype. The material of the model must be capable of simulating creep, elastic aftereffect and plastic flow.

4. Possibility of obtaining transparent, optically sensitive alloys with different structures.

5. The appearance during the process of deformation of residual stresses of the first, second and third kind.

3. Classification of Materials.

In view of the fact that the materials being utilized for the method of photoplasticity have been studied relatively little, it is not possible at the present time to enumerate the materials whose rheological behavior corresponds not only to the classes but to the sub-classes of the classification proposed in Chapter I. It appears that the most expedient manner of classifying all materials being used for the optical methods of analysis of states of stress is to divide them into three groups: (1) elastic; (2) viscous; (3) plastic. Such a division corresponds to the basic classes of the proposed classification.

materials which either completely or to a large extent simulate the properties of metals and alloys.

The materials utilized in the photoplastic method must also have the following distinctive characteristics in addition to such properties as a high optical sensitivity and transparency:

1. Plasticity. Resistance of such materials to shear must depend upon the degree of deformation and be independent of its rate. In the process of plastic deformation there must occur a change in structure and properties. We must be able to vary the grain size and obtain the proper structure in the material by combining deformation and thermal treatment.

2. Absence of an initial double refraction. When double refraction is present, we must be able to select such thermal treatment as will assure complete removal of residual stresses or reduce them to an acceptable magnitude.

3. Similarity of rheological curves to the corresponding curves of the material in the prototype. The material of the model must be capable of simulating creep, elastic aftereffect and plastic flow.

4. Possibility of obtaining transparent, optically sensitive alloys with different structures.

5. The appearance during the process of deformation of residual stresses of the first, second and third kind.

3. Classification of Materials.

In view of the fact that the materials being utilized for the method of photoplasticity have been studied relatively little, it is not possible at the present time to enumerate the materials whose rheological behavior corresponds not only to the classes but to the sub-classes of the classification proposed in Chapter I. It appears that the most expedient manner of classifying all materials being used for the optical methods of analysis of states of stress is to divide them into three groups: (1) elastic; (2) viscous; (3) plastic. Such a division corresponds to the basic classes of the proposed classification.

STAT

Among the materials to be enumerated in the first group we must list glass, celluloid, bakelite, phenolite, trolon, viskhomlit, plexiglass, gels and others; in the second group we find synthetic and natural resins; in the third group we find haloid salts of silver, thallium and their alloys ("transparent metals"). Certain materials which we have enumerated in one group may be successfully utilized for solving problems which specifically apply to another group. Thus, there are data which indicate the possibility of utilizing elastic materials -- celluloid [13] and plexiglass -- for the study of a state of stress accompanied by plastic deformation. In testing these materials at high temperatures, it is possible to simulate in models processes involving viscous flow.

We shall give a brief characteristic of the basic properties of elastic, viscous and plastic materials used in the photoelastic and photoplastic procedures.

Glass. Glass satisfies the majority of the requirements for materials used in the method of photoelasticity. This serves as the basis for its application as the very first material for solution of practical problems.

Glass is the most transparent material, it has a high modulus of elasticity, it is rigid, isotropic, insensitive to temperature variations, free of creep and is comparatively inexpensive. However, it has not received any wide application in the photoelastic method of analysis in view of its low optical sensitivity and the difficulties involved in its fabrication. One of its basic shortcomings is the formation of nonhomogeneous and anisotropic structure when models are prepared from glass by casting process. The preparation of complex models from separate glass prisms by cementing involves considerable expenditure of money.

Celluloid. This material is an organic substance ($C_6HN_3O_{11}$), which is obtained from a solution of nitrocellulose in a mixture of alcohol and ether after this solution is treated with camphor. It is sufficiently transparent

and isotropic. Its optical sensitivity is greater than that of glass by a factor of five. The basic advantage of celluloid is its good cementability by means of acetone, butyl acetate, and ethyl acetate. This permits us to prepare from this material complex models of large dimensions. The properties of celluloid improve and become stabilized with time. After being aged for a period of several years, it has a very slight creep.

The transparency of celluloid decreases considerably as the thickness of the plate increases. The transparency decreases still further after it is exposed to ultraviolet light. Celluloid has comparatively low mechanical strength.

The stress-strain diagram of celluloid in tension shows [13] that it is capable of producing small elastic-plastic deformations in the range of stresses of 200-500 kg/cm^2. At the same time, the difference in the optical paths is proportional to the stresses beyond the elastic limit approximately up to 500 kg/cm^2. This permits us to utilize celluloid for the study of stresses at elastic-plastic deformations.

Bakelite. (BT-61-893). This material is a phenol-formaldehyde plastic; bakelite also satisfies the majority of the basic requirements specified for the materials used in the photoelastic method.

Bakelite is transparent and colorless, is sufficiently hard and is not excessively brittle; this permits us to machine it with ordinary tools without difficulties. Being isotropic, it shows a linear relationship between stresses and strains up to 420 kg/cm^2 and a linear relationship between the stresses and fringe order up to 500 kg/cm^2 [12]. Bakelite has considerable tensile strength. Its properties at room temperature are practically constant. Its high optical sensitivity permits us to obtain a high order of fringes, thus increasing considerably the precision of the experiments.

Bakelite is a two-phase system whose components have different melting points [12]. A change of temperature within the limits of 15-30°C practically

STAT

has no effect upon the fringe value (sensitivity), its modulus of elasticity and Poisson's ratio. At temperatures of 60 to 110°C the fringe value and the modulus of elasticity decrease rapidly. At a temperature of approximately 110°C the change in the properties of bakelite practically ceases. At high temperatures it is a completely elastic material since the optical effect and the deformations caused by the load disappear completely upon removal of the load. The relationships between stresses and deformations, and between stresses and the order of the fringes are linear. At room temperature, the material is hard and its deformations are elastic. As the temperature is increased, there occurs a failure by flow (viscous) which corresponds to its transition to a liquid state. As the temperature is changed, the load is gradually transferred to a solid grid. The value of τ_0 decreases sharply. This process continues up to a temperature of 110°.

As the heated and deformed bakelite is cooled, there occurs solidification of the liquid component phase which leads to "freezing" of the deformations of its primary grid. This prevents the disappearance of the grid as the load is removed. The fringes of the "frozen" pattern coincide completely with the configuration of the fringes obtained at room temperature. In all other respects the bakelite behaves just as the material of the type known as viskhomlit.

Material IM-44 (Type of Viskhomlit). An optically sensitive material designated as IM-44 prepared in the Institute of Machine Design, Academy of Sciences USSR, satisfies the majority of the requirements specified for materials used in the photoelastic method.

Preparation of the material is carried out in three stages. In the first stage, a resin is obtained by condensation of phenol with formaldehyde in the presence of oxalic acid as a catylyst; in the second stage the alcohol in the lacquer obtained during the condensation is evaporated and the material is cast into molds; in the third stage polymerization of the product occurs as

STAT

the temperature is increased [14].

The product obtained after evaporation is quite plastic and soluble (resin of stage A). In the polymerization process the resin is transformed into the final state (into an insoluble and nonfusible resin of stage C). Its structure consists of an insoluble three-dimensional grid filled with a soluble and fusible product. Arrangement of the molecules of the nonfusible three-dimensional frame is random and is not subject to any crystallographic law. Therefore, the material is isotropic in all its properties. The mechanical and optical properties of viskhomlit depend upon the purity of the raw materials, the degree and method of polymerization, and the temperature and duration of material under load. At temperatures up to 50°C the phenol-formaldehyde plastic remains an elastic material [15], in the range of temperatures of 50-110°C the material is elastic-viscous, and at temperatures from 80-110° to 180°C (depending upon the grade) it remains an elastic material while its properties are but slightly sensitive to changes in temperature. At room temperature we observe a mechanical and optical creep, but their values can be decreased if the measurements are made 10-15 minutes after the model is loaded (within the limits of porportionality).

The material IM-44 finds successful application in the study of stresses in three-dimensional models. If the model is loaded at a temperature of 80-110°C and is then cooled to room temperature, the fringe pattern obtained under load is "frozen." Then the model may be cut into any number of parts while the optical pattern observed under load is not destroyed. The difference in the optical paths at a given point of the model being deformed is proportional to the maximum shearing stress.

The material IM-44 has certain residual stresses and consequently a certain degree of double refraction immediately after being formed. This is caused by nonuniform shrinkage of the material during its polymerization. In addition to internal stresses distributed throughout its volume, there is

STAT

produced along the contours a special layer with a considerable degree of double refractivity. The appearance of the edge effect is explained by physical-chemical processes (primarily by evaporation or absorption of moisture). The aging of this material over a period of several years improves its quality. The magnitude of the edge effect increases with time. The sign of the internal stresses caused by the edge effect depends upon the method of the preliminary machining of the material.

Material of type IM-44 has characteristics which are equal to those of bakelite of grade BT-61-893, which is widely used in the United States for the photoelastic method. This can be seen from data given in Table 1 [12].

Table 1

Indexes	IM-44		Bakelite BT-61-893	
	at 20°	at 110°	at 20°	at 110°
Fringe value τ_0 in kg/cm^2	6.0	0.9	7.7	0.286
Modulus of elasticity E in longitudinal direction in kg/cm^2	40-42·10^3	200	43.2·10^3	86
Poisson's ratio	0.37	0.42	0.365	0.5
Proportional limit σ_{pr} in kg/cm^2	500	10	492	11.3
Tensile strength σ_v in kg/cm^2	1300	25	1200	28.2-31.6

Organic Glass (plexiglass). This material is a plasticized polymer of methyl ether of metacryllic acid [16]. It is the most transparent plastic of all. An increase in the model thickness does not appreciably reduce its transparency. Ultraviolet light has no effect on the transparency of the organic glass for practical purposes. Plexiglass is low in optical sensitivity. In order to obtain isochromatic lines of several orders it is necessary to apply considerable force. It has a desirable property of being able to deform plastically. Models of large dimensions may be prepared from this

STAT

material by cutting from a whole piece or by cementing separate parts. Plexiglass can be used to measure distribution of stresses at elevated temperatures (up to 120°), whereupon its optical sensitivity increases considerably.

Gelatin-Glycerine Optically Sensitive Material. This material is prepared from photo-gelatin (with molecular weight of the order of 900), glycerine, ethyl alcohol, sodium chloride, and β-naphthol. The gelatin-glycerine material is transparent, has a very high coefficient of optical sensitivity (several hundred times as large as that of viskhomlit and bakelite). This makes it applicable in studying stresses caused by three-dimensional forces.

Sensitivity of the material depends in many respects on the concentration of photo-gelatin, concentration of glycerine, salt and temperature.

Being elastic and weak, the gelatin-glycerine material (after being formed) is destroyed under appreciable load. However, if it is aged for a long period at room temperature or if it is subjected to a lengthy steam bath, it becomes more dense, stronger and slightly darker, thus losing some of its optical sensitivity. However, after such treatment, the material becomes suitable both for a short-term as well as a sustained test and it is able to resist considerable loads.

In a short-term load test, gelatin-glycerine models undergo only elastic deformations. The pattern of isochromatic lines observed under load vanishes immediately upon removal of the load. In the case of a load maintained for long time (of the order of several days), plastic deformation is observed and the model changes its form permanently.

Figure 12 shows three stages of flow of a model from a container under a sustained load test. Photograph a indicates the form and dimensions of the model prior to the test; b shows the beginning of an irreversible change of form; c shows the form of the model after flow of a considerable amount of material through a die. After the model was removed from the container, its

dimensions changed somewhat due to the removal of the elastic component of deformation, but the residual stresses remained in the material.

The character of distribution of the isochromatics and their order in the model under test may be seen in Figure 13, which was obtained by illuminating with circularly polarized light (see insert between pages 46-47). This pattern remained in the model over a considerable period of time (more than three years).

a b c

Figure 12. Flow of gelatin-glycerine material from a container: a--model before test; b--beginning of an irreversible change in form; c--model after a sustained test.

Figure 14 shows photographs obtained with such a model after a certain period. Comparison of Figures 13 and 14 a shows that no significant changes in the isochromatic pattern have occurred. Figure 14 b shows a photograph made after the model was cut into two parts along the axis of flow. As can be seen, the isochromatics were preserved in the two separate parts of the model. This shows that there develops in the model during the process of plastic deformation a texture indicated by the double refraction shown in the photograph.

Figure 15 shows a color photograph which indicates the disposition of the isochromatics and their order in the model deformed by settlement in a flat container (see insert between pages 46-47).

Thus, when we use gelatin-glycerine material prepared in the indicated manner, we can study the character of the distribution of the residual stresses in models subjected to finite plastic deformations.

Figure 14. An isochromatic pattern in a specimen of gelatin-glycerine material obtained three years after deformation: a -- before the model was cut; b -- after the model was cut into two parts along the axis of flow.

Resins. Rosin (a mixture of resinous acids) in its solid state possesses optical sensitivity. The rosin acquires different colors and degrees of transparency depending upon the degree of oxidation of its components. The resinous acids which are oxidized to lesser extent ($C_{20}H_{30}O_2$) yield lighter grades of rosin. The latter are most suitable for preparation of plastic optically sensitive materials. Since the rosin itself is very brittle, it cannot be used for the photoelastic method, and certainly not the photoplastic method. However, by plasticizing we can obtain from the hard rosin materials of the required properties. In order to plasticize this material, we can use various mineral and vegetable oils; however, some of them when mixed with the rosin do not yield materials of the required properties. We must use as a plasticizer such oils as when mixed with the rosin yield a material which resists oxidation.

In order to obtain an optically sensitive, transparent plastic material which meets the basic requirements specified for materials to be used in the photoplastic method, it is best to use a rosin of high grade and a pure rosin oil. A rosin oil of the highest fraction is obtained by distilling rosin of light grades under vacuum (distilling temperature 300°C, pressure 5 mm Hg). A mixture of rosin with rosin oil* in certain proportions yields a material

* The rosin oil was obtained in the Laboratory of Technical Catalysis and Kinetics, Academy of Sciences BSSR

of different hardness and plasticity. In mixing rosin and rosin oil in the ratios of 2:1 and 3:1 we obtain a very plastic material in which the pattern of isochromatics under load is preserved only a very short time. In this case it is difficult to fix the pattern of isochromatics and isoclinics which accompany the process of plastic deformation. By mixing the components in the ratios of 5:1 and 6:1 we obtain a hard elastic material in which the isochromatic pattern due to loading is preserved for a considerable length of time. However, models prepared from such a material are likely to be destroyed even for relatively small deformations.

The mixture most suitable for the method of photoplasticity proved to be one consisting of four parts of rosin and one part of rosin oil. The material is transparent, has a light-yellow color, produces a bright and vivid isochromatic pattern and permits large plastic deformations at high rates of deformation. It proved to be possible to remelt the material repeatedly without any appreciable loss of transparency (darkening). In order to guard against possible contamination during the repeated use of the same batch of material it may be filtered through gauze in a molten state. Our experiments were conducted in the main with material of this composition.

The optical sensitivity of the resin described is quite high. The experimentally determined fringe value for this material at a stabilized process of flow for the yellow line of mercury and a temperature of 20°C is τ_o = 2.20 ± 0.015 kg/cm. For a sufficiently small dimension of the monochromatic source of light and well regulated optical apparatus and the use of a light filter, it is possible to obtain in the photograph up to 40 fringes (Figure 46c).

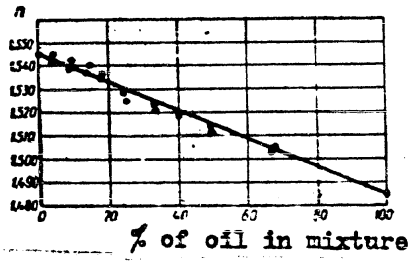

Figure 16. Variation of the index of refraction of the rosin mixed with rosin oil with the oil content.

Tests of the resin at various temperatures show that its sensitivity

a b

Figure 2. Colored fringe pattern obtained:
a) with resin; b) with gelatin-glycerine material.

Figure 13. Isochromatics retained by the model of gelatine-glycerine material after test.

STAT

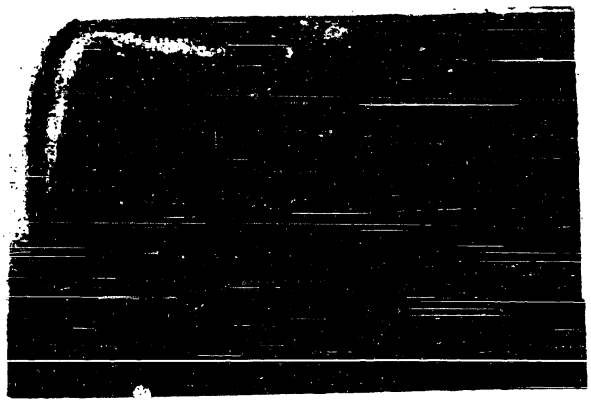

Figure 15. Isochromatics retained by the model of gelatine-glycerine material after a compressive test.

Figure 17. Isochromatic pattern observed during the flow of rosin-butadiene hydrocarbon dioxide mixture.

STAT

increases with temperature. The sensitivity of the material changes also with the proportions of its components. The smaller the amount of resin in the mixture, the greater the sensitivity. The index of refraction varies with the composition linearly (Figure 16).

Physical tests of cylindrical specimens (d = 10 mm, h = 14 mm) of the resin of indicated composition show that the static deformation at various speeds of the testing machine (10, 20, 40 and 80 mm/min) indicates, as might be expected, that the material has no defined flow limit. The rate of flow of the resin, and consequently the rate of its deformation at room temperature within wide limits (from 1.19 to 33.7 kg/cm^2) is proportional to the shearing stress. The relationship between the coefficient of internal friction and the temperature for a temperature range of 12 to 27°C is shown in Table 2. For a temperature change of 1°C the viscosity of the resin decreases approximately by a factor of 1.4.

When we study the process of plastic deformation by means of resin models, we must keep in mind the possibility of large reduction of viscosity at points of stress concentration associated with temperature rise. This circumstance may lead to a redistribution of stresses in the model under test.

Table 2

$t°C$	12	15	18	21	24	27
$10^{-7}\eta$	355	205	81	25	8.1	3.45

The result of physical tests at room temperature show that the resin is the most suitable material for models in the study of the process of plastic deformation of solid bodies under conditions of viscous flow.

Dioxide of Butadiene Hydrocarbon ($C_{20}H_{22}O_2$)*. The dioxide is obtained by oxidizing hydrocarbon $C_{20}H_{22}$ in vacuum. It is a viscous fluid of light yellow color. The higher the fraction of the material, the denser the dioxide. When

* Obtained in the Laboratory for Organic Chemistry of the Academy of Sciences of BSSR.

mixed with a resin it yields a transparent optically sensitive material of varying plasticity (depending upon the proportions of the components).

The most suitable material was obtained from a mixture of rosin and the dioxide fraction obtained at a temperature of 204-218°C and a pressure of 1.5 mm Hg for a component ratio of 1:2. This material is transparent and has a light-yellow color. The isochromatic pattern has bright and vivid colors (see insert, Figure 17). For large rates of loading the material is destroyed, while for low rates it deforms plastically. It permits repeated use by re-melting without exceeding the temperature of the melting point. When this temperature is exceeded the material gradually darkens and loses its transparency, thus becoming unsuitable for further work.

The mixture of dioxide of butadiene hydrocarbon with rosin of higher grades yields isochromatics of high orders.

Abietinic acid ($C_{20}H_{30}O_2$)*. This material is a crystalline substance of monoclinic structure obtained by isomerization of primary resin acids. It has a melting point of 172-173°C. In its molten state it is transparent; after cooling this material becomes amorphous and after a certain length of time begins to crystallize and lose its transparency.

Abietinic acid mixed with rosin oil in the ratio of 3:1 yields a material of light-yellow color of high optical sensitivity. The isochromatic pattern is bright but disappears rapidly, and the colors are vivid. For a component ratio of 4:1 we obtain a material which has the properties indicated above, is plastic, and retains its isochromatic pattern for a long time. When the model is loaded until a fringe of the tenth order is obtained, the fringe pattern is retained in excess of 20 minutes (at room temperature). Being an unstable material, abietinic acid oxidizes rapidly when heated (for repeated melts), darkens and becomes unsuitable for further use. In view of this, repeated use of this material is quite limited.

* Obtained in the Laboratory of Chemistry of Forest Products, Academy of Sciences, BSSR.

STAT

Canadian Balsam. When this material is evaporated to an almost solid state, it is adequately transparent, plastic and optically sensitive. When models made of this material are deformed, we observe bright and vivid isochromatics. Canadian balsam may be used repeatedly upon being remelted.

Silver-Fir Balsam. In the solid state this material possesses optical sensitivity. In order to make this material plastic (viscous) it must be boiled with xylol (or some other solvent). Varying the quantities of the components, we can obtain materials of various plasticity and transparency. When models made of such a material are deformed they produce bright and vivid isochromatics. This material permits repeated melts without any noticeable loss of transparency.

Materials obtained with Canadian or silver-fir balsam as a base possess high optical sensitivity, plasticity and other required properties, but they adhere tenaciously to instruments. Besides that, they are quite expensive and in short supply.

Chloric Silver. This material has a crystalline structure /4/. Its crystals have a simple cubic grid of the type of NaCl and have a period $a = 5.54$ kx. By combining mechanical and thermal treatments of a casting, it is possible to obtain transparent and almost colorless specimens of any dimension and form. The volume of the specimen (casting) under a given set of conditions may be filled with a single or several grains, while under another set of conditions it may contain hundreds and even millions of grains. The grains may have different dimensions, form and orientation in one and the same casting, just as is the case with ordinary metals and alloys. We may obtain textured specimens and also specimens with an almost homogeneous grain structure, with grains of uniform size. Specimens of chloric silver may have the structure of cast products, recrystallized metal, etc. In order to obtain the required structure, we utilize ordinary methods of treatment of metal.

Haloid salts of silver and thallium have mechanical properties at room

temperature which are quite different from the ordinary properties of the component masses of salts and minerals. The mechanical properties of chloric silver are such that it can be truly called "transparent metal." It can be treated at room temperature by all the types of treatment applicable to metals. Chloric silver may be forged, rolled, stamped, pressed, etc. At room temperature it is approximately ten times weaker than copper; like lead, it may be scratched by nail, it can be easily flexed by hand, and it has a metallic ring. The mechanical properties of chloric silver both by itself and in alloyed form, depend upon the magnitude of deformation. In the process of plastic deformation it becomes less plastic. In this respect, chloric silver shows its ability to be strengthened by cold working at room temperature.

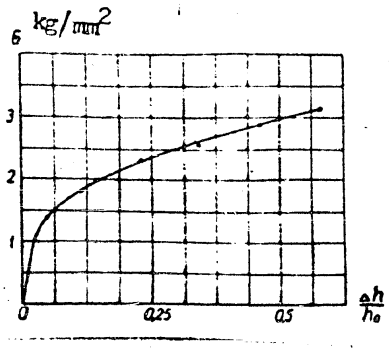

Figure 18. Curve of true stresses obtained for a static compression of specimens of chloric silver.

The test by the method of indentation with a cone shows that the hardness of chloric silver increases considerably after it is deformed. Specimens which are compressed 75% have their hardness increased approximately by a factor of 1.75 compared with undeformed specimens. Thus, if the hardness of the undeformed specimens is 10.5 kg/cm^2, specimens compressed 60 and 75% have hardness values of 16.2 and 18.5 kg/cm^2 respectively.

Curves of the true stresses obtained from the diagrams of static compression for specimens of chloric silver having a cylindrical form (8 mm in diameter and 12 mm long) prepared from a casting which had previously been deformed 60% in compression and then heat treated for 5 cycles of 5 hours each at a temperature of 150°C, are quite similar to analogous curves for a "cold worked" metal. The curve of true stresses for the indicated case is shown in Figure 18.

The thermal treatment of cold worked specimens of chloric silver brings about the removal of stresses, which may be either relaxation or complete recrystallization depending upon the temperature of the heat treatment. As a result of thermal treatment the cold worked specimen is returned to its initial soft and plastic state as may be seen in Figure 19. For purpose of comparison there are given in Figure 20 stress-strain diagrams of polycrystalline specimens of copper.

The character of the flow of chloric silver and also the nature of fractured and compressed specimens are similar to the corresponding phenomena observed for metals. Fracture occurs with a formation of a necked-down section. For heat treated specimens the fractured section degenerates into a point (Figure 21). The entire length of the specimen participates in accumulation of residual elongation. During a tensile test of cold worked specimens we observe formation of a necked-down section and in addition to that we observe the formation of the surface of fracture. Specimens compressed to a high degree do not show any symptoms of fracture (Figure 22).

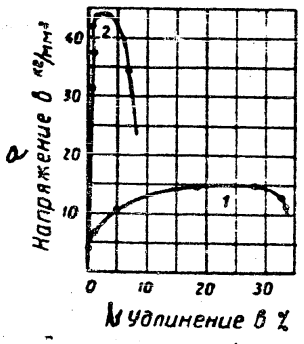

Figure 19. Stress-strain diagrams of polycrystalline specimens of chloric silver in tension: 1 -- heat treated; 2 -- cold worked (from A. V. Stepanov)
Legend: a) stress in kg/mm²
b) elongation in %

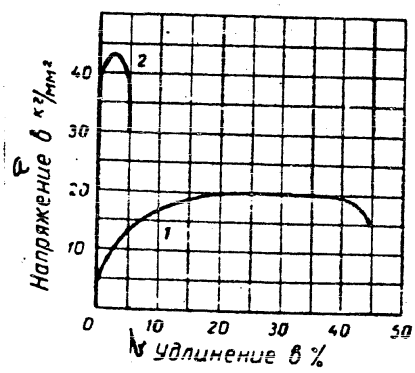

Figure 20. Stress-strain diagrams of polycrystalline specimens of copper in tension: 1 -- heat treated; 2 -- cold worked (from Muller).
Legend: same as Figure 19

Crystals of chloric silver being in the cubic system are optically isotropic. If a specimen of this material is subjected to external mechanical forces, it becomes doubly refractive. A characteristic peculiarity of the

piezo-optical properties of chloric silver is its high optical sensitivity. That places it among the best contemporary substances having high optical sensitivities (viskhomlit, bakelite, resin).

Figure 21. A specimen of chloric silver tested in tension (from A. V. Stepanov).

Figure 22. A cylindrical specimen of chloric silver compressed 60%.

Up to certain small values of loads chloric silver behaves as elastic material. For larger loads the material develops permanent double refractivity. This indicates that plastic deformation brings about residual stresses in this material. In a deformed specimen of chloric silver one can observe residual stresses of the first, second and third types. Residual stresses brought about as a result of plastic deformation may be removed by means of special heat treatment.

Optically sensitive chloric silver has high piezo-optical coefficients which are of the same order of magnitude as for viskhomlit and bakelite. The transparency of chloric silver is reduced considerably under the action of light. However, this is not a serious obstacle in working with this material. The process of decomposition of this material is not very intensive. Application of light filters which block the short-wave portion of the spectrum reduces considerably the decomposition of chloric silver in light.

A very desirable property of chloric silver is its ability to regenerate and its ability to be used several times over for experimental work.

4. Effect of the Nature of the Material Being Deformed on the Character of

STAT

Stress Distribution.

Study of the effect of the nature (structure) of materials and their mechanical properties on the stress distributions of a deformed body or a body undergoing deformation is one of the basic problems of the method of photoplasticity. Depending on whether the material is amorphous or crystalline, the model undergoing deformation under given conditions (type of loading, geometry of the model and type of instrument) will yield a completely definite picture of the distribution of stresses.

The process of plastic deformation is accompanied by formation of residual stresses. In homogeneous bodies one can observe only residual stresses of the first type, while in crystalline bodies residual stresses of first, second and third type may be observed. Thus, the distributions of stress in crystalline and amorphous bodies subjected to identical conditions of deformation differ in this essential respect.

In order to confirm the stated postulate we shall compare fringe patterns observed for a load of the same type in models prepared from elastic, viscous, and plastic material.

For the purpose of comparative tests the authors utilized a flat model loaded with a die. Figures 23, 24 and 25 show the fringe pattern in the entire field of models loaded approximately to the same extent.

In the case of elastic material the fringes are continuous and form circles which touch the corners of the die. This confirms the well-known postulate that for the loading under consideration fringes are circular and pass through the edges of the die. As the load was removed, the fringe pattern accompanying the load was completely removed.

In the case of viscous material the fringes are continuous and well defined. They form ovals elongated in the direction of movement of the die. As the model is unloaded, the fringes persist for a long time, and gradually disappear. The fact that these lines are continuous indicates that the

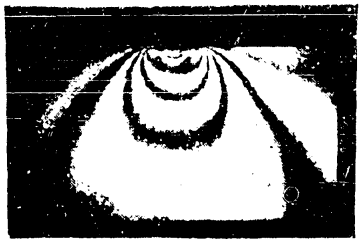

Figure 23. Fringes observed upon deforming a viscous material (resin).

Figure 24. Fringes observed upon deforming an elastic material (viskhomlit).

Figure 25. Fringes observed upon deforming of a plastic polycrystalline material with a fine grain structure (chloric silver).

residual stresses being observed are of the first type. Figures 26 and 27a show fringe patterns immediately after models of various dimensions are completely unloaded. Figure 27b shows the fringes several minutes after the model is unloaded, the model corresponding to Figure 27a.

In the case of polycrystalline material with a sufficiently fine grain structure we note considerable distortion of the fringes even in the first stages of finite plastic deformation. However, even in this case the fringes have an oval shape. As the model is loaded, the order of the fringes increases (Figure 116). After the model is unloaded, a portion of the fringes corresponding to elastic deformation disappears immediately. However, it retains fringes of a certain order. The fringe pattern retained by the model corresponds to the residual stresses of the first, second, and third type. In Figure 117 we may consider the two well defined fringes in the right hand side of the model as being caused by residual stresses of the first type. In the remaining portion of the model, the fringes are considerably distorted and do not give us any clear picture

STAT

of the orderly distribution of residual stresses. These stresses are in essence residual stresses of the second and third type in this portion of the model.

Figure 10b which shows the fringe pattern obtained with a model of considerable dimensions made of plastic polycrystalline material with a coarse structure (1-2 mm) is even more characteristic in this respect. In this view it is impossible to see any well defined continuous fringes.

Figure 26. Fringe pattern retained by a model of resin after removal of the load.

Each grain behaves in a distinct manner, yielding its own individual pattern of stress distribution. This is revealed by the different coloring of the grains in polarized light. The individual properties and the different disposition of the discrete grains give their own optical pattern, departing from the orderly fringe pattern which we would have obtained in the presence of residual stresses of the first type only. In the given case the residual stresses of the second and third type are larger in magnitude than the residual stresses of the first type. Here we are dealing with a structural isochromatic picture.

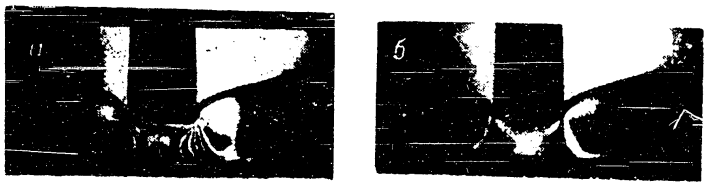

Figure 27. Fringe patterns observed in models of resin: a -- immediately after removal of load; b -- several minutes after removal of load.

For a fine and homogeneous grain structure the distorting influence of the residual stresses of the second and third type is not as strongly indicated

and in this instance one can observe a certain orderliness in the fringe pattern -- a pattern which shows the distribution of forces throughout the volume of the deformed model.

CHAPTER III

SPECIAL FEATURES OF EXPERIMENTAL TECHNIQUE

1. Optical Installation and Apparatus.

Optical installations for the photoplastic method as distinct from those used in a photoelastic method must have primarily devices for assuring constant rates of loading over a broad range of loads and rates. Therefore, such installations must have a mechanical device meeting this requirement and they must have a recorder for recording the load-deformation curves.

Such an apparatus was installed in the FTI and AN BSSR [23]. Its general view is shown in Figure 28.

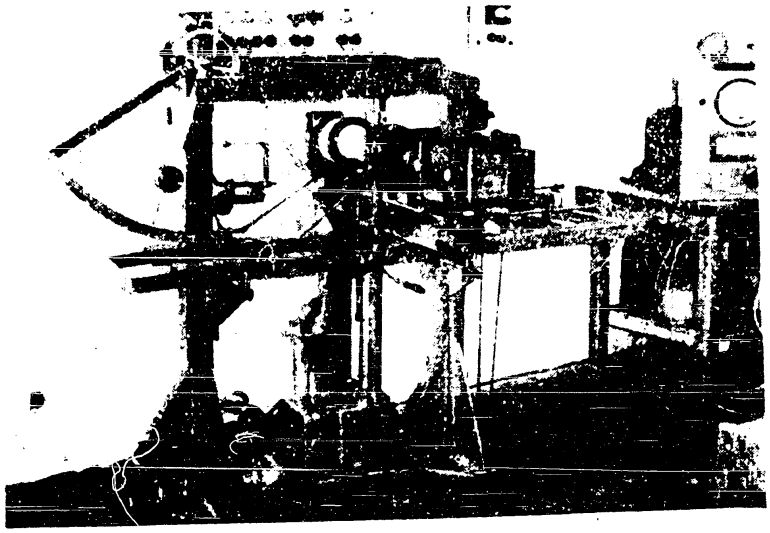

Figure 28. Optical installation of the Physical-Technical Institute of AN BSSR.

The optical installation consists of an optical and loading portion. The arrangement of the optical portion does not differ in principle from the ordinary apparatus applied in the photoelastic method (Figure 29).

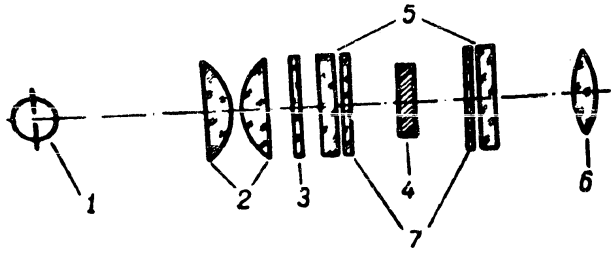

Figure 29. Diagram of the optical part of the installation: 1 -- source of light; 2 -- condenser; 3 -- filter; 4 -- model; 5 -- polaroids; 6 -- objective; 7 -- "quarter-wave" plates.

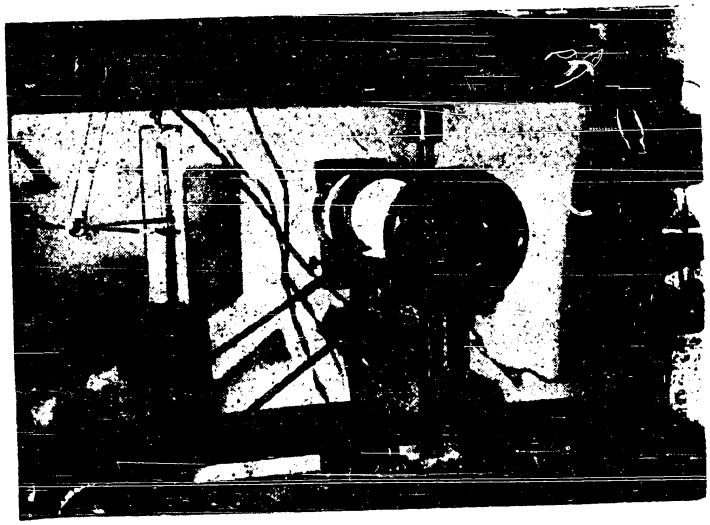

Figure 30. Position of the container with the model in the field of the optical installation.

In investigating various processes of plastic deformation, the model is placed in the container between polaroids (Figure 30). Loading of the model is achieved according to various schemes by the loading portion of the equipment. The loading mechanism permits recording of loads from 100 g to 180 kg. The necessity of obtaining an even application of load and very low rates of loading with highly optically sensitive plastic materials dictated the requirement that the range of speeds of the loading crosshead be maintained from 0.3 to 300 mm per minute. The load being applied to the model is measured

STAT

automatically by a lever-pendulum mechanism consisting of several levers, a pendulum indicator and a load scale. The record of "load deformation" is obtained by a recording mechanism.

The study of the processes of deformation under conditions of plane strain is carried out in universal devices -- flat containers shown in Figures 31 and 32.

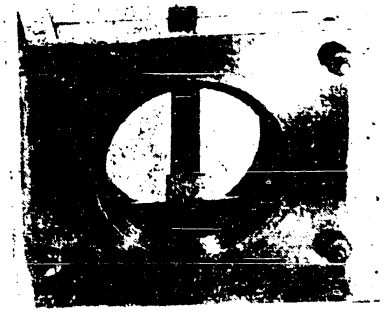

Figure 31. Container in assembled form.

In the container shown in Figure 31, the openings in the front and rear walls are covered with quartz plates 25 mm thick. The space between the plates contains steel inserts of required form and thickness. The model under investigation is placed between the inserts and is loaded by them.

The container shown in Figure 32 may be used for testing of models of various thicknesses. The portions of the container with the die opening are made of steel plates of various thicknesses (Figure 33). Optically flat plates of the required thickness are attached to the interior portions of the container by means of side bars of rectangular section and bolts. The width of the working portion of the container (in which the model is placed) may be adjusted by the width of the loading die.

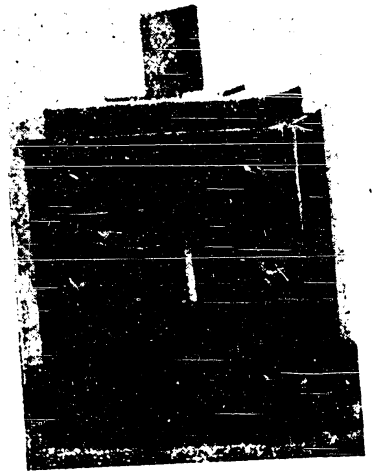

Figure 32. Container in assembled form.

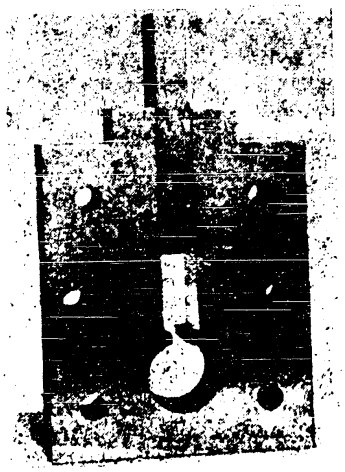

Figure 33. One of the interior plates of the container shown in Figure 32.

For the study of the stamping process, stamps of the required form are fabricated and placed in the containers.

In the first container (Figure 31) the diameter of the openings in the front and rear walls is equal to 84 mm, which permits the testing of 60x60x16 mm models; in the second, the diameter of the openings is 52 mm, which permits the testing of 38x38x50 mm models. The construction of these devices permits the casting of models directly into the almost assembled container. After test, the containers are taken apart and the models are removed from them without difficulty.

2. Fabrication and Machining of Models.

Models of Resin.

The procedure used in preparing models of resin differs in substance from the corresponding procedure used for the elastic method. The laboratory for forming of metal by pressure of the FTI AN BSSR has developed by experience its own procedure for preparation of materials and preparations of models of resin.

In view of the fact that models of the required form and thickness cannot be cut or machined from a slab or piece of resin because of its brittleness and adhesion to the cutting tools, the following procedure is used.

The mixture (consisting of the components taken in proper proportions by weight) is thoroughly stirred with a glass rod and after air bubbles are expelled, it is poured into molds made of synthetic rubber. Other materials are not suitable for this purpose, since the highly adhesive resin sticks to them and it is impossible to strip the molds without spoiling the model. The molds have the dimensions and the form of the required model. The molten resin is cast with some excess since as it cools the material shrinks. After the model cools, the form or its parts are easily stripped from the model without disturbing it. The excess of the model thickness is removed by rubbing on a stretched strip of gauze with application of suitable alcohol. The

STAT

alcohol dissolves the resin quite easily and it is only necessary to expend several minutes to remove a thickness of material of about 1 mm. The other dimensions of the model are similarly adjusted by polishing with gauze wetted with alcohol. By means of this treatment, it is possible to prepare a model of any form and dimensions. The finished model is coated lightly with a pure transformer or vegetable oil which increases its transparency.

The model prepared in this manner is placed in a container and is tested or aged for the necessary length of time.

When imperfections in the fit of the model are noted, it is loaded lightly prior to the test. This is done in the first place in order to obtain intimate contact between the model and the various parts of the container and in so doing to eliminate imperfections on the model surface; in the second place, this is done to remove from the field of the model those fine lines which are due to the presence of droplets of lubricating oil. However, when the model is loaded, stresses are induced in it. In order to remove these stresses, the model is sometimes unloaded, while in other cases 2-3 minutes are allowed to elapse until the optical pattern disappears and the model becomes quite clear and transparent.

After the preliminary operations are completed, the test of the model is initiated.

The method of preparation of models of resin described above is not the only possible one. The model may be cast into the container which is almost completely assembled. In order to do this, the molten resin is cast (taking into account the thickness of the model and the excess needed to account for shrinkage) directly into the mold formed by the walls of the instrument and inserts of synthetic rubber. After the model cools, it is polished until the required thickness is obtained on one surface only (the front). Then the front part of the container or the face plate is placed, the parts are bolted together and the model may be tested. Such a procedure eliminates the operation

STAT

required to fit the dimensions and shape of the model to the container.

Models of Chloric Silver.

Optically sensitive chloric silver is prepared in accordance with the procedure developed by A. V. Stepanov [17].

The powder of chloric silver is obtained from a 33-percent solution of silver nitrate as a precipitate produced with a 15-percent solution of sodium chlorides. In order to obtain the precipitate the component materials must be chemically pure. Before the solutions are mixed, they are heated to a temperature of 60°. This accelerates the coagulation of the particles of chloric silver.

After the precipitate is obtained from the reaction which is accompanied by a vigorous stirring of the solutions, the mixture is permitted to stand for 8-12 hours to permit the sedimentation of the flakes of the precipitated chloric silver. After this, half of the portion of the clear solution which is above the chloric silver at the bottom of the vessel, is siphoned out and is replaced by pure distilled water. During the following washings and decantations the precipitate of chloric silver is separated from the soluble products of the reaction. In practice this operation is repeated 14-18 times. This assures the presence in the final solution of soluble products in an amount not exceeding 1/16,000 - 1/250,000 parts of the initial amount.

After washing, the powder of chloric silver is dried at a thermostatically controlled temperature of 60-80°C. In this process of drying, the powder becomes finer.

The entire process of preparation of the product (AgCl) is carried out in a dark-red light.

In order to obtain a transparent optically sensitive material it is necessary to melt the powder of chloric silver (melting temperature 457.5°), and having cast the material into a crucible of thin glass it must be slowly cooled. However, the material obtained decomposes rapidly and darkens (in

view of liberation of metallic silver). The darkened chloric silver is restored to transparency by refinement with chlorine. In order to do this, dry chlorine obtained during the reaction of potassium permanganate with hydrochloric acid is passed through the melt at a temperature of 500-525°. The refinement takes from 10-30 minutes depending upon the degree of darkening of the material. The transparent chloric silver with an oily sheen obtained after this process may now be utilized in the investigation.

However, there are still certain impurities in the chloric silver thus obtained which may cause the material to decompose rapidly while exposed to light during the test. The removal of these impurities is carried out by means of crystallization. As the result of formation of a crystalline grid during the slow cooling of the molten chloric silver, all the foreign bodies and metallic silver are displaced to the end of the casting and may be removed when the model is machined. This is achieved by virtue of the fact that the cooling of the melt proceeds from one end and the boundary between solid and liquid chloric silver slowly moves from the lower part of the crucible to the top. During this process, the impurities are gradually displaced into the upper portion of the casting and form a dark layer at the top.

After the melt of chloric silver is refined, it is cast in a crucible of molybdenum glass and is then placed in a vertical crystallizer. In order to obtain a completely transparent casting without any defects it is necessary to obtain certain conditions in the crystallizer furnace. After the crucible with the molten material is maintained for a certain length of time in the upper part of the furnace of the crystallizer at a temperature not exceeding 525°, a device is started which moves the crucible downward at a speed of 1-6 cm/hour. The fineness of the grain structure will depend upon the rate of movement of the crucible. Beginning with the lower end, the crucible passes through a ring diaphragm (furnace) in which the temperature is maintained within the limits of 495-500°C and the melt begins to crystallize.

STAT

After the entire crucible passes through the ring diaphragm and the crucible cools slowly at the bottom part of the furnace of the crystallizer to a temperature of 100-120°, the crucible with the casting is removed. Because of the large difference in the coefficients of thermal expansion of chloric silver (32.94×10^{-6}) and molybdenum glass (5.5×10^{-6}), during cooling the casting is in a condition corresponding to three-dimensional tension. Therefore, in order to prevent cracking within the casting, the walls of the crucible are made so thin (0.2-0.3 mm) that the glass is destroyed by the compressive stresses before the casting can be damaged by the tensile stresses.

The casting must then be heat treated at a temperature of 360-370°C for a period of 6 hours with a consequent slow cooling in the furnace during a lengthy period (10 hours).

Chloric silver is very weakly soluble in water and the majority of other substances. In order to show the magnitude and boundaries of the grains, it is necessary to etch the casting. For this purpose, one may use solutions of ammoniac, hyposulphate or potassium cyanide, which are all good solvents of chloric silver.

Various methods of mechanical and thermal treatment of the material are used depending upon the function to be served by the models prepared from plastic optically sensitive substances.

In order to obtain a fine and sufficiently homogeneous grain structure upon recrystallization, it is necessary to realize a preliminary plastic deformation of sufficiently high magnitude under conditions of absolute homogeneity. In this instance the thermal treatment must be carried out at low temperatures. When such a procedure of mechanical and thermal treatment is used, we succeed in obtaining specimens with grains of the order of 0.1-0.05 mm.

Specimens in the shape of discs (cylinders) about 24-30 mm high, are cut from the casting obtained by crystallization of the melt and heat treatment at an elevated temperature. The height of the cylinders must not be greater

STAT

than twice the diameter and the ends must be perpendicular to the axis. The cylinders are compressed between flat polished plates of plexiglass or chrome plated steel plates in a hydraulic press. As a lubricant one must use a pure transformer oil, liquid vaseline, or grease. The degree of deformation is from 90-92%, i.e., the cylinder with an initial height of 26 mm is transformed into a plate with a thickness of 2.4-2.6 mm. The plates thus obtained are polished to the required dimension after which models of required dimensions are cut from the plates. Then finer polishing of the model surfaces is carried out on frosted glass plates with abrasives of different fineness and a solution of hyposulphate. The models are polished on felt, wool cloth, or chamois and are then placed on flat and parallel thick glass plates to be heat treated in a thermostatically controlled furnace.

As was already shown, in order to obtain a sufficiently fine grain structure, the temperature for the heat treatment must not be high. Thus, for a deformation of 92-95% it must not exceed 100°C [187], while for a deformation of 90 percent it must not exceed 150°C. Naturally, for a temperature of the heat treatment of 100°C the time of the treatment must be rather long (of the order of 10-12 hours); for 150°C it may be considerably reduced to approximately 2-5 hours.

In order to obtain a more uniform grain structure it is necessary that the coarser grains in the original casting be sufficiently uniform. If in the original structure there are significant inhomogeneities, then the recrystallized grains will be quite inhomogeneous. The large and fine grains will be found side by side in the heat treated specimen. Therefore, if in the original casting there is present a significant inhomogenity of grains, it is recommended that the casting be subjected to a preliminary treatment consisting of compression of the order of 40-50 percent with subsequent heat treatment. After such a preliminary treatment the material is subjected to treatment indicated above.

Adequate results are obtained in preparation of plates in the following manner. The disk is compressed from 13 to 7.6 mm. In doing so, the deformation attains a value of 42 percent. After that the casting is heat treated at a temperature of 170°C over a period of 4 hours and is then compressed to 2.2 mm. During this operation the deformation attains a value of 71 percent. The subsequent heat treatment is again performed at a temperature of 170°C over a period of 3-4 hours. The models are prepared from the plate obtained in this fashion. Figure 115 shows the isochromatic pattern obtained in a model prepared in the indicated manner for the case where the load is applied with a die 10 mm wide. The isochromatic lines are continuous. The model behaves mechanically and optically as a continuous and homogeneous body. During this process there occurs an averaging process of the optical phenomena in the model of quasi-isotropic fine grain structure, and the optical isoclinic coincides with the elastic one. In view of the fact that the averaged difference in optical paths varies continuously, there will be observed a system of continuous isochromatics.

In models having a thickness of 2 mm, one of which is indicated in Figure 10b, there are approximately 20-40 grains in the path of the polarized ray of light. This number is sufficient to obtain in the field of view of the deformed model a system of continuous isochromatics and isoclinics.

The heat treatment of the models must be performed in air. It is still better to use paraffin for this purpose by virtue of the greater heat capacity which facilitates the regulation of temperature in the heat treatment.

The development of chloric silver of finely crystalline structure makes it possible to obtain a macro-pattern of the distribution of stresses throughout the volume of the specimen (model). However, in order to solve a series of problems, specimens with a coarser grain structure are needed. For example, in investigating certain fatigue properties specimens are needed in which individual grains occupy the entire width and thickness of the specimens. It

becomes important to study the state of stress in individual grains and also at the boundaries of the grains. For this purpose specimens are needed which are prepared in such a manner that the path of the ray of light contains only a single grain.

The procedure for preparation of polycrystalline specimens of chloric silver (monocrystalline in the direction of thickness) was developed by S. O. Tzobkallo [19] and applied by him in the study of the nature of fatigue failures by optical means. This method consisted of carrying out special processes of crystallization and mechanical and thermal treatments.

In order to obtain specimens monocrystalline in the direction of thickness, the crystallization of chloric silver is carried out in a horizontal crystallizer with an application of flat glass inserts. In this process we obtain plates with elongated grains with a magnitude up to 20 mm. Crystals obtained in this fashion have an uneven surface and must be ground and then polished. The best results are obtained by recrystallization of strips of chloric silver obtained by pressing. In strips having a cross-section of 1x10 mm pressed in a container having a diameter of 15 mm with a deformation of 94 percent it is possible to obtain grains having dimensions of 1.5-2.0 mm by application of the high temperature heat treatment (340°C) over a period of 24 hours. The graph in Figure 34 shows the relationship between the grain size and the temperature of recrystallization.

In certain special cases (such as determination of piezo-optical constant) it is necessary to have specimens containing but a single grain both in direction of thickness and in the direction of the width. This may be achieved in the following manner [20]. We start with a strip having a cross-section of 1x10 mm and a grain size of 1.5-2.0 mm obtained by pressing in a container. These strips, which receive a preliminary cold working process by compression (or tension, which is worse) up to the critical deformation of 3 percent, are then heat treated in the following manner. The specimens are maintained in a

STAT

furnace for 24 hours at a temperature of 310°C after which the temperature is raised to 340°C over a long period of time (10 hours) and the specimens are maintained at that temperature for 20 hours. Then the temperature is raised to 360°C in a period of 4 hours and the specimens are maintained at that temperature for 2 hours. After such a treatment the specimens must be slowly cooled. Such a procedure makes it possible to obtain specimens having a grain thickness of 1 mm and a width of 8 mm. In Figure 35 there is shown the relationship between grain size and the extent of deformation in compression.

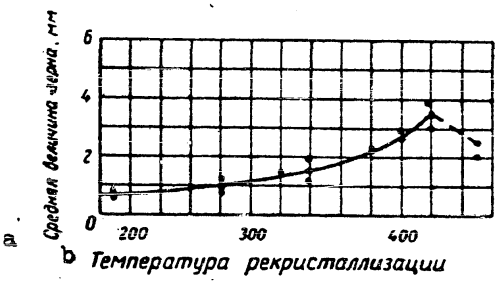

a

b

Figure 34. Relationship between the grain size and the temperature of recrystallization.

a) Average grain size, mm.
b) Temperature of recrystallization.

By utilizing a very low rate of crystallization of molten chloric silver and other haloid salts of thallium and their alloys, it is possible to obtain monocrystals of considerable dimensions.

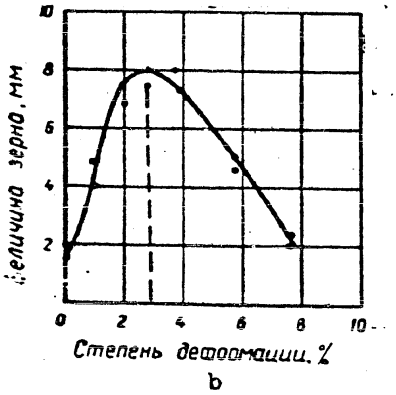

a

b

Figure 35. Relationship between the grain size and the magnitude of plastic deformation in compression.

a) Grain size, mm.
b) Magnitude of deformation, %.

V. M. Krasnov and A. V. Stepanov [21 and 22] reported in their work the use of anisotropic plates of the alloy of bromic and iodic thallium (TlBr -- 60 percent, TlI -- 40 percent) having dimensions of 3.28x37.00x35 mm in which they studied the state of stress under

the action of a concentrated load. The plates were heat treated prior to the test at a temperature of 150°C for a period of 6 hours. Following the heat treatment, only slight residual stresses, which had no significant effect on the results of the experiments, were observed. In the second case [22] monocrystalline plates of a fluoric casting having dimensions of 20.87x22.55x3.28 mm and others were utilized for the study of initiation of fracture. In this instance the heat treatment was carried out at a temperature of 700°C over a period of 10 hours.

Thus, when we use a proper method of mechanical and thermal treatment we can obtain from the salts of silver and thallium both monocrystals of various dimensions and polycrystalline materials with a very fine grain structure.

3. Experimental Technique.

In order to obtain quantitative results by the photoplastic method it is necessary to utilize models of considerable thickness, as will be shown below. An increase in the thickness of the model is associated with a series of experimental difficulties. The transparency of the model decreases noticeably and the intensity of the transmitted polarized light is correspondingly reduced. This leads to considerable increase in the exposure time in photographing the optical pattern. However, the more serious difficulties are those related to the problem of obtaining a sharp outline of the model, which is associated with the volumetric effect -- formation of shadows around the contour of the model. When the outline is poorly visible, the determination of the true values of stress at the edges as well as at other points of the model is considerably more difficult.

The shadows which are observed along the edges of the model are associated with improper experimental procedure: improper installation of the model and poor machining of the surfaces of the model and apparatus, failure to secure a rectangular section and rounding of the edges (Figure 36).

STAT

However, the volumetric effect may also occur for other reasons. If the model and the apparatus are well machined and the model is correctly installed on the optical bench but the optical arrangement does not assure parallelism of the polarized rays of light, then in investigating models of considerable dimensions we observe shadows along its edges (Figure 37). In the given case, the necessary condition for a sharp image of the edge of the model is that the polarized rays of light in the working portion of the installation must be rigorously parallel.

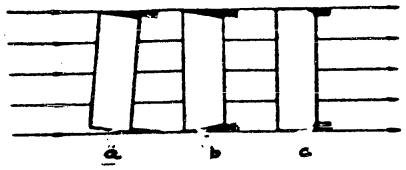

Figure 36. Causes of poor visibility of the model edges: a -- properly machined but improperly installed model; b -- improperly machined edge surface; c -- rounding of edges during improper polishing of the model.

The indicated difficulties may be largely avoided by observing a number of conditions.

1. Use of a point source of light of high intensity. Mercury lamps of intense luminosity, such as lamps SVDSh-250 and SVDSh-1000, may be used.

2. Use of highly transparent materials for preparation of the models. For this purpose the models must be machined from originally very pure materials having a transparency of high order.

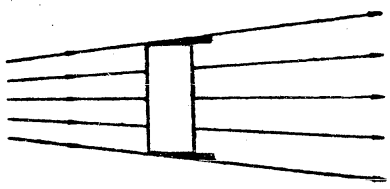

Figure 37. Edge effect caused by lack of parallelism of the rays of polarized light.

3. Carefully adjusted position of the components of the optical system and in particular the condenser (in order to obtain a rigorously parallel beam of light). For this it is necessary that the ratio of the diameter of the light source to the focal length of the condenser be a minimum.

STAT

4. Careful fit of the model dimensions to the contour and thickness of the holder.

5. Assurance of constant thickness of the model over its entire surface. When the model is placed between the polaroids, its surfaces must be rigorously perpendicular to the optical axis of the system and its center must coincide with the axis. Failure to secure a rectangular section of the model and its improper orientation with respect to the direction of polarized light becomes evident first of all in the magnitude of the volumetric effect. This effect may cause experimental errors in the determination of the order of the fringes by as much as 10 percent.

In photographing the optical pattern one must use photographic objectives of high capacity, highly sensitive film of high contrast, developers which tend to increase the contrast in the negatives, use of thin negatives and the proper type of photosensitive paper.

In testing models of resin in a flat container with glass sidewalls the observed optical pattern reveals the fact that the resin adheres to the glass plates of the container. If a lubricant is used, it is displaced at the contact points of the resin model and the glass in the process of deformation. The glass surfaces in contact with the resin are acted upon during the flow of the material. In view of this there are created considerable shearing stresses and this fact causes the appearance of a certain optical effect in the glass plates themselves. This optical effect, which affects the optical pattern, must be taken into account in planning the experiment.

This indicated effect may be reduced to a minimum by using in the container glass plates with a low optical sensitivity. Then we shall not observe any appreciable change in the optical paths within the glass and in certain cases the effect of double refractivity in the glass plates may be neglected.

Thus, it follows from the above that the experimental procedure in the photoplastic method has its characteristic features which distinguish it

basically from the photoelastic method.

4. Photographing of Isochromatics and Isoclinics.

The photographing of optical effects observed with linearly and circularly polarized light with deformed models undergoing viscous flow has its special characteristics.

While in the testing of models by the photoelastic method we photograph a static fringe pattern, in the tests of models of resin we obtain a pattern which varies with time. Therefore, all the experimental procedures must be rigorously planned so that the photographing is carried out at those stages of the experiment which are of greatest interest to the experimenter. Therefore, it is necessary to use photographic apparatus of high quality which is convenient to operate, and photographic materials of high sensitivity so as to reduce the exposure to a minimum.

For this purpose the universal photographic camera (UFK) is quite suitable; it has an "Industar-13" lens with a focal length of 300 mm and receives 9x12 cm film. Even more convenient is a camera with a lens having a focal length of 110 mm. In this instance a removable plate holder is used for photographing with 6x9 cm film.

Distortion of the form of the model and the fringe pattern cannot be tolerated in the polariscope. In order to eliminate this distortion, a proper optical system is used. In order to check the presence of distortions on the ground glass of the camera, a rectangular grid is engraved upon the ground glass which aids in controlling the appearance of distortions.

In using narrow film the most convenient camera is one of the reflex type, especially a "Kino-Exacta" with a "Biotar" (1:2) or "Zenith" lens. In order that the film accommodate the entire optical pattern, it is necessary to make the proper adjustment in magnification.

In order to obtain high contrast negatives with the cameras as described, one must use highly sensitive aerial photographic film, high contrast,

STAT

"Iso-ortho" plates, 6x9 "Isopan" film, or fine grained motion picture film MZ.

In order to obtain color negatives, one must use film of type B. In this instance the light source must be a vertical projection lamp of 500 watts. This yields bright and vivid color photographs, both of the isochromatics and isoclinics.

Good results are obtained by photographing isoclinics with ordinary photographic material (MZ) using a monochromatic source of light. The use of a filter and a slight overexposure aids in increasing the sharpness of the isoclinics in the general fringe pattern.

Isoclinics may be sketched directly on a sheet of paper by utilizing a ground glass camera back or by using a special attachment for projecting the lines on a horizontal surface. In particularly important cases, one must obtain both a photographic record and a recorded sketch. Each record supplements the other and aids in locating with precision the location of isoclinics in various parts of the model. In such cases one must also take into account the particular properties of these lines along free boundaries or the contours in which shear loads are absent.

Development of the negatives in high contrast developers improves the contrast quality of the negatives. However, even with correctly exposed and developed negatives it is possible to improve the contrast by thinning out the negatives or certain parts of it. The use of different grades of paper, partial exposure, equalization during exposure, partial development of selected portions of the positive, various grades of developer, retouching, etc, may successfully aid in improving the quality of the positive.

STAT

CHAPTER IV

VISCOUS PHOTOPLASTICITY

An irreversible change in the form of a body occurs by virtue of viscous and plastic flow. Each of these forms of flow has its specific features which require different modelling procedures. In this chapter we shall consider the basic principles involved in modelling of processes of viscous flow, and we shall devote particular attention to those aspects which differ in the photoelastic and photoplastic methods.

1. Viscous Flow.

As was previously indicated, the basic distinction of viscous flow is the dependence of the deviational portion of the stress tensor upon the rate of deformation and its independence of the magnitude of deformation. This form of flow is common to all amorphous bodies, which include among them the majority of natural and synthetic plastics. It must be remembered, however, that viscous flow also occurs in bodies of crystalline structure. Thus, deformations which follow the law of viscous flow are observed in the case of tectonic flow of rock formations and in the creep of metals. Apparently, deformation in the form of viscous flow is common to all bodies in nature. In crystalline bodies this deformation is as a rule accompanied by structural changes, a fact which complicates considerably the observed relationships.

The kinetic-molecular theory of viscous flow proposed by Eiring [24] and further developed by Frenkel, establishes the relation between the shearing stresses and the rate of shearing deformation:

$$\tau = c_1 \, Arsh \, (c_2 \dot{\gamma}). \qquad (6)$$

where τ is the shearing stress;

$\dot{\gamma}$ is the rate of shearing deformation;

C_1, C_2 are constants which characterize the properties of the substance at a given temperature.

For small shearing stresses, when $C_2\gamma \ll 1$, Arsh $(C_2\gamma)$ may be represented approximately by $C_2\gamma$, and formula (6) assumes the form

$$\tau = c_1 c_2 \dot{\gamma}.$$

In this case, the product $C_1 \cdot C_2$ is the ordinary coefficient of internal friction. This relationship is observed experimentally in liquids and in certain solid bodies, such as resins. As an example of such linear relationship the authors can cite the results obtained by them in experimenting with rosin plasticized by rosin oil. These results are shown in the graph of Figure 38. In the case where $C_2\gamma \geqslant 1$, formula (6) approaches asymptotically the form of

$$\tau = c_1 \ln (2c_2 \dot{\gamma})$$

or

$$\tau = c_0 + c_1 \ln \gamma,$$

where $C_0 = C_1 \ln (2C_2)$.

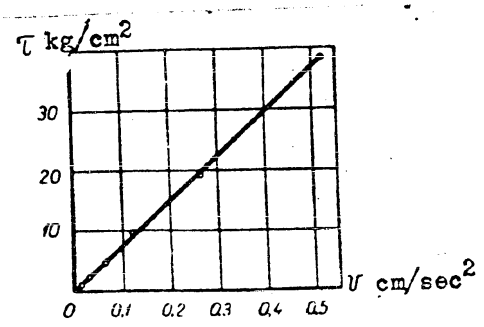

Figure 38. Relationship between the shearing stress and the rate of indentation of the ball in Hepler's consistency apparatus.

Relationships of this type between stresses and the rate of deformation are observed in stabilized processes of creep in metals.

In considering the problems of investigation by means of models, we need not be concerned with the mechanism of different types of change in the form

STAT

of the body. In this instance we are only concerned with the relationship between the tensors of stresses, deformations, and the rates of deformations. These relationships are always determined experimentally.

In the following material we shall consider the flow of material having a viscosity in excess of 10^7 poises. In this case, the internal frictional forces exceed the body forces in most processes which are of interest to us, and consequently the forces due to mass and inertia may be neglected. Under these hypotheses, the relationship between the stress components and the rates of flow may be represented by the following equations up to certain magnitudes of shearing stresses:

$$\begin{aligned}
\sigma_x &= \sigma + 2\eta \frac{\partial v_x}{\partial x}, \; a \\
\sigma_y &= \sigma + 2\eta \frac{\partial v_y}{\partial y}, \; b \\
\sigma_z &= \sigma + 2\eta \frac{\partial v_z}{\partial z}, \; c \\
\tau_{xy} &= \eta \left(\frac{\partial v_x}{\partial y} + \frac{\partial v_y}{\partial x} \right), \; d \\
\tau_{yz} &= \eta \left(\frac{\partial v_y}{\partial z} + \frac{\partial v_z}{\partial y} \right), \; e \\
\tau_{zx} &= \eta \left(\frac{\partial v_z}{\partial x} + \frac{\partial v_x}{\partial z} \right), \; f
\end{aligned} \tag{7}$$

where σ is the average stress equal to $\frac{\sigma_x + \sigma_y + \sigma_z}{3}$;

η is the coefficient of the internal friction.

Together with the differential equations of equilibrium

$$\begin{aligned}
\frac{\partial \sigma_x}{\partial x} + \frac{\partial \tau_{xy}}{\partial y} + \frac{\partial \tau_{xz}}{\partial z} &= 0, \; a \\
\frac{\partial \sigma_y}{\partial y} + \frac{\partial \tau_{yx}}{\partial x} + \frac{\partial \tau_{yz}}{\partial z} &= 0, \; b \\
\frac{\partial \sigma_z}{\partial z} + \frac{\partial \tau_{zx}}{\partial x} + \frac{\partial \tau_{zy}}{\partial y} &= 0, \; c
\end{aligned} \tag{8}$$

and the condition of invariability of volume

$$\frac{\partial v_x}{\partial x} + \frac{\partial v_y}{\partial y} + \frac{\partial v_z}{\partial z} = 0 \tag{9}$$

These equations describe completely the process of flow under the indicated conditions.

If we confine ourselves to consideration of the cases in which the

STAT

coefficient of internal friction η may be assumed to be constant, then substituting the values of the components of the tensor of the stresses (7) in (8), and taking into account equation (9), we shall obtain:

$$\frac{\partial \sigma}{\partial x}+\eta\Delta v_x=0, \quad a$$

$$\frac{\partial \sigma}{\partial y}+\eta\Delta v_y=0, \quad b \qquad (10)$$

$$\frac{\partial \sigma}{\partial z}+\eta\Delta v_z=0. \quad c$$

In these equations, the operator Δ has the usual value

$$\Delta=\frac{\partial^2}{\partial x^2}+\frac{\partial^2}{\partial y^2}+\frac{\partial^2}{\partial z^2}.$$

Differentiating equations (10a) with respect to x, (10b) with respect to y, (10c) with respect to z, adding, and taking into account condition (9), we obtain an equation for σ given by:

$$\Delta\sigma=0. \qquad (11)$$

In the system of equations (10) it is also easy to eliminate σ and to obtain a system of equations only for the rates of flow. Viscous materials whose flow is described by equations (10) have the property of adhering completely to the instrument causing deformation. Thus, the rate of flow of the material undergoing deformation at the surface of the instrument equals its velocity. To consider a particular case, the rate of flow for a stationary instrument surface is equal to zero. This property yields a boundary condition for the rate of flow. The consequence of this is the fact that the normal stresses on the surface of the instrument are equal to the mean stress σ.

In order to prove this assertion, let us consider the stresses at an arbitrary point on the surface of the instrument. Without imposing any limitations on the general nature of the proof, we can assume that the plane tangent to the surface of the instrument at this point is parallel to the plane XOY. Because of the complete adherence, $\frac{\partial v_x}{\partial x}=\frac{\partial v_y}{\partial y}=0$, and on the basis of (9)

$\frac{\partial v_z}{\partial z} = 0$ also, whence we obtain on the basis of (7c) that $\sigma_z = \sigma$.

Equations (9), (10) and (11) are linear, and their use is well developed; this permits us to apply them to the calculations and analysis of many processes of flow.

In spite of this, in those cases where the deformation is characterized by a geometrically complex plastic pattern, the calculations are either too time consuming or impossible to solve in practice.

It must be borne in mind, however, that in reality the coefficient of internal friction η is a function of the average stress σ and the temperature. As was already shown, the dependence of the coefficient of internal friction on the mean stress has the form

$$\eta_{(\sigma)} = \eta_{(0)} e^{-\alpha\sigma}. \qquad (12)$$

According to the authors' experiments to be described below, for resin material α has a value of the order of 0.012 cm^2/kg. Consequently, if at two points in the resin material whose flow process is under study the difference between average stresses is equal to 100 kg/cm, then the viscosity of the material at these two points will differ by a factor of more than three. It is quite apparent that an assumption that the coefficient of internal friction is constant is not applicable under these conditions. If, however, this coefficient η in equation (7) assumes the form of (12), we shall then obtain nonlinear differential equations the solutions of which lead to great mathematical difficulties even for the simplest processes. In view of this, the study of many processes of viscous flow at the present time is only possible in an experimental form. One of the experimental methods may be the photoplastic method.

In modelling various physical processes, particularly when we wish to obtain quantitative results, the questions of similitude are of paramount importance. As is usual in such cases, we shall consider as similar those

processes which possess a similarity in those fields of physical variables which are of interest to us in the process under study. Similarity of the fields of the physical magnitudes is present in the case where one field may be obtained from the other by changing the scales of measurement. In studying the process of viscous flow we are primarily interested in the fields representing rates of flow and stresses. In the following, we shall consider two processes as being similar if the rates of flow and the stresses at corresponding points are proportional. (The coefficients of proportionality for the rates of flow and the stresses are in general different.)

The basic theorem of the theory of similarity, the theorem of Kirpichev-Gukhman, states that: "Two phenomena are similar if they are described by one and the same system of differential equations and if they have similar conditions which determine the sign" [25]. In the case under consideration, among the conditions of similarity which assure constancy of sign we must include geometric similarity and similarity of boundary conditions. The necessity of geometric similarity is obvious and needs no special explanation. Under conditions of surface sticking, similarity of boundary conditions is always present. Let us establish those conditions of similarity which make it possible to describe the processes by a single system of differential equations.

As was already shown, in the study of many processes of viscous flow it is necessary to take into account the dependence of the coefficient of internal friction η upon the average stress. Let us derive the conditions of similarity taking this dependence into account. When the relationship between η and σ is of the form given in (12), the flow process of a very viscous incompressible medium is described by equations (7), (8), (9) and (12). Substituting the value of the coefficient of internal friction (12) in (7), we obtain:

$$\sigma_{ik}=\sigma\delta_{ik}^{*}+\eta_0 e^{\sigma\sigma}\left(\frac{\partial v_i}{\partial x_k}+\frac{\partial v_k}{\partial x_i}\right), \tag{13}$$

* δ_{ik} denotes a tensor with components equal to 1, when i = k, and equal to 0, when i ≠ k.

where i, k assume the values of x, y, z.

The medium undergoing deformation is characterized by two coefficients: $\eta_{(0)}$, the viscosity in the case where the average stress is zero, and α, the parameter indicating the sensitivity of the internal friction to changes in the mean value of stress. The media which we are considering may have various values of $\eta_{(0)}$ and α.

Let us reduce equation (13) to a dimensionless form. In doing this, let us change the scale of the quantities which enter into the equation in such a manner that dimensional values may be canceled in the equation. Let us represent each dimensional quantity in the equation as a product of a constant dimensional value which may be regarded as a new unit of measurement and a dimensionless variable quantity.

Let

$$\begin{aligned} &\sigma_{ik}=\sigma_p\Sigma_{ik};\ v_i=v_pV_i;\ \eta_{(0)}=\eta_p\cdot 1;\\ &\sigma=\sigma_p\Sigma;\qquad x_i=x_pX_i;\ \alpha=\alpha_p\cdot 1. \end{aligned} \tag{14}$$

Here all the letters with the subscript p denote constant dimensional values, and the capital letters denote variable dimensionless quantities. Substituting (14) in (13), we obtain

$$\sigma_p\Sigma_{ik}=\sigma_p\cdot\Sigma\cdot\delta_{ik}+\eta_p e^{-\alpha_p\sigma_p\Sigma}\frac{v_p}{x_p}\left(\frac{\partial V_i}{\partial X_k}+\frac{\partial V_k}{\partial X_i}\right). \tag{15}$$

Dimensional factors in equation (15) may be eliminated provided that

$$\sigma_p=\eta_p\frac{v_p}{x_p}. \tag{16}$$

In addition to that, since the exponent of e is dimensionless,

$$\alpha_p\sigma_p=\kappa. \tag{17}$$

Here k is a dimensionless constant. It can be easily demonstrated that equations (8) and (9) do not impose any conditions on the selection of the scale.

Let us consider two processes which we shall in the following call the 1st and 2nd processes. The quantities which appear in each of these processes will be designated by the appropriate subscript.

The conditions for the 1st process are given by

$$\sigma_{p_1} = \eta_{p_1} \frac{v_{p_1}}{x_{p_1}}, \quad a$$
$$\alpha_{p_1} \sigma_{p_1} = \kappa \quad b \qquad (18)$$

and for the 2nd, given by

$$\sigma_{p_2} = \eta_{p_2} \frac{v_{p_2}}{x_{p_2}}, \quad a$$
$$\alpha_{p_2} \sigma_{p_2} = \kappa \quad b \qquad (19)$$

Both processes are described by the same equations but with different units of measurement. Therefore, the processes are similar.

Let us divide the expressions (18a) by (19a), and (18b) by (19b):

$$\frac{\sigma_{p_1}}{\sigma_{p_2}} = \frac{\eta_{p_1}}{\eta_{p_2}} \cdot \frac{v_{p_1}}{v_{p_2}} \cdot \frac{x_{p_2}}{x_{p_1}}, \quad a$$
$$\frac{\alpha_{p_1}}{\alpha_{p_2}} \cdot \frac{\sigma_{p_1}}{\sigma_{p_2}} = 1. \quad b \qquad (20)$$

The ratios of the analogous values which characterize the 1st and 2nd process are called multipliers of similarity.

Let

$$\frac{\eta_{p_1}}{\eta_{p_2}} = C_\eta; \quad \frac{\alpha_{p_1}}{\alpha_{p_2}} = C_\alpha; \quad \frac{\sigma_{p_1}}{\sigma_{p_2}} = C_\sigma; \quad \frac{v_{p_1}}{v_{p_2}} = C_v;$$
$$\frac{x_{p_1}}{x_{p_2}} = C_x. \qquad (21)$$

By means of these designations the conditions of similarity may be written in the form:

$$C_\sigma = \frac{C_\eta \cdot C_v}{C_x}, \quad a$$
$$C_\alpha \cdot C_\sigma = 1. \quad b \qquad (22)$$

Let us suppose that we must study by means of a model the flow process of a material characterized by the constants $\eta_{(0)}$ and α. We have at our disposal a material for preparation of a model whose constants are $\eta_{(0)1}$ and α_1. The scale of the model is usually selected by considering the experimental means and the means of machining the models and also by taking into account the available equipment. Thus, C_α, C_η and C_x may be considered to be preassigned.

Using equation (22b), we determine

$$C_\tau = \frac{1}{C_\alpha}. \tag{23}$$

On the basis of (22a)

$$C_v = \frac{C_x}{C_\eta C_\alpha}. \tag{24}$$

Since C_v is the ratio of the velocities of flow at the corresponding points of the model and the actual process, it is equal to the ratio of the speeds of the machines causing the loads. At the same time on the basis of (23) all the stresses in the corresponding points of the model will be reduced by a factor of C_α. In an analogous manner we can obtain the ratios between the loads in the model and the actual process which assures similarity in the distribution of stresses. It is useful to note that, as follows from (23) and (24), varying only the speed of the machine and utilizing one material for the models we can determine stress distributions similar to those which exist in the actual material undergoing a process of flow with η and α assuming arbitrary values. If we can neglect in the processes under consideration the effect of the mean value of stress on the coefficient of internal friction, then the condition (22b) vanishes. The distribution of stresses in such processes is always similar and the ratio of stresses at corresponding points is determined by the expression (22a). We must note that in deriving the conditions of similarity we did not take into account the heating of the

material in the flow process and the reduction of the viscosity associated with the increase in temperature. In a number of cases this factor must be taken into account.

2. Optical Anisotropy in Conditions of Viscous Flow.

In Chapter II it was indicated that during viscous flow of certain bodies the initially isotropic medium acquires optical anisotropy. This phenomenon is observed among resins, plastics, glasses and fluids. The effect of double refraction in viscous flow was studied primarily in fluids having a viscosity of the order of 10^{-2} - 10 poises. Ordinarily this effect is called the Maxwell effect. It is established that for molecular fluids and with very small rates of shear the difference between the indexes of refraction of the ordinary and extraordinary rays is proportional to the rate of shear, and the directions of the principal optical axes form an angle of 45° with the plane of shear. In the case where the fluid is a colloidal suspension or a solution of polymers, the relationships become more complicated. Thus, the angle between the major optical axis and the plane of shear decreases with an increasing rate of shear approaching a certain constant. The relationship between the difference of the indexes of refraction and the rate of shear in this case proves to be more complex and is different for different substances. These data yield information on the form of molecules of the polymers and on the degree of their polymerization. Considerable work in this field was accomplished by Tsvetkov and his associates.

Modern molecular theories of Maxwell's effect indicate several possible explanations of the forced anisotropy caused by the presence of the velocity gradient [26]. First of all, this phenomenon may occur if the medium contains molecules which may be polarized anisotropically and have in addition an elongated form. In the absence of deformation in the fluid, these molecules are oriented at random and the fluid is isotropic as a whole. If we now create in the fluid a velocity gradient, it aids in orientation of the

STAT

elongated molecules along certain directions. The directions of orientation of the molecules cease to be equally probable, directions of predominant orientation appear and the fluid acquires optical anisotropy. While the velocity gradient introduces order in the orientation, the thermal movement of the molecules destroys this order continuously. The simultaneous effect of these opposing factors leads to the state where a certain degree of orderliness is established in the liquid, depending on the relationship of the indicated factors. Calculations show that in the cases where the equilibrium state of orderliness is small, the directions of predominant orientation of the major axes of the molecules form an angle of 45° with the direction of the velocity gradient. These directions then become the directions of the major optical axes. Such a mechanism of anisotropy presupposes saturation, since there is a limit value which is attained upon complete orientation. In such a case, the relation between the difference in the indexes of refraction and the velocity gradient may be nearly linear only as long as the degree of orderliness is not great.

The forced anisotropy may also be the consequence of deformation of molecules under the action of stresses. This mechanism may be the predominant one for deformation of polymers.

In addition to that, if the medium contains elongated particles for which the index of refraction differs from the mean index of refraction of the medium, then in the case of ordered orientation of these particles we also obtain anisotropy. We must keep in mind the fact that the latter mechanism of optical anisotropy may exist only in those cases where the particles have dimensions exceeding the wavelength of light.

The theories which consider the indicated mechanisms of Maxwell's effect yield results which only agree qualitatively with the experimental results.

In order to utilize double refraction for the purpose of study of processes of viscous flow we must know those relationships which exist between

STAT

the observed optical effect and the various parameters of the process. Of greatest interest to us is the relationship between the magnitude of forced anisotropy, rate of deformation, and the state of stress.

The authors have made measurements of the difference in the paths of ordinary and extraordinary rays passing through deformed resin consisting of 80 percent rosin and 20 percent of rosin oil. Viscosity of such a material at $t = 20^{\circ}$ is $\eta_{(0)} = 2.5 \times 10^{8}$ poises. Data which characterize the rheological behavior of this resin are shown in Figure 38. The linear relationship between the rate of deformation and the maximum shear stress indicates that in the given case we are dealing with a viscous flow described by equations (7).

Those methods of deforming bodies which are used in similar tests of materials in the method of photoelasticity are naturally not applicable in the case of flow of the medium. In a given case we must have a plane stationary process of flow in which the state of stress and the rates of deformation are known with precision. We have obtained deformation by means of concentric shear, and the substance of this method will become clear from examination of the diagram shown in Figure 39. This method of deforming a body is ordinarily employed also in the study of Maxwell's effect in fluids.

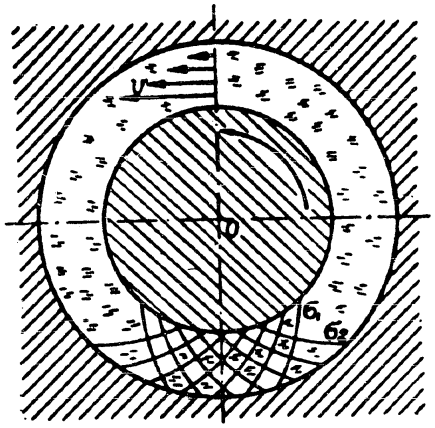

Figure 39. Diagram illustrating deformation by the method of concentric displacement.

Figure 40.

The essential parts of the instrument were two concentric rings, the clearance between which was filled with the material under investigation.

After hardening the material adhered tenaciously to the walls of the rings. Figure 40 shows the rings with the specimen. The outer ring was fixed while the inner ring was subjected to a given torque. During rotation of the inner ring each point of the specimen was deformed by the method of applying simple shear. For any isotropic material subjected to such a deformation, the trajectories of maximum shearing stresses are concentric circles, while trajectories of principal stresses form two families of logarithmic spirals of the following form:

$$r = Ae^{\pm \varphi}$$

(Figure 39). At the same time, the principal stresses are equal in magnitude but have opposite signs.

The maximum shearing stress is determined by the expression

$$\tau_{max} = \tau_{r\varphi} = \frac{M}{2\pi r^2 d}, \qquad (25)$$

where M is the torque;

r is the radius of the point under consideration;

d is the thickness of the specimen.

At the same time the distribution of velocities of flow is established in the specimen by the following equation [27]:

$$v_r = 0; \; v_\varphi = \omega \frac{r_1^2 (r_2^2 - r^2)}{r (r_2^2 - r_1^2)}. \qquad (26)$$

Here v_r and v_φ are respectively the radial and tangential components of the velocity;

ω is the angular velocity of rotation of the inner ring;

r_1 is the radius of the inner ring;

r_2 is the radius of the outer ring;

r is the radius of the point in the specimen being considered.

Consequently, the rate of shear is

$$\dot{\gamma} = \frac{\partial v_\varphi}{\partial r} - \frac{v_\varphi}{r} = -2\omega \frac{r_1^2 r_2^2}{r^2 (r_2^2 - r_1^2)}. \qquad (27)$$

The apparatus with the specimen was placed in the field of the polariscope. The illumination was directed along the axis of the rings. The optical diagram of the experimental setup was shown previously in Figure 29. After a given torque was applied to the inner ring, it began to rotate. The field of view of the specimen became covered with fringes. At some time each fringe shifted from the center to the periphery and the radii of the fringes increased. However, after a certain length of time the fringes became stable and their location was dependent on the magnitude of the applied torque. After this the optical pattern was photographed and the radius was determined from the negative taking into account the change of scale in the photographic process. The corresponding shearing stress was computed by formula (25).

In the given case, just as is done in the photoelastic method, it is convenient to measure the difference in the paths of the rays in terms of the wavelengths of the light being used. In this instance the difference in the paths at the point of the model under consideration is equal to the fringe order. In Figure 41, there is shown a graph illustrating the relationship of the fringe order to the magnitude of the shearing stress for a specimen 1 cm thick. These data were obtained with the yellow line of mercury (λ = 5770/90 Å) at a temperature of 20°C.

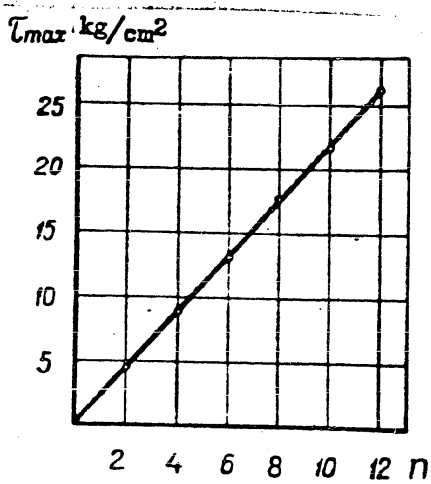

Figure 41. Relationship between the maximum shearing stress and the fringe order for deformation in resin.

The experimental results indicate that a linear relationship exists between the difference in the paths of light and the magnitude of the maximum shearing stress up to a limiting value of at least 26 kg/cm^2. Since in the given case the rate of shear is proportional to the shearing stress, we may speak of proportionality between the difference in the paths of the rays and

the rate of shear. The linear relationship thus obtained makes it possible to characterize the optical sensitivity in terms of the fringe value of the material, just as in the photoelastic method. As we know, the fringe value for the material is measured by the magnitude of the maximum shearing stress which produces a difference of one wavelength of given light, for a path of light traversing a medium 1 cm thick.

According to the definition, the fringe values are calculated according to the formula

$$\tau_0 = \frac{\tau_{max}\, d}{n}, \tag{28}$$

where τ_0 is the fringe value of the material;

n is the order of the fringe.

Or, as applied to the experiments described above,

$$\tau_0 = \frac{M}{2\pi r^2 n}. \tag{29}$$

The fringe value of the material under consideration as obtained from 20 specimens for t = 20°C proved to be equal to 2.2 $\pm$ 0.015 kg/cm for a yellow line of mercury. In all the experiments the isoclinics were situated along the radii forming an angle of 45° with the plane of polarization irrespective of the magnitude and stage of loading. Thus, the optical isoclinics coincide with mechanical isoclinics.

In order to obtain a more detailed explanation of certain peculiarities of the increase in the path difference with time while the specimen is under a constant load, analagous tests were conducted at a lower temperature. The reduction of temperature was accompanied by an increase in viscosity, and as a result the stabilization process of the optical pattern became drawn out. At the same time, the following was observed. At the instant the load is applied, the difference in the paths of the rays attains a certain value in a single increment and then gradually increases under conditions of creep for a

sustained load. At first the rate of increase in the difference of the paths of the rays is large, although it has a finite value. As the flow process develops, the rate of increase of the path difference decreases and approaches zero. When the load is suddenly removed, a certain part of the path difference disappears together with the load, and the remainder decreases over a period of several seconds, and even scores of seconds. If the direction of the load is reversed after it has been applied for a considerable length of time (say, by reversing the direction of applied torque), the path difference is reduced to zero in 1-2 seconds, and then increases having changed its sign.

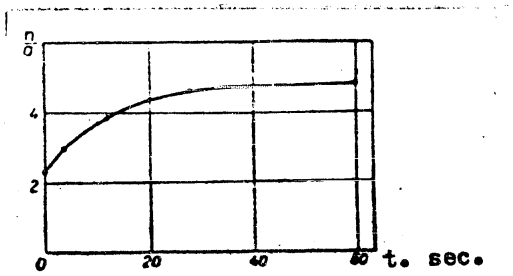

Figure 42. Change in the path difference for rays passing through resin undergoing flow under a constant load (t = 0 at the instant of application of load).

In Figure 42 there is shown a graph illustrating the increase in the difference of the paths of rays with time under a constant load. This experiment was conducted at 14°C. It can be seen from the graph that the final path difference is approximately twice as large as the value corresponding to the instant of application of the load. This must be taken into account in experiments involving models. All the measurements and photographing must be done only after the pattern under observation becomes stabilized.

The indicated peculiarity in the change of difference in the paths of the rays during the flow process is definite evidence of the fact that in the given case optical anisotropy is due basically to the fact that an orderly orientation of molecules comes about as a result of deformation. In connection with this, we must consider the question of the possible magnitude of mechanical anisotropy which occurs in the flow process, since an orderly orientation of molecules must assuredly bring about mechanical anisctropy. In particular, the coefficient of internal friction η must become a tensor quantity.

STAT

As was already indicated, the anisotropy caused by orientation of molecules has a limit which is attained when complete orderliness is achieved. The curve showing the variation of the difference between indexes of refraction has the shape of a saturation curve which approaches asymptotically its limiting value. In this case the proportionality between the difference of the two indexes of refraction and the shearing stress under conditions of viscous flow may exist only as long as the distribution of molecule orientations approaches a uniform distribution. However, according to experimental data this proportionality is well observed up to τ_{max}=26 kg/cm^2 as a limit. This forms a basis for a hypothesis that for shearing stresses within these limits, the degree of orderliness in orientation is quite small. We shall also consider how large is the relative difference between the indexes of refraction of the ordinary and extraordinary rays which is observed in analogous experiments. As can be easily shown, the difference between the indexes of refraction is related to the magnitude of the maximum shearing stress as follows:

$$|n_o - n_e| = \lambda \frac{\tau_{max}}{\tau_o}.$$

Even in the case where the shearing stress τ_{max} = 100 kg/cm^2, when we utilize the previously obtained values of λ and τ_o we arrive at the fact that the difference of the indexes of refraction $|n_o - n_e|$ = 0.0026, which constitutes only 0.175 percent of the mean value of the index of refraction of the material under study. There are reasons to believe that the magnitude of mechanical anisotropy is of the order of the optical one. All this gives us grounds to consider resin as being mechanically an isotropic material under the indicated conditions of deformation (that is, we can consider the coefficient of internal friction as being a scalar quantity).

It proved to be possible to conduct the experiment with concentric shearing displacements only up to 26 kg/cm^2 as a limiting stress, since the specimens fail at stresses exceeding this value. Usually the failure occurred

along spiral lines which coincided fairly well with the trajectories of principal compressive stresses. A photograph of a specimen after failure is shown in Figure 43. It is obvious that the material is destroyed in tension under the action of a tensile stress having a magnitude of the order of 26 kg/cm^2, which then imposes a limit upon the shearing stress that can be used in the method of concentric shearing displacements.

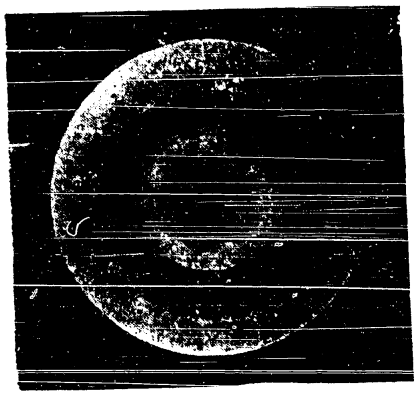

Figure 43. View of a specimen which failed at τ_{max} = 26 kg/cm^2.

One of the special attributes of the deforming process by means of concentric displacements is that the mean stress is equal to zero. On the other hand, the mean stress generally attains considerable values in models which represent various processes of deformation. Thus, there arose the necessity of verifying the observed fringe value for a specimen subjected to hydrostatic pressure varying within wide limits. This proved to be possible to achieve experimentally by forcing the material under investigation through a channel of square cross section. The general view of the apparatus and the diagram of the experimental set-up are shown in Figures 44 and 45.

A slit 5 mm wide was cut through a steel plate 5 mm thick. Optically flat glass plates were bolted to both sides of this plate by means of two other plates and six bolts. The slit, covered on both sides with glass plates, formed a channel. One end of the channel was sealed with an accurately machined aluminum washer and then the channel was filled with the cast material being studied. A die which exerted pressure through the washer had a cross section somewhat smaller than the channel so as to minimize resistance to its movement. The optical arrangement in the experiment was analogous to that shown in Figure 29. Photographs of the optical patterns obtained in

STAT

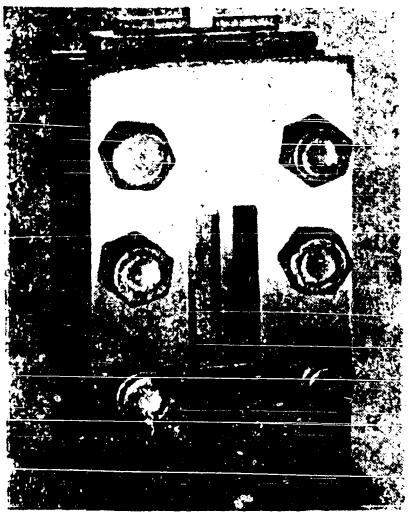

Figure 44. General view of the apparatus used for forcing resin through a channel.

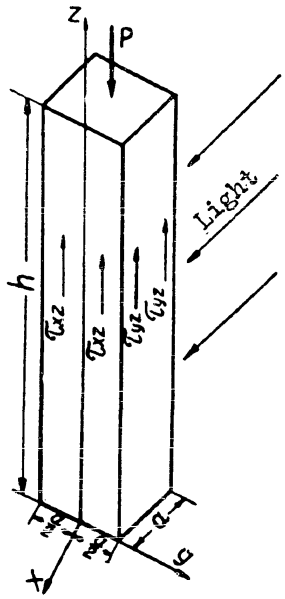

Figure 45. Diagram of the experimental set-up in forcing the material through a channel.

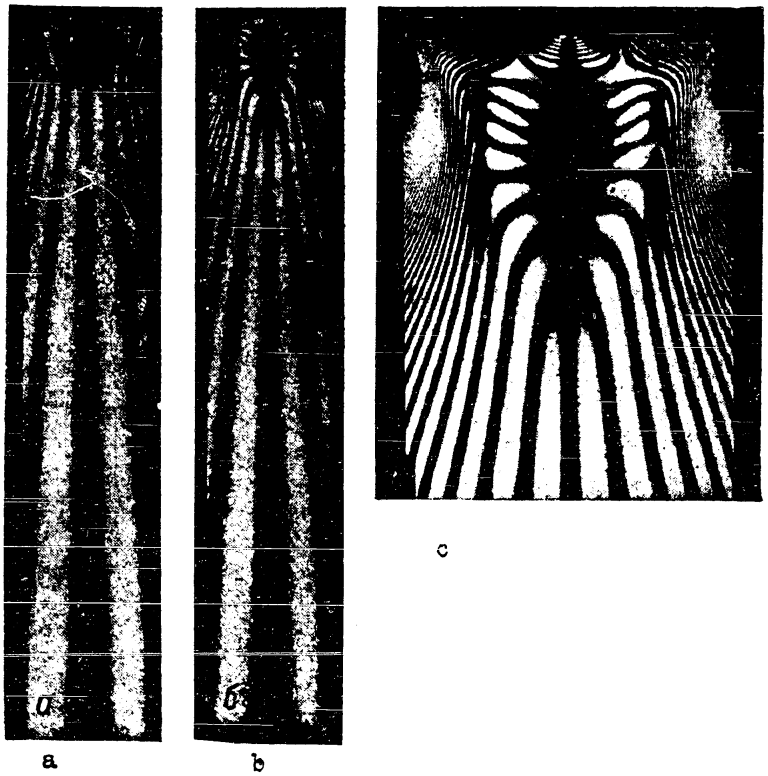

Figure 46. Fringe pattern in forcing resin through channel: a -- at a load of 120 kg; b -- at a load of 150 kg; c -- fringes near the loading washer.

linearly polarized light are shown in Figure 46. The dark line along the axis of symmetry is the neutral line, or the line of zero order. Near the ends, it passes over into an isoclinic with a parameter equal to zero.

When a specimen is forced through the channel, the pressure upon the material from the washer end is equalized by the tangential forces on the sidewalls of the channel. Thus, we have an equality

$$P = 4 \int_0^h \int_0^a \tau_{zy}\, dx\, dz, \tag{30}$$

where P is the force on the washer;

h is the height of the specimen;

a is the side of the square section;

τ_{zy} defines the stress in the plane of the wall of the channel.

Since the material under investigation adheres to the surfaces of the instrument, the latter are the surfaces where the maximum shearing stresses exist (this question will be considered in greater detail in the following pages). Consequently, on the surfaces of the channel $\tau_{zy} = \tau_{max}$. Taking into account the fact that

$$\int_0^a \tau_{zy}\, dx = \int_0^a \tau_{max}\, dx = \tau_0\, n_{(z)},$$

equation (25) may be rewritten in the form

$$P = 4\, \tau_0 \int_0^h n_{(z)}\, dz, \tag{31}$$

where $n_{(z)}$ is the fringe order at the wall of the channel at a section z.

The experimentally determined pressure forces P_E are compared in Table 3 with the forces P_P computed from equation (31). The integration in formula (31) was replaced by a summation, and the variation of $n_{(z)}$ between adjacent experimental points was assumed to be linear. The fringe value used in the calculations was that observed in the experiments involving a concentric shearing displacement.

STAT

Table 3

P_e, Kg	P_p, kg	$P_e - P_p$, kg	$\frac{P_e - P_p}{P_e}$, %	$\frac{P_e - P_p}{P_e}$ % aver.
	40	2	4.8	
	43	-1	-2.4	
42	38	4	9.5	6
	39	3	7.2	
	59	3	4.9	
	56	6	9.7	
62	57	5	8.1	5.7
	62	0	0.0	
	76	9	10.6	
	78	7	8.2	
85	81	4	4.7	8.8
	75	10	11.8	
	119	11	8.5	
	115	15	11.5	
130	114	16	12.3	9.6
	122	8	6.2	

The tabulated data show that the computed pressure, as a rule, is somewhat smaller than that applied to the pressure washer. This can apparently be explained by the fact that a part of the force is resisted by the pressure washer, a fact which we do not take into account. In spite of a certain amount of scatter in the computed values of the force, these results enable us to conclude that the fringe value does not depend upon the mean value of stress.

Let us now consider the optical pattern obtained for the field of view of the channel. At the same time, let us confine our attention to the flow process as it proceeds at sections sufficiently far removed from the ends of the specimen. Experiments have shown that the distorting influence of the ends is only appreciable at distances from the ends not exceeding the width of the channel. When we take into account the effect of the hydrostatic pressure on the viscosity, the flow process is described by equations (7), (8), (9) and (12) (the medium is assumed to be incompressible). As a boundary condition, we assume that the velocity of flow along the side walls of

STAT

the channel is equal to zero.

Let us make two simplifying assumptions. First, let us assume that at all points the flow velocity has a direction parallel to the axis of the channel. Consequently, $V_x = 0$, $V_y = 0$. Whence, utilizing (9), we obtain

$$\frac{\partial V_z}{\partial z} = 0 \quad \text{or} \quad V_z = V_{z(x,y)}$$

Thus, this condition for an incompressible medium is tantamount to the assumption that distribution of flow velocities is one and the same for all transverse sections of the channel.

Secondly, we shall assume that the average stress σ is governed only by the relationship $z \div \sigma = \sigma_{(z)}$

It must be noted that when η is independent of σ, these hypotheses are exact. However, in the case we are considering, both of these conditions can be satisfied only approximately. It is impossible to obtain exact solutions on the basis of the indicated hypotheses.

Substituting expressions (7) and (12) into (8), and taking into account (9) and the indicated hypotheses, we shall obtain

$$\frac{d\sigma_{(z)}}{dz} + \eta_{(0)}\, e^{-a\sigma(z)}\, \Delta V_{z(x,\,y)} = 0. \tag{32}$$

Let us rewrite equation (32) in the form

$$\Delta V_{z(x,\,y)} = -\frac{e^{a\sigma(z)}}{\eta_{(0)}} \cdot \frac{d\sigma_{(z)}}{dz}. \tag{33}$$

In this expression, the left hand side contains only x and y, while the right hand side contains only z. Equality is possible only when each of them is equal to one and the same constant, which we shall denote by B. We shall obtain two equations:

$$\Delta V_{z(x,\,y)} = B; \tag{34}$$

STAT

$$\frac{e^{n\sigma(z)}}{\tau_{k(0)}} \cdot \frac{d\sigma_{(z)}}{dz} = -B. \tag{35}$$

Equation (34) describes the distribution of flow velocities at a transverse section and constitutes Poisson's equation with a constant right hand side. By virtue of the adherence of the medium to the apparatus and utilizing the notation of Figure 45, the boundary conditions may be written as follows:

$$V_{(o,y)} = V_{(-a,\ y)} = V_{(x,\ -a/2)} = V_{(x,\ a/2)} = 0$$

The solution of equation (34) for the indicated boundary conditions has the following form [28]:

$$V_z = B\left[\frac{4a^2}{\pi^3}\sum_{m=0}^{\infty}\frac{sh(2m+1)\pi\frac{y}{a}\cdot\sin(2m+1)\pi\frac{x}{a}}{(1+2m)^3\cdot ch(2m+1)\frac{\pi}{2}} - \frac{1}{2}x(a-x)\right]. \tag{36}$$

The series contained in this expression can be differentiated and integrated term by term, and as a consequence, by utilizing (7) we can obtain the magnitude of the shearing stress τ_{yz}:

$$\tau_{yz} = \eta\frac{\partial V_z}{\partial y} = \frac{4\eta Ba}{\pi^2}\sum_{m=0}^{\infty}\frac{sh(2m+1)\pi\frac{y}{a}\cdot\sin(2m+1)\pi\frac{x}{a}}{(1+2m)^2 ch(2m+1)\frac{\pi}{2}}. \tag{37}$$

Taking into account the fact that $\frac{\partial v_x}{\partial x} = \frac{\partial v_y}{\partial y} = \frac{\partial v_z}{\partial z} = 0$, and utilizing (7a, 7b, 7c), we obtain $\sigma_x = \sigma_y = \sigma_z = \sigma$; consequently, the trajectories of the quasi-principal stresses* at any section x = const (planes perpendicular to the direction of incident light) form an angle of 45° with the axis z and

* Quasi-principal stresses are computed as principal stress from the components in a selected plane, for instance in a plane perpendicular to the direction of incident light. Thus, in the case under consideration they are computed by the formula

$$(\sigma_1, \sigma_2)_x = \frac{\sigma_y + \sigma_z}{2} \pm \frac{1}{2}\sqrt{(\sigma_y - \sigma_z)^2 + 4\tau^2_{yz}}$$

τ_{yz} is a quasi-maximum shearing stress. This conclusion is verified experimentally: the entire field of view of the channel, except for small regions near the ends, is occupied by an isoclinic having a parameter equal to 45°. Thus, the fringe order is given by the expression

$$n = \frac{1}{\tau_0} \int_0^a \tau_{yz}\, dx. \tag{38}$$

Substituting into (38) the value of τ_{yz} from (37), we obtain

$$n = \frac{8B\eta a^3}{\tau_0 \pi^3} \sum_{m=0}^{\infty} \frac{sh(2m+1)\pi \frac{y}{a}}{(2m+1)^3 ch(2m+1)\frac{\pi}{2}}. \tag{39}$$

Let us establish the relationship of the fringe order to z. In order to do this, let us integrate equation (35), and as a result we obtain

$$\frac{e^{a\sigma(z)}}{a\eta_{(0)}} = C - Bz.$$

The constant of integration C we shall determine on the basis of the following boundary conditions: σ = 0, at the exit from the channel, with z = 0. Thus

$$\frac{e^{a\sigma(z)}}{a\eta_0} = \frac{1}{\eta_0} - Bz. \tag{40}$$

But since $\frac{e^{a\sigma(z)}}{\eta_{(0)}} = \frac{1}{\eta_i}$,

it follows that

$$\eta_i = \frac{\eta_{(0)}}{1 - aB\eta_{(0)}z}. \tag{41}$$

Substituting the value of η' from (41) into (39), we obtain finally the equation of the fringes in the field of view of the channel:

$$n_{(y,z)} = \frac{8Ba^2\eta_{(0)}}{\pi^3\tau_0(1 - Ba\eta_{(0)}z)} \sum_{m=0}^{\infty} \frac{sh(2m+1)\pi \frac{y}{a}}{(2m+1)^3 ch(2m+1)\frac{\pi}{2}}. \tag{42}$$

As regards the constant B, its sign and magnitude may be obtained from (36). It is convenient to express B in terms of the volume of the material passing through the transverse section of the channel in a unit of time. In this case, we have on the basis of (31)

$$B = \frac{28{,}4U}{a^4}, \qquad (43)$$

where U is the volume of the medium passing through the transverse section of the channel in a unit of time;

a is the side of the square cross section.

Let us compare the experimentally obtained distribution of fringe order in the field of view of the channel with that based on expression (42).

Figure 47 shows a graph of the fringe order distribution at a transverse section of the channel. The solid line shows the ratio of the fringe order at a given point to the order of the fringe at the edge of the channel for the same section based on expression (42). The same graph also shows the values of this ratio obtained experimentally. The experimental points were obtained for various sections whose distances from the ends were equal to or exceeded 5 mm. The overall length of the specimens in this instance was 30-35 mm. It follows from examination of the graph that the distribution of the fringe orders at a transverse section of the specimen in its middle portion agrees satisfactorily with the computed values.

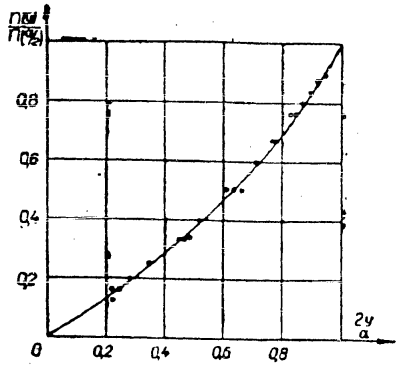

Figure 47. Relative order of the fringe at a transverse section of a square channel.

Let us consider the distribution of the order of fringes in the field of the view of the channel along its longitudinal sections. Since the distributions of the order of fringes at various transverse sections proved to be

similar, in the given case we may confine ourselves to a comparison of computed and experimental values along a single arbitrarily selected section. In view of the fact that the order of the fringes is highest at the edges of the channel, the results we obtain are most accurate when we examine the distribution of the order of the fringes precisely along the edges of the specimen. For this purpose, let us solve the expression (42) for z and present it in the form

$$z = z_o - \frac{A}{n_{(z)}}; \tag{44}$$

here

$$z_0 = \frac{1}{B\alpha\tau_{i(0)}}; \tag{45}$$

$$A = \frac{8a^2}{\alpha\tau_0\pi^3}\sum_{m=0}^{\infty}\frac{th(2m+1)\frac{\pi}{2}}{(2m+1)^3} = \frac{a^2}{4\alpha\tau_0}. \tag{46}$$

Thus, z_o is a constant of the given experiment which depends upon the flow velocity, and A is a general constant of all experiments. The values of z_o and A may be computed by the method of least squares from the experimental values of z and $n_{(z)}$. The values of A determined in this fashion from the data of 10 experiments proved to be concordant. If we substitute the computed values of z_o and A in (44), we shall find that the values of z computed by this formula agree well with the experimental values. Figure 48 shows the results of such a comparison.

As can be seen from the graph, a systematic divergence of experimental and computed results is first observed in the vicinity of the pressure washer at a distance from it equal approximately to the width of the channel. This is quite natural since the calculations cited do not take into account those distortions in the flow process which are introduced by the proximity of the pressure washer.

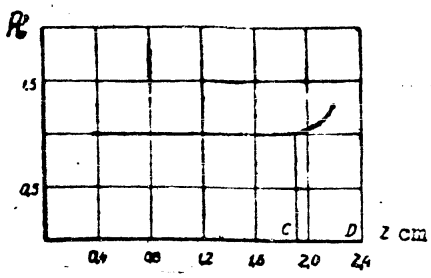

Figure 43. Ratio of the observed order of the fringe in the field of view of the channel to that computed by formula (44). Point D corresponds to the location of the washer; CD is equal to the length of the side of the square section of the channel.

The constant A may be computed more simply by means of two experimental points. Knowing the order of fringes at two points n_1 and n_2 and the distance $z_2 - z_1$ between them, we obtain on the basis of (44)

$$A_{1,2} = \frac{(z_2 - z_1)n_1 n_2}{n_2 - n_1} \qquad (47)$$

Utilizing the experimental values τ_0 and A, and taking into account (46), we can compute the value of α. According to the data of the series of experiments where rosin oil was used as a plasticizer, $\alpha = 0.012 \pm 0.0005$ cm^2/kg. The thermodynamic theory of viscosity gives the value of α in the form of $\alpha = \frac{V}{RT}$ /7/. If we assume that the molecular weight of the rosin oil is 342 and its density is 1.09, we obtain from this theory for a temperature of 20°C, a value of α of 0.0127 cm^2/kg. Agreement with the experimentally obtained value may be considered to be good. This result confirms anew the correctness of our calculations, and also confirms the validity of a previous deduction regarding the independence of the optical sensitivity of the resin from the hydrostatic pressure and the related change in viscosity.

On the whole, the results of our experiments with pressing of resin through a channel furnished convincing evidence that it is possible to conduct a quantitative study of the state of stress of a material undergoing viscous flow by the method of photoplasticity.

3. Certain Special Features of the Problem of Plane Models Undergoing Viscous Flow.

Results of investigations cited in the previous paragraphs show that the basic relationships between the state of stress and the optical anisotropy in conditions of viscous flow of resin, are analogous to the corresponding

relationships for the case of elastic deformation in amorphous bodies. Thus, many of the experimental procedures and methods of reduction of data which are used in the photoelastic methods may also be used in the models designed for the study of viscous flow.

However, the use of models under conditions of viscous flow also has a number of substantial special features. The process of plane flow, in particular, gives rise to a number of considerable difficulties.

Let us consider this question in more detail. A plane process, as we know, is one in which the variable physical quantities which characterize it are independent of one of its coordinates (in our case these variables are the flow velocities and the stresses). In the use of models in the photoelastic method a plane state of stress is realized relatively simply. For this purpose we select a model having a thickness which is small compared with its other dimensions and apply the load only along the periphery of the model. In accordance with Saint Venant's principle, the variation of stresses across the thickness decreases rapidly with the distance from the loaded periphery and the state of stress approaches a state of plane stress. It may be noted that the state of plane stress is approximated more closely as the thickness of the model decreases.

The basic difference in the modelling technique for processes involving an irreversible change in the form of the bodies is the fact that in the great majority of such processes it is impossible to confine the application of forces to the periphery of the specimen. (In the following discussion all surfaces of the apparatus touching the specimen which are parallel to the direction of incident light will be termed as peripheral surfaces, and those which are perpendicular to the direction of light will be termed side surfaces.)

Let us consider this special feature of the modelling of a process involving plane plastic deformation by means of a model representing extrusion. The diagram illustrating the process is shown in Figure 49. The specimen is

illuminated in the direction of axis of x. The unavoidable presence of side surfaces 1 and 2 and the frictional forces on them, leads to the creation of shearing stresses τ_{zx} in the deformed body. From symmetry it is clear that the shearing stresses at corresponding points of sides 1 and 2 are equal in magnitude but are opposite in sign, while at the plane of symmetry for x = 0, the shearing stresses τ_{zx} are equal to zero. Consequently, these shearing stresses vary in the direction of incident light and the flow process is definitely not a plane one. It must be noted that, as was previously mentioned, the shearing stresses τ_{xz} and τ_{zx} do not reveal their presence through an optical effect in the present case; however, their presence causes the distribution of all other components of the stress tensor to be different from a plane one, and the optical pattern obtained experimentally does not correspond to the case of a plane problem. In the final analysis the distortion in the plane flow is due to the frictional forces on the side surfaces of the apparatus.

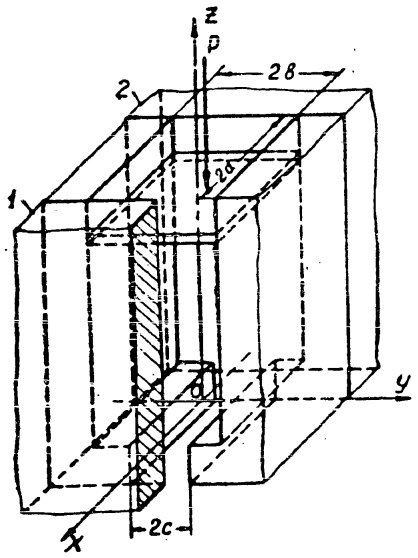

Figure 49. Diagram illustrating modelling of an extrusion process.

In order that the state of deformation in the three-dimensional process approximate a plane state of deformation, it is obviously necessary to reduce the effect of the side walls on the distribution of flow of velocities and stresses. This can be achieved in two ways. One method consists of reduction of the friction on the side walls to a minimum by utilizing a lubricant. However, this method is not very useful with models made of resin since transparent lubricants dissolve the resin. In addition to that, it becomes impossible to take friction into account in the presence of a lubricant. Another

method consists of increasing the dimension of the model in the direction of the incident light making this dimension considerably larger than its other dimensions. From Figure 49 it can be seen that as we increase the ratio d/b the effect of the side walls on the process of flow decreases compared with the edge effect of the periphery, and as a result the process approaches a state of plane deformation. It is true, of course, that the distortion of the plane process near the walls occurs for all thicknesses of the model; however, the optical pattern being observed is a result of the cumulative difference in the path of rays in the direction of the light across the entire thickness of the model, and, therefore, it reflects the averaged values of stresses in the specimen. This averaged value approaches the value of stress which we obtain in the plane flow process, as the thickness of the model increases. More precisely, the observed optical pattern approaches the pattern which corresponds to a plane flow process. Increasing the thickness of the model relative to its other dimensions enables us, in principle, to achieve any degree of approximation of a plane flow process; however, experimental difficulties arise increasingly when this is done. In a number of cases it proves to be possible to evaluate the degree of approximation of the process to a plane flow process and by these means to select rationally the thickness of the model.

Let us consider the conditions of approximation of the process to a plane flow process for the case of extrusion of resin through a channel of rectangular cross section. The experimental setup is analogous to that shown in Figure 45. First of all, let us establish how the ratio of the tangential forces acting on the side and peripheral surfaces of the channel varies with its cross section and with the ratio d/b. Here d is the dimension of the cross section of the channel in the direction of incident light and b is the width of the channel. The flow of the material in the immediate vicinity of the pressure washer is analogous both for the peripheral walls and the side walls.

STAT

The latter becomes clear if we take into account that the material under consideration adheres both to all the walls of the container and to the surface of the washer whose velocity naturally is constant with respect to all the walls. In view of the fact that the shearing stresses are functions of the flow velocities, these stresses on all the walls approach one and the same value as we approach the pressure washer, and depend only upon the distance to the pressure washer. This question is treated in greater detail in section 4 of the present chapter.

Let us designate the tangential force acting upon a unit length of wall by t with a subscript indicating the width of the wall under consideration. Corresponding to this definition, we have:

$$t_a = \int_0^a \tau_{yz}\,dx\,; \qquad t_b = \int_0^b \tau_{xz}\,dy. \tag{48}$$

Since in the vicinity of the pressure washer τ_{yz} and τ_{xz} approach one and the same value which depends only upon the distance from the pressure washer, the ratio of the tangential forces acting upon the peripheral surfaces to the tangential forces acting upon all the walls will approach the following magnitude in the vicinity of the pressure washer:

$$x_1 = \frac{d}{b + d} \tag{49}$$

This ratio will decrease with the distance from the pressure washer.

As was previously shown, there is observed a distribution of velocities satisfying the following equation at distances from the pressure washer which exceed the width of the channel:

$$\Delta v_z = \text{const}. \tag{50}$$

Utilizing the solution of this equation for a rectangular region of an experimental case cited in section 2, we can obtain the values x_2 for sections at some distance from the pressure washer. The computation of x_2 may be carried

STAT

out by the following approximate formula with a sufficient degree of precision for the condition that $d/b \geqslant 2$.

$$x_3 = \frac{1 - 0{,}633\,\frac{b}{d}}{1 - 0{,}106\,\frac{b}{d}}. \tag{51}$$

The values of x_1 and x_2 obtained constitute two limiting values of x. All the observed values of x must be confined between them.

Experimental confirmation of these deductions based on the optical patterns for d/b = 2 proved their correctness. In Figure 50 there is shown a graph of values of x_1 and x_2 computed from formulae (49) and (51). As can be seen from the graph, all possible values of x for arbitrary values of d/b are situated within relatively narrow limits, which enables us to estimate approximately that part of tangential forces which acts upon the side walls.

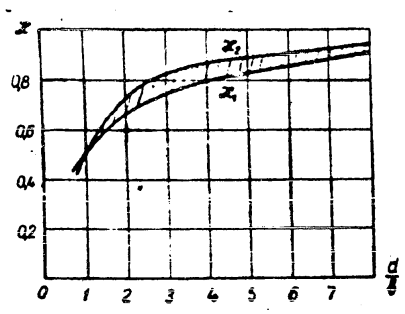

Figure. 50

However, the value of x still does not give us a complete understanding of the degree of approximation of the process to a plane flow process. In order to have a complete understanding we must also know to what extent the observed optical pattern of the entire field of the model corresponds to a plane process. As was already shown, a plane distribution of velocities of flow, and consequently, of the stresses, will only exist in the absence of frictional forces on the side walls. In that case, using the designations of Figure 49, the velocity of flow in the channel will depend only upon y. Let us seek a solution of equation (50) in the form $v_z = v_{z(y)}$ for boundary conditions

$$v\left(\frac{b}{2}\right) = v\left(-\frac{b}{2}\right) = 0.$$

As can be easily demonstrated, the following expression is such a solution:

$$v_z = k\left[y^2 - \left(\frac{b}{2}\right)^2\right],$$

where k is a constant;

b is the width of the channel.

Utilizing (7), we shall obtain the components of the tensor of the stresses:

$$\sigma_x = \sigma_y = \sigma_z = \sigma,$$
$$\tau_{xy} = \tau_{xz} = 0,$$
$$\tau_{yz} = 2k\eta y;$$

Consequently, $\tau_{yz} = \tau_{max}$. At the same time, the fringe order is determined by the expression

$$n = \frac{2k\eta dy}{\tau_o}. \qquad (52)$$

Since all the quantities in the right hand side of this expression other than y do not depend upon y, it follows that for any transverse cross section of the channel in the case of plane flow process the fringe order n is proportional to y, and the fringes will be uniformly spaced. In Figure 51, are shown photographs of fringes obtained for channels with various ratios of d/b.

It can be seen in all the photographs that the fringe order increases in the direction away from the outer section of the channel and toward the pressure washer. As was previously established, this is due to the fact that the coefficient of internal friction increases with hydrostatic pressure. As regards the distribution of fringe orders at an arbitrary transverse section, it proved to be similar for each given ratio of d/b except for those sections which are situated close to the end of the specimen. As the ratio d/b increases, the distribution of fringes at a transverse section approaches a uniform one.

In Figure 52 are shown graphs of the ratio $\frac{n(y)}{n(b)}$ obtained from the data

STAT

of the optical patterns with indicated ratios of d/b. Each of these curves was obtained on the basis of measurements of four photographs.

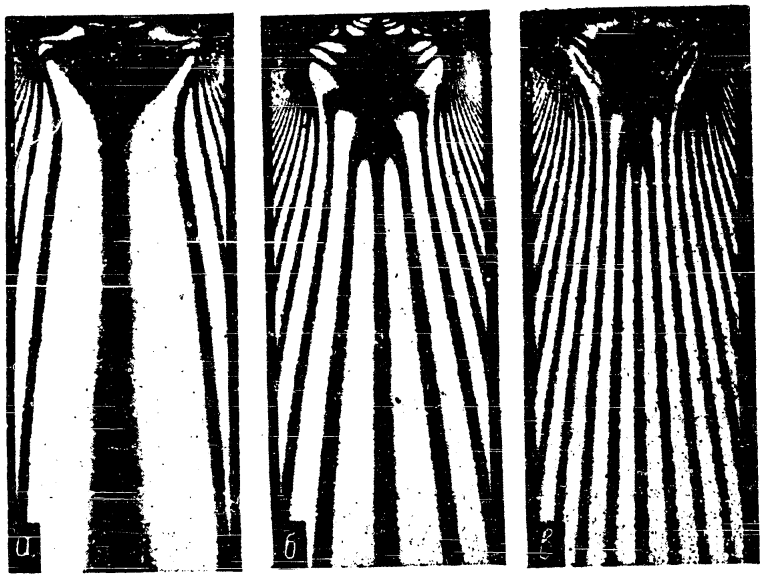

a b c

Figure 51. Fringe patterns in the field of the channels for various ratios of sides of cross sections: a -- channel with a section of 5 x 10 mm ($\frac{d}{b} = \frac{1}{2}$); b -- 5 x 5 mm ($\frac{d}{b} = 1$); c -- 10 x 5 mm ($\frac{d}{b} = 2$).

It is clear from the examination of the curves that when we use thin models (d/b being small) the distribution of fringes is far from that corresponding to a plane flow process. As the ratio d/b increases the distribution of fringes in the field of the channel approaches the plane case and only approaches closely the distribution corresponding to a plane process for $\frac{d}{b} = 2$.

These data certainly do not exhaust the problem of the rational selection of the model thickness and the evaluation of the errors introduced by the presence of frictional forces on the side walls. However, in modelling various technological processes involving deformation they may be utilized for purposes of orientation. Thus, in modelling the process of extrusion we can let the width of the container equal the width of the channel as a first approximation. Obviously, the selection of the model thickness depends upon the requirements which specify the precision of the results.

STAT

In our opinion, in order to obtain reliable quantitative results, the thickness of the model must be at least twice as large as its other dimensions. For a qualitative study of the distribution of stresses we may limit the thickness of the model to approximately its width.

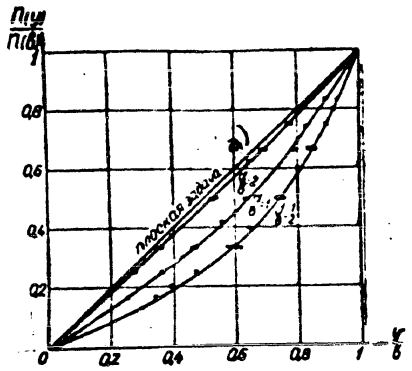

Legend: a) plane problem

Figure 52. Relative fringe order at a transverse section of channels for various ratios of sides of section (the straight line corresponds to fringe order in the case of a plane flow process.

4. The Simplest Plane Problems of Viscous Flow.

One of the ways in which it is possible to determine whether the photoplastic method is applicable to the study of processes of viscous flow is to compare the computed and experimental values of one and the same problem. Certain similar comparisons were made in the preceding paragraphs of this chapter. In the following material there is given the solution of four plane problems of viscous flow and a comparison of these solutions with experimental results obtained by the photoplastic method is presented. All the problems cited are solved for the case in which the coefficient of internal friction may be presumed to be independent of the value of mean stress.

Problem 1. A Viscous Medium Compressed Between Flat Parallel Plates. This process is shown diagramatically in Figure 53.

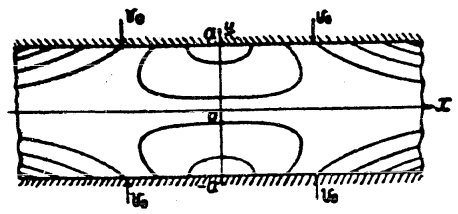

Figure 53. Diagram of compression of material between flat plates and the computed fringe pattern.

Let the plates move towards each other with a velocity v_o each, and let

the distance between them (the thickness of the strip) at the given moment equal 2a. Because of the adherence of the material, the velocity of the layers of the medium adjacent to the surfaces of the plates is equal to the velocity of the plates.

Thus, the boundary conditions for the flow velocities may be written in the form:

$$v_x = 0,\ v_y = \pm v_0 \text{ при } y = \pm a.$$

Let us differentiate equation (10a) with respect to y, equation (10b) with respect to x and let us subtract the latter from the former. After cancelling the term η we shall obtain

$$\frac{\partial}{\partial y}\Delta v_x - \frac{\partial}{\partial x}\Delta v_y = 0. \tag{53}$$

Let us express v_y in the form $v_y = v_y(y)$. (54)

Then on the basis of (9)

$$v_x = -x\frac{dv_y}{dy} + f(y). \tag{55}$$

Here f(y) is an arbitrary function of y.

Since along the axis of symmetry $v_x = 0$ for $x = 0$, $f(y) = 0$

$$v_x = -x\frac{dv_y}{dy}. \tag{56}$$

Substituting (54) in (56) into (53) and cancelling x, we obtain

$$\frac{d^4 v_y}{dy^4} = 0. \tag{57}$$

A general solution of this equation has the form

$$v_y = C_0 + C_1 y = C_2 y^2 + \tilde{C}_3 y^3. \tag{58}$$

The process of flow is symmetrical with respect to axis of x and consequently, $C_0 = 0$, $C_2 = 0$. On the basis of boundary conditions

$$C_1 = \frac{3v_0}{2a}\,;\; C_3 = -\frac{v_0}{2a^3}\,. \tag{59}$$

Thus, taking into account (59) and (56), we shall obtain the following flow velocities:

$$v_x = \frac{3v_0}{2a}\left(1 - \frac{y^2}{a^2}\right)x, \quad a$$

$$v_y = -\frac{3v_0}{2a}\left(y - \frac{y^3}{3a^2}\right). \quad b \tag{60}$$

Utilizing (7), we obtain the components of the stress tensor:

$$\sigma_x = \sigma + \frac{3v_0\eta}{a}\left(1 - \frac{y^2}{a^2}\right), \quad a$$

$$\sigma_y = \sigma - \frac{3v_0\eta}{a}\left(1 - \frac{y^2}{a^2}\right), \quad b$$

$$\tau_{xy} = \frac{3v_0\eta}{a^3}xy. \quad c \tag{61}$$

Applying the known formula of the theory of plane stress

$$\tau_{max} = \frac{1}{2}\sqrt{(\sigma_x - \sigma_y)^2 + 4\tau^2_{xy}}$$

we obtain in the given case

$$\tau_{max} = \frac{3v_0\eta}{a^3}\sqrt{(a^2 - y^2)^2 + x^2y^2}\,. \tag{62}$$

Consequently, the equation of the family of fringes will have the form

$$n = \frac{3v_0\eta d}{a^3\tau_0}\sqrt{(a^2 - y^2)^2 + x^2y^2}\,. \tag{63}$$

None of the quantities in the expression (63) which are in the term preceding the radical depend upon x and y; therefore, using the designation

$$\frac{a^3\tau_0}{3v_0\eta d} = k,$$

equation (63) may be written in the form

$$k^2 n^2 = (a^2 - y^2)^2 + x^2 y^2. \tag{64}$$

The family of fringes corresponding to equation (64) is shown in Figure 53. In Figure 54 is shown a photograph of the fringes obtained at the instant when the specimen is compressed 7 mm with the thickness of the layer in the direction of light being equal to 40 mm. The agreement between the experimental and computed fringe patterns may be considered satisfactory.

Figure 54. Fringe pattern for compression between flat parallel plates.

Problem 2. Flow of viscous material in an angle formed by two mutually perpendicular walls, one of which is moving in its plane. The diagram of the process is shown in Figure 55.

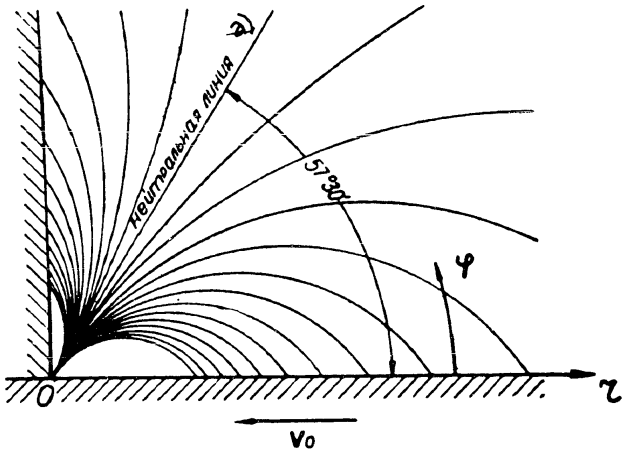

Figure 55. Diagram of the process and the family of fringes for flow through an angle.
Legend: a) neutral line

Both walls are assumed to be infinite. The flow in dihedral angles formed by the pressure washer and walls of a container which serves to represent the process of extrusion, is analogous in character.

In order to solve this problem it is most convenient to use a polar system of coordinates in which the equations analogous to equations (10) for the case of plane problem have the following form [27]:

$$\frac{\partial \sigma}{\partial r} + \eta\left(\frac{\partial^2 v_r}{\partial r^2} + \frac{1}{r^2}\frac{\partial^2 v_r}{\partial \varphi^2} + \frac{1}{r}\frac{\partial v_r}{\partial r} - \frac{2}{r^2}\frac{\partial v_\varphi}{\partial \varphi} - \frac{v_\varphi}{r^2}\right) = 0;$$

$$\frac{1}{r}\frac{\partial \sigma}{\partial \varphi} + \eta\left(\frac{\partial^2 v_\varphi}{\partial r^2} + \frac{1}{r^2}\frac{\partial^2 v_\varphi}{\partial \varphi^2} + \frac{1}{r}\frac{\partial v_\varphi}{\partial r} + \frac{2}{r^2}\frac{\partial v_r}{\partial \varphi} - \frac{v_\varphi}{r^2}\right) = 0. \qquad (65)$$

Here v_r and v_φ are respectively the radial and tangential components of velocity.

The equation of incompressibility in the given case is transformed into

$$\frac{\partial v_r}{\partial r} + \frac{1}{r}\frac{\partial v_\varphi}{\partial \varphi} + \frac{v_r}{r} = 0. \qquad (66)$$

The components of the stress tensor are defined by the expressions

$$\sigma_r = \sigma + 2\eta\frac{\partial v_r}{\partial r};$$

$$\sigma_\varphi = \sigma + 2\eta\left(\frac{1}{r}\frac{\partial v_\varphi}{\partial \varphi} + \frac{v_r}{r}\right);$$

$$\tau_{r\varphi} = \eta\left(\frac{1}{r}\frac{\partial v_r}{\partial \varphi} + \frac{\partial v_\varphi}{\partial r} - \frac{v_\varphi}{r}\right). \qquad (67)$$

Let the wall a be fixed and let the wall b move in its plane with the velocity v_0. Taking into account the adherence of the material to the walls and utilizing the designations indicated in Figure 55, let us set down the boundary conditions in the following manner:

for $\varphi = 0 \qquad v_\varphi = 0, \qquad v_r = v_0;$

for $\varphi = \frac{\pi}{2} \qquad v_\varphi = 0, \qquad v_r = 0.$

Let us seek solutions for v_r and v_φ in the form:

$$v_r = v_r(\varphi); \qquad v_\varphi = v_\varphi(\varphi). \qquad (68)$$

Under conditions (68) equations (65) will be rewritten in the following manner:

$$\frac{\partial \sigma}{\partial r} + \frac{\eta}{r^2}\left(\frac{d^2 v_r}{d\varphi^2} - 2\frac{dv_\varphi}{d\varphi} - v_r\right) = 0, \quad a$$

$$\frac{\partial \sigma}{\partial \varphi} + \frac{\eta}{r}\left(\frac{d^2 v_\varphi}{d\varphi^2} + 2\frac{dv_r}{d\varphi} - v_\varphi\right) = 0. \quad b \tag{69}$$

Equation (66) may be written as follows when we take into account (68):

$$\frac{dv_\varphi}{d\varphi} + v_r = 0. \tag{70}$$

After differentiating equation (69a) with respect to φ, and equation (69b) with respect to r, the latter is subtracted from the former. After cancelling η and taking into account equation (70), we obtain the following ordinary differential equation for v_φ

$$\frac{d^4 v_\varphi}{d\varphi^4} + 2\frac{d^2 v_\varphi}{d\varphi^2} + v_\varphi = 0, \tag{71}$$

whose general solution will be given by

$$v_\varphi = A\sin\varphi + B\cos\varphi + \varphi(C\sin\varphi + D\cos\varphi). \tag{72}$$

where A, B, C, D are arbitrary constants. On the basis of the boundary conditions the constants are determined with respect to sign:

$$A = -1.675\ v_0; \quad B = 0; \quad C = 1.062\ v_0; \quad D = 0.675\ v_0.$$

Thus, the velocity components are determined by the expressions:

$$v_\varphi = v_0[-1{,}675\sin\varphi + \varphi(1{,}062\sin\varphi + 0{,}675\cos\varphi)];$$
$$v_r = v_0[\cos\varphi - 1{,}062\sin\varphi - \varphi(1{,}062\cos\varphi - 0{,}675\sin\varphi)]. \tag{73}$$

The components of the stress tensor may be expressed in the following form on the basis of (67):

$$\sigma_r = \sigma;$$
$$\sigma_\varphi = \sigma;$$
$$\tau_{r\varphi} = 2{,}52\eta\frac{v_0}{r}\sin(\varphi - 57°30'). \tag{74}$$

Since $\sigma_r = \sigma_\varphi$, $\tau_{r\varphi} = \tau_{max}$, and consequently, the trajectories of the maximum shearing stresses may be represented by radii and circular arcs, and the trajectories of the principal stresses form two families of logarithmic spirals of the form $r = ce^{\pm\varphi}$.

Substituting (74) into (28), we obtain an equation of the family of fringes

$$n = \frac{2{,}52\eta d}{\tau_0} \cdot \frac{v_0}{r} \sin(\varphi - 57°30'). \tag{75}$$

Thus, the fringes represent circular arcs which are tangent at the origin of coordinates to the straight line $\varphi = 57°30'$. This straight line is a neutral line, since shearing stresses are absent from it. Figure 55 shows a family of fringes corresponding to formula (75). In Figure 56 there is shown a photograph of fringes obtained experimentally for an angle formed by the wall of the container and the pressure washer.

Comparison of Figures 55 and 56 shows that the computed fringe pattern near the vertex of the angle coincides satisfactorily with the experimental one. These patterns diverge more and more with the distance from the vertex of the angle since the computations were carried out for the case in which the extent of the medium in the radial direction is large compared with the distances from the vertex to the points in the model being considered.

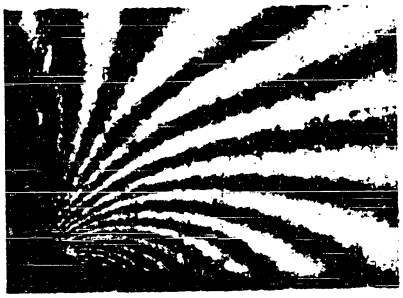

Figure 56. Fringe pattern in the angle formed by the wall of the container and the pressure washer.

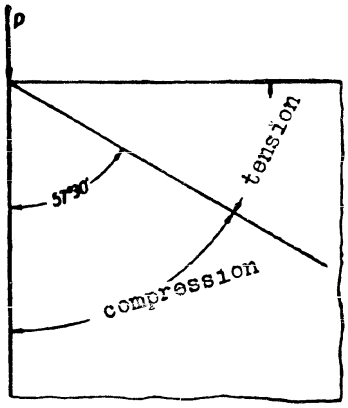

Figure 57. A schematic diagram of load applied to an elastic plate for which the family of fringes is the same as that for flow of a viscous medium through an angle (Figure 55).

STAT

It is interesting to note that the fringe pattern obtained is completely analogous to that which we observe in loading the vertex of a right angle of an elastic plate with a concentrated load in the direction of one of the sides of the angle. A schematic diagram of such a loading is shown in Figure 57. Although the fringe patterns in both of these cases are the same, still the states of stress are basically different. In the case of the loaded elastic plate the trajectories of the principal stresses coincide with the radii and circular arcs, and the trajectories of the maximum shearing stresses form logarithmic spirals. Thus, the trajectories of the principal and maximum shearing stresses interchange their loci in the transition of one process to the other.

Problem 3. Flow of a Viscous Medium through a Narrow Slot. A schematic diagram of the process is shown in Figure 58.

The problem may be stated in the following manner. The volume bounded by planes z = 0 and z = d (situated at the top in Figure 58), is filled with a viscous medium which flows through a narrow slot of infinitesimal width, the slot being situated along the axis of z. The flow process is a plane one and the flow velocity does not depend on z. The boundary conditions are:

for $$\varphi = \pm \frac{\pi}{2} \quad v_r = 0, v_\varphi = 0.$$

It is natural to suppose that the flow velocity in this case is directed along the radii. Therefore we shall seek a solution in the form:

$$v_\varphi = 0; \quad v_r = \frac{\Phi(\varphi)}{r}. \tag{76}$$

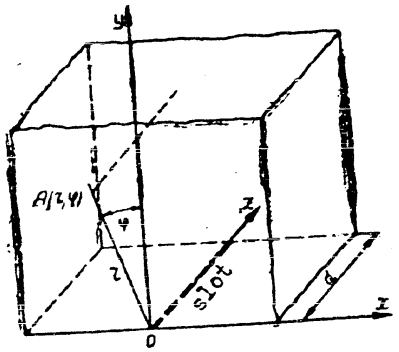

Figure 58.

Substituting values of v_r and v_φ in the form of (76) into (65), we obtain:

$$\frac{\partial \sigma}{\partial r} + \frac{\eta}{r^3}\frac{d^3\Phi}{d\varphi} = 0, \quad a$$
$$\frac{\partial \sigma}{\partial \varphi} + \frac{2\eta}{r^2}\frac{d\Phi}{d\varphi} = 0. \quad b \qquad (77)$$

Let us differentiate equation (77a) with respect to φ and equation (77b) with respect to r and subtract the latter from the former. After cancelling η we shall obtain the following equation for Φ:

$$\frac{d^3\Phi}{d\varphi^3} + 4\frac{d\Phi}{d\varphi} = 0, \qquad (78)$$

whose solution has the form

$$\Phi = A\cos 2\varphi + B\sin 2\varphi + C.$$

Since the process must be symmetrical with respect to axis of x, B = 0. On the basis of the boundary conditions C = A.

Thus, the flow velocity may be written in the form

$$v_r = \frac{2A\cos^2\varphi}{r}. \qquad (79)$$

The constant A may be expressed in terms of the volume of the medium which flows through the opening in a unit of time, $A = \frac{U}{\pi}$. Here U is the volume of the medium flowing through the opening in a unit of time. Utilizing (79) and (67) we shall compute the components of the stress tensor:

$$\sigma_r = \sigma + \frac{4U\eta}{\pi}\cdot\frac{\cos^2\varphi}{r^3}; \quad a$$
$$\sigma_\varphi = \sigma - \frac{4U\eta}{\pi}\cdot\frac{\cos^2\varphi}{r^3}; \quad b$$
$$\tau_{r\varphi} = \frac{2U\eta}{\pi}\cdot\frac{\sin^2\varphi}{r^3}. \quad c \qquad (80)$$

On the basis of (80) the maximum shearing stress will be equal to

$$\tau_{max} = \frac{4U\eta}{\pi}\cdot\frac{\cos\varphi}{r^2}. \qquad (81)$$

Consequently, the equation of the fringes has the form

$$n = \frac{4U\eta d}{\pi\tau_0} \cdot \frac{\cos\varphi}{r^2}. \qquad (82)$$

This equation is an equation of a family of similar ovals which are tangent to the straight line $\varphi = \frac{\pi}{2}$ at the origin of coordinates. The dimensions of these ovals vary inversely as the square roots of the fringe order.

As indicated by the statement of the problem, in comparing the computed values with experimental data we may expect them to coincide only at points sufficiently far removed from the opening. More precisely, the distance of the points from the slot must be considerably larger than the width of this slot. As will be seen from the following exposition, the fringe pattern is close to that described by equation (82) even for points which are situated at a distance of twice the width of the slot measured from the middle of the slot.

Moreover, as was already repeatedly indicated, in order to assure that the flow process be plane it is necessary that the tangential forces on the side walls be eliminated. In practice this is impossible to achieve. However, at distances from the slot which are small in comparison with the distance between the side walls ($d > r$), the relative effect of the side walls on the flow process is small and the observed optical pattern must be close to that yielded by equation (82). In Figure 59 there is shown a photograph of fringes obtained in extruding resin through a slot 0.8 mm wide. The distance between side walls in this experiment was equal to 28 mm.

In Figure 60 there is shown for purpose of comparison a computed fringe pattern. With the exception of the region in the immediate vicinity of the slot the coincidence of these two patterns must be accepted as satisfactory.

Problem 4. Flow of medium through a slot of finite width. This problem differs from the preceding one in that in this case we do not neglect the dimensions of the slot and thus obtain a description of the flow process in the immediate vicinity of the slot as well. As a consequence, we may obtain

Figure 59

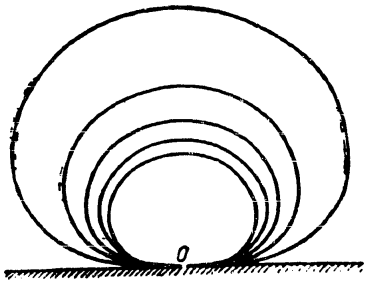

Figure 60

certain new results which are applicable to actual processes.

Let us formulate the problem in the following manner. The space occupied by the viscous medium is divided by a thin plane wall into two parts. The wall has a slot of a constant width. The pressures in the medium on either side of the wall are constant at infinitely large distances from the wall but are different in magnitude. In view of the difference of the pressures the medium is extruded through the slot and at the same time it adheres to the wall. In the entire volume filled by this medium a certain field of flow velocities and stresses is established. The process is assumed to be a plane one. The computed pattern for the plane xy is shown in Figure 61. The purpose of the problem is to determine the indicated fields of velocities and stresses.

As will be seen from the following, this problem can be solved most conveniently by means of elliptical coordinates. To simplify the calculations the width of the slot is assumed to equal to 2.

Let us consider the process in the coordinate system given by λ and μ, which are related to the coordinates x and y through the equations:

$$x^2 = (1 + \lambda)(1 + \mu);$$
$$y^2 = -\lambda\mu. \qquad (83)$$

Excluding from equations (83) the term μ, we obtain the following

equation of one family of coordinate lines:

$$\frac{x^2}{1+\lambda}+\frac{y^2}{\lambda}=1. \qquad (84)$$

As λ varies from 0 to ∞ each of the lines of this family represents an ellipse with foci at points (- 1.0) and (1.0); λ is equal to the square of the minor semiaxis.

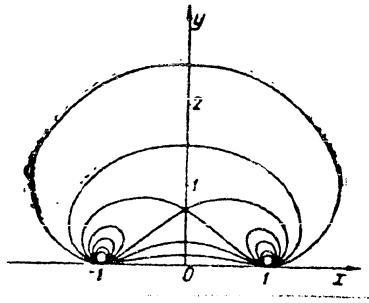

Figure 61. Computed diagram of the lines indicating equal maximum shearing stresses for a plane flow of viscous medium through a slot.

In an analogous manner having excluded λ from (84), we obtain the second family of coordinate lines in the form

$$\frac{x^2}{1+\mu}+\frac{y^2}{\mu}=1. \qquad (85)$$

As μ varies from -1 to 0 this equation forms a family of hyperbolae having foci at precisely the same points, (-1.0) and (1.0). In the present case the absolute value of μ is equal to the square of the distance to the vertex of the corresponding hyperbola from the nearest focus.

It is easy to demonstrate that the families of ellipses and hyperbolae being considered are mutually orthogonal. Through each point of the plane xy there passes one ellipse of the family (84) and one hyperbola of the family (85). Thus, the quantities λ and μ determine with respect to sign any point within the limits of a single quadrant of the plane and these quantities may be considered as the coordinates of the point.

Let us note that for these coordinates the equation of the axis of x between points -1 and 1 will be $\lambda = 0$, the equation of the axis of x beyond the limits of the indicated interval will be $-\mu = 0$, and the equation of the axis of y will be $\mu = -1$.

In utilizing the curvilinear coordinates a very important role is played

by Lamé's coordinates, which represent arbitrary arcs of a coordinate line for a given coordinate. For the chosen system of coordinates, Lamé's coefficients have the form:

$$H_\lambda = \frac{ds_\mu}{d\lambda} = \frac{1}{2}\sqrt{\frac{\lambda-\mu}{(1+\lambda)\lambda}},$$

$$H_\mu = \frac{ds_\lambda}{d\mu} = \frac{1}{2}\sqrt{\frac{\lambda-\mu}{-(1+\mu)\mu}}. \tag{86}$$

The components of the stress tensor may be presented in the following form analogously to the preceding cases:

$$\sigma_\lambda = \sigma + \sigma'_\lambda,$$
$$\sigma_\mu = \sigma + \sigma'_\mu,$$
$$\tau_{\lambda\mu} = \tau'_{\lambda\mu}, \tag{87}$$

where in accordance with the theory of orthogonal curvilinear coordinates (see for example [32]) the components of the "viscous" tensor of the stresses for coordinates λ and μ are given by the following expressions:

$$\sigma'_\lambda = \frac{2\eta}{H_\lambda}\left(\frac{\partial v_\lambda}{\partial\lambda} + \frac{v_\mu}{H_\mu}\cdot\frac{\partial H_\lambda}{\partial\mu}\right);$$

$$\sigma'_\mu = \frac{2\eta}{H_\mu}\left(\frac{\partial v_\mu}{\partial\mu} + \frac{v_\lambda}{H_\lambda}\cdot\frac{\partial H_\mu}{\partial\lambda}\right);$$

$$\tau'_{\lambda\mu} = \frac{1}{H_\mu}\cdot\frac{\partial v_\lambda}{\partial\mu} + \frac{1}{H_\lambda}\cdot\frac{\partial v_\mu}{\partial\lambda} -$$
$$- \frac{1}{H_\lambda H_\mu}\left(v_\lambda\frac{\partial H_\lambda}{\partial\mu} + v_\mu\cdot\frac{\partial H_\mu}{\partial\lambda}\right). \tag{88}$$

Equations of motion of a very viscous incompressible medium in the same coordinates may be written in the form:

$$\frac{\partial\sigma}{\partial\lambda} = \left(\sigma'_\mu - \sigma'_\lambda\right)\frac{\partial \ln H_\mu}{\partial\lambda} - \frac{\partial\sigma'_\lambda}{\partial\lambda} -$$
$$- \frac{H_\lambda}{H_\mu}\cdot\frac{\partial\tau_{\lambda\mu}}{\partial\mu} - \frac{2}{H_\mu}\cdot\frac{\partial H_\lambda}{\partial\mu}\tau'_{\lambda\mu};$$

$$\frac{\partial \sigma}{\partial \mu} = (\sigma'_\lambda - \sigma'_\mu)\frac{\partial \ln H_\lambda}{\partial \mu} - \frac{\partial \sigma'_\mu}{\partial \mu} - \frac{H_\mu}{H_\lambda}\cdot\frac{\partial \tau'_{\lambda\mu}}{\partial \lambda} - \frac{2}{H_\lambda}\cdot\frac{\partial H_\mu}{\partial \lambda}\tau'_{\lambda\mu}. \tag{89}$$

Here σ'_λ, σ'_μ, $\tau_{\lambda\mu}$ are determined by expressions (88).

The equation of continuity in the given case has the form:

$$\frac{\partial}{\partial \lambda}(H_\mu v_\lambda) + \frac{\partial}{\partial \mu}(H_\lambda v_\mu) = 0. \tag{90}$$

Let us now consider the boundary conditions. The condition of adherence to the wall is expressed in the following manner:

$$\text{for } \mu = 0 \quad v_\lambda = 0 \quad \text{and} \quad v_\mu = 0 \tag{91}$$

The conditions at infinity may be obtained from the following considerations. At infinity ($\lambda \longrightarrow \infty$) the distribution of flow velocities into a slot of a finite width must become the same as the distribution which occurs for a flow through a slot of infinitesimal width (79). Let us seek a solution for the velocities of flow in the form:

$$v_\lambda = v_\lambda(\lambda, \mu); \; v_\mu = 0. \tag{92}$$

In other words, let us assume that the lines of flow coincide with the hyperbolae of the family (85).

Substituting (92) into (90), we obtain

$$\frac{\partial}{\partial \lambda}(H_\mu v_\lambda) = 0,$$

whence, taking into account the value of H_μ from (86),

$$v_\lambda = f(\mu)\sqrt{\frac{-(1+\mu)\mu}{\lambda - \mu}}. \tag{93}$$

Here $f(\mu)$ is an arbitrary function of μ and is determined by the condition of transition at infinity of equation (93) into (79).

As can be easily verified, the latter is achieved for

$$f(\mu) = A \frac{\mu}{\sqrt{-(1+\mu)\mu}},$$

where A is an arbitrary constant.

Thus, if the supposition (92) is correct, the velocity of flow has the form

$$v_\lambda = \frac{A\mu}{\sqrt{\lambda - \mu}}. \tag{94}$$

The velocity of flow in form (94) satisfies both equation (90) and the boundary conditions. It remains to be shown that it also satisfies equations (89).

In order to do this, and substituting (94) into (88) we obtain:

$$\begin{aligned} \sigma'_\lambda &= -2A\eta \frac{\mu\sqrt{(1+\lambda)\lambda}}{(\lambda-\mu)^2}; \\ \sigma'_\mu &= 2A\eta \frac{\mu\sqrt{(1+\lambda)\lambda}}{(\lambda-\mu)^2}; \\ \tau'_{\lambda\mu} &= 2A\eta \frac{\lambda\sqrt{-(1+\mu)\mu}}{(\lambda-\mu)^2}. \end{aligned} \tag{95}$$

Further, taking into account (86) and (95), equations (89) may be rewritten in the form:

$$\begin{aligned} \frac{\partial\sigma}{\partial\lambda} &= A\eta \frac{\lambda(1+\mu)+\mu(1+\lambda)}{(\lambda-\mu)^2\sqrt{(1+\lambda)\lambda}}, \quad a \\ \frac{\partial\sigma}{\partial\mu} &= -2A\eta \frac{\sqrt{(1+\lambda)\lambda}}{(\lambda-\mu)^2}. \quad b \end{aligned} \tag{96}$$

Differentiating the first of these with respect to μ and the second with respect to λ, and subtracting the latter from the former on both the right and left sides we obtain 0 identically. Thus, the flow velocity in the form (94) is actually the solution being sought. The constant A is related to the volume of the medium passing through the slot of unit length in a unit of time

by the relationship

$$A = \frac{2U}{\pi}. \tag{97}$$

Let us compute the value of the average stress σ.

From the conditions of the problem it is apparent that the value of is determined only with a precision given by an arbitrary increment, since the flow of the medium is caused by a difference in the mean stresses (difference in pressures) on both sides of the wall. From the expression (96b) it follows that the mean pressure along the slot (for $\lambda = 0$) is constant. Let us assume that it is equal to zero. Then the mean stress may be obtained by integrating (96a) with respect to λ from 0 to λ.

$$\sigma = -\frac{4U\eta}{\pi}\frac{\sqrt{(1+\lambda)\lambda}}{(\lambda-\mu)}. \tag{98}$$

As $\lambda \longrightarrow \infty$ the mean stress approaches a constant independently of the value of μ:

$$\sigma_\infty = -\frac{4U\eta}{\pi}. \tag{98a}$$

The latter defines the relationship between the volume of the medium passing through a slot of unit length in a unit of time, and the difference in the pressures.

Further, when we substitute (95) into (87) with (97) taken into account, the components of the stress tensor finally assume the form:

$$\sigma_\lambda = \mp\frac{4U\eta}{\pi}\frac{\lambda\sqrt{(1+\lambda)\lambda}}{(\lambda-\mu)^2};$$

$$\sigma_\mu = \mp\frac{4U\eta}{\pi}\frac{(\lambda-2\mu)\sqrt{(1+\lambda)\lambda}}{(\lambda-\mu)^2};$$

$$\tau_{\lambda\mu} = \pm\frac{4U\eta}{\pi}\frac{\lambda\sqrt{-(1+\mu)\mu}}{(\lambda-\mu)^2}. \tag{99}$$

Here the upper sign corresponds to that portion of the region from which the medium flows, while the lower sign corresponds to the region which receives

the flow.

Let us pause briefly and consider the bounds of applicability of the computed data thus obtained. The solution obtained is precise for the case where the medium occupies the entire volume on both sides of the wall. Let us immediately note that such a character of flow is impossible to achieve in the vicinity of the slot in that part of the region which receives the flow. Indeed, it is apparent from (99) that the normal stresses attain arbitrarily large values on the wall ($\mu = 0$) near the points which define the slot ($\lambda \longrightarrow 0$).

However, a given medium can support without failure only certain tensile stresses. Thus, in that part of semi-infinite volume which receives the flow in the vicinity of the points forming the boundary of the slot, there must occur a failure of bond between the medium and the wall.

We are usually interested in the case where the medium occupies the space on one side of the wall and flows freely through a slot. In the initial stage of the flow process when the medium occupies the space only on one side of the wall, the solution we obtained is exact. After a certain amount of flow of the medium through the slot has taken place, the effect of that portion of the medium on the distribution of velocities and stresses in the semi-infinite medium on one side of the wall is quite small and in practice its effect is the same as in the initial stage.

Let us evaluate the applicability of these results to those cases in which the medium undergoing deformation occupies a finite space. In the process just considered the major portion of the energy of deformation is expended near the slot. In this region we also find the largest changes in stresses. In Figure 62 are shown the graphs illustrating the changes in the ratios

$$\frac{\sigma}{\sigma_-}, \frac{\sigma_y}{\sigma_-} \text{ and } \frac{\tau_{max}}{\sigma_-}$$

along the y axis obtained on the basis of (98) and (99). From these graphs it is seen that at distances from the slot equal to twice its width the stresses are already close to their limiting value, and at distances of the order of 3 widths the mean value of stress is 98 percent of σ_∞.

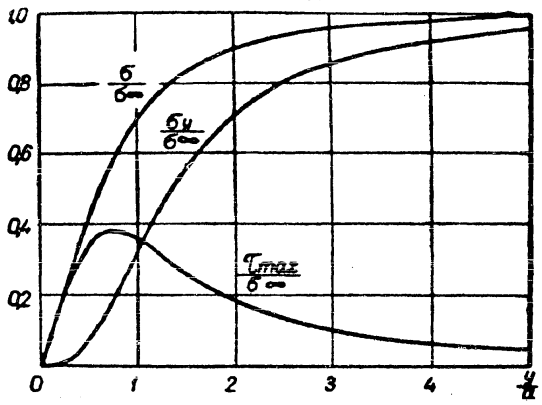

Figure 62. Graphs of the ratios of σ, σ_y and τ_{max} to the difference between stress at infinity and that at the slot for a flow of viscous medium through a slot having a width 2a.

Thus, the results obtained on the distribution of stresses for the case of flow of medium through a slot are applicable to concrete examples of processes of flow of a viscous medium in those cases where the dimensions of the space occupied by the medium undergoing deformation exceed the width of the slot by a factor of 3-5.

On the basis of the data on the state of stress given by (99) we can obtain a computed fringe pattern. The order of the fringes n can be given in the following manner on the basis of (99), (28) and (98a) as it was done in the preceding problems:

$$n = \frac{\sigma_\infty d}{\tau_0} \cdot \frac{\sqrt{-\mu\lambda}}{(\lambda-\mu)^{3/2}},$$

or, adopting Cartesian coordinates, by:

$$n = \sigma_\infty \frac{d}{\tau_0} \cdot \frac{y}{[(x^2+y^2-1)^2-4y^2]^{1/4}}. \qquad (100)$$

Figure 63 shows an experimentally obtained fringe pattern for a slot width of 5 mm and a thickness of layer d of 28 mm. As can be seen from the

direct comparison with the family of fringes (Figure 61) corresponding to equation (100), the computed fringe pattern coincides quite satisfactorily with the experimental one.

In all the problems cited, one can compute the trajectories of principal stresses and isoclinics. Along with fringes it would be possible to compare computed and observed isoclinics; however, isochromatics are always obtained experimentally with greater precision than isoclinics and this assures more reliable conclusions regarding their correspondence to computed values.

The material considered in this discussion confirms the previously expressed opinion that it is possible to solve plane problems in viscous flow by experimental means. As regards the solution of three-dimensional problems, this question belongs to the future. There are reasons for believing that the method utilizing scattered light is quite applicable in this case. The photoplastic method even now may be applied in a number of cases for checking the theoretical solutions of three-dimensional problems (for instance, as it was done in considering the flow through a channel).

Figure 63.

5. Singularities of the State of Stress at the Periphery of the Model and Some of the Methods of Reduction of Experimental Data.

As was previously shown, we may obtain by the method of photoplasticity the fringe order and the inclination of the trajectories of the principal stresses in the entire model field. Knowing the fringe value for a given material, it is possible to determine the state of stress at any point of the

STAT

model on the basis of these data by one of the methods known in photoelasticity. In this instance the following formulae of the theory of plane stress distribution are generally utilized:

$$\tau_{xy} = \tau_{max} \cdot \sin 2\theta; \tag{101}$$

$$\sigma_y = \sigma_x \pm 2\tau_{max} \cdot \cos 2\theta; \tag{102}$$

$$\frac{\partial \sigma_x}{\partial x} + \frac{\partial \tau_{xy}}{\partial y} = 0; \tag{103}$$

$$\frac{\partial \sigma_y}{\partial y} + \frac{\partial \tau_{yx}}{\partial x} = 0. \tag{104}$$

The shearing stress τ_{xy} is determined on the basis of formulae (28) and (101) according to the data on the fringe order and parameter of the isoclinics from the expression

$$\tau_{xy} = \frac{\tau_0 n}{d} \sin 2\theta. \tag{105}$$

As regards the normal stresses, they are determined from the optical data only with a precision given by a constant term in view of the fact that the anisotropy is independent of the mean stress. For a complete determination of the normal stresses we must have in addition to the fringe and isoclinic patterns the value of one of the normal stresses at some point of the model.

Let us assume that we know σ_x at the point (x_o, y_o); then on the basis of equation (103) σ_x is determined by the following expression at any point on the straight line $y = y_o$:

$$\sigma_x (x, y_0) = \sigma_x (x_0, y_0) - \int_{x_0}^{x} \frac{\partial \tau_{xy}}{\partial y} \, dx. \tag{106}$$

Here $\sigma_x (x_o, y_o)$ is σ_x at the starting point having coordinates (x_o, y_o).

The integration in this formula is performed along the straight line $y = y_o$.

In order to compute the integral in the formula (106) we may proceed in the following manner. Let us divide an interval of the straight line $y = y_o$ by the points x_1, x_2 ... into small increments Δx_i, where $\Delta x_i = x_i - x_{i-1}$. Through the mid-points of the increments of the straight line let us pass straight lines parallel to the y axis. Let us select on each of these straight lines two points close to each other and situated on both sides of the straight line $y = y_o$. Utilizing the experimental values of n and θ, let us compute the values of τ_{xy} at these points. Dividing the difference between the values of τ_{xy} at the indicated points by the distance between them, we shall obtain the approximate value of the derivative $\frac{\partial \tau_{xy}}{\partial y}$ in the interval Δx_i. Further, after we substitute a summation sign for the integral sign in (106) this formula may be approximated by the following one:

$$\sigma_x(x_n, y_0) = \sigma_x(x_0, y_0) - \sum_{i=1}^{n} \frac{\Delta \tau_{xy_i}}{\Delta x_i} \Delta y_i. \tag{107}$$

Knowing σ_x, σ_y is computed at the same point by means of formula (102).

In order to compute σ_y along any straight line parallel to the y axis, an analogous formula will be given by

$$\sigma_y(x_0, y_n) = \sigma_y(x_0, y_0) - \sum_{i=1}^{n} \frac{\Delta \tau_{yx_i}}{\Delta x_i} \Delta x_i. \tag{108}$$

In the calculations we may take as the starting point any point where the state of stress is known. By keeping track of the movements along intervals of straight lines parallel to the coordinate axes, it is possible to reach any point in the model and thus to determine the magnitude of the components of the stress tensor in the entire model field. Any point along the free boundary of the specimen undergoing deformation may serve as the point of the model where the stresses are known. In view of the fact that external

loads are absent along the free boundary, the boundary itself becomes a trajectory of one of the principal stresses. The second principal stress whose trajectory is perpendicular to the free boundary is equal to zero at each point of that boundary. Thus, the parameter of isoclinics which enters a free boundary is equal to the slope of the tangent of the boundary at the point of entry. Since the maximum shearing stress is equal to half of the sum of the principal stresses, it follows that the principal stress acting in the direction of the tangent to the boundary is determined by the following expression and the known order of the fringe:

$$\sigma_2 = 2\tau_0 n. \tag{109}$$

The method of computation which was briefly described here is called the method of differences of tangential stresses. It is described in greater detail in a monograph "Photoelasticity" by M. Frocht [12].

When we study flow processes by means of photoplastic models, we must keep in mind certain singular attributes of a state of stress at the boundaries of the model in contact with the apparatus. We have already indicated in this chapter that for a viscous flow the boundaries of the apparatus are the trajectories of maximum shearing stresses. In view of the importance of this assertion, we shall show that it follows from equations (7), (9) and the condition of adherence. Without limiting the general nature of this proof, let us select for simplicity the coordinate axes in such a manner that the tangent to the boundary at the point under consideration is parallel to the x axis. In this case, in view of the adherence of the medium to the apparatus, $\frac{\partial v_x}{\partial x} = 0$ at the point on the boundary. On the basis of (9) $\frac{\partial v_y}{\partial y} = 0$ at the same point. Utilizing formulae (7a) and (7b), we obtain $\sigma_x = \sigma_y = \sigma$. Applying the formula of the theory of plane state of stress

$$\operatorname{tg} 2\theta = \frac{2\tau_{xy}}{\sigma_x - \sigma_y},$$

we obtain the value of θ

$$\operatorname{tg} 2\theta = \infty, \quad \theta = \pm 45^{\circ}.$$

Thus, at all points where the deformed medium is in contact with the apparatus the trajectories of the principal stresses form an angle of 45° with the periphery of the apparatus, and the periphery itself constitutes a trajectory of the maximum shearing stresses. The utilization of this property of the state of stress along the boundary facilitates considerably in many cases the reduction of experimental data and increases the precision of the results. In planning the reduction of experimental data, it often proves to be expedient to compute first of all the state of stress along the boundary. For the points on the boundary the state of stress can be conveniently expressed by the stress normal to the boundary and the shearing stress acting in the plane tangent to the boundary. This shearing stress being a maximum shearing stress is computed by formula (28).

Let us show how the normal stress along the boundary may be calculated by integrating along the boundary. In order to do this, let us express all the components of the stress tensors in terms of the average stress, maximum shearing stress and the angle θ

$$\sigma_x = \sigma + \tau_{max} \cdot \cos 2\theta; \tag{110}$$

$$\sigma_y = \sigma - \tau_{max} \cdot \cos 2\theta; \tag{111}$$

$$\tau_{xy} = \tau_{max} \cdot \sin 2\theta. \tag{112}$$

Substituting expressions (110) and (112) into (103), we obtain

$$\frac{\partial \sigma}{\partial x} - 2\tau_{max} \cdot \sin 2\theta \cdot \frac{\partial \theta}{\partial x} + \cos 2\theta \cdot \frac{\partial \tau_{max}}{\partial x} +$$

$$+ 2\tau_{max} \cdot \cos 2\theta \cdot \frac{\partial \theta}{\partial y} + \frac{\partial \tau_{max}}{\partial y} \cdot \sin 2\theta = 0. \qquad (113)$$

If the x axis is chosen as a line parallel to the tangent to the boundary at the point under consideration, then $\theta = 45^\circ$, $\sin 2\theta = 1$, $\cos 2\theta = 0$, the derivative with respect to x coincides with the derivative along the arc of the boundary, the derivative with respect to y will be equal to the derivative along the normal to the boundary, and $\frac{\partial \theta}{\partial x}$ will be the curvature to the boundary (Figure 64).

Taking these relationships into account and expressing the curvature in terms of the radius of curvature, we shall obtain

$$\frac{\partial \sigma}{\partial s} + \frac{\partial \tau_{max}}{\partial N} - \frac{2\tau_{max}}{r} = 0. \qquad (114)$$

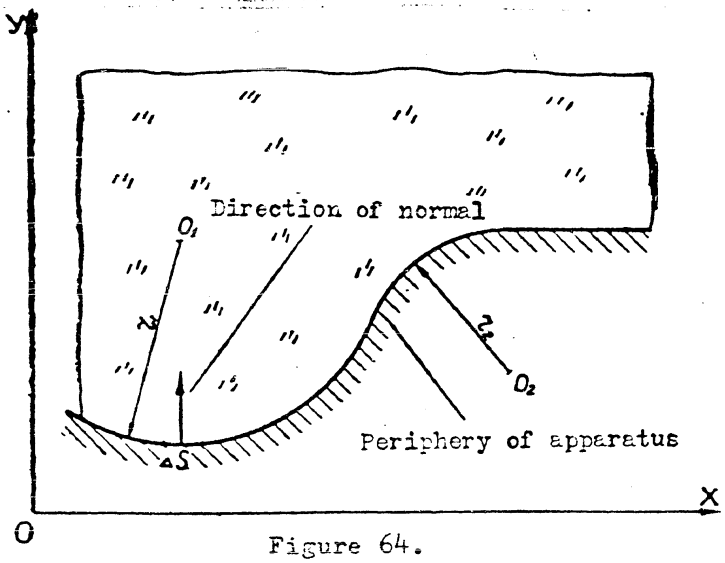

Figure 64.

Here $\frac{\partial \sigma}{\partial s}$ is a derivative of the mean stress along the arc of the periphery; $\frac{\partial \tau_{max}}{\partial N}$ is a derivative of the maximum shearing stress in the direction of the normal to the periphery; r is the radius of curvature of the periphery.

Thus, on the basis of (114) the mean stress at the boundary points may be computed by the formula

$$\sigma(s) = \sigma(s_0) + \int_{s_0}^{s} \left(\frac{2\tau_{max}}{r} - \frac{\partial \tau_{max}}{\partial N} \right) ds. \qquad (115)$$

Taking into account (28), formula (115) may be rewritten in the form

$$\sigma(s) = \sigma(s_0) + \tau_0 \int_{s_0}^{s} \left(\frac{2n}{r} - \frac{\partial n}{\partial N} \right) ds. \tag{116}$$

Keeping in mind the fact that the mean stress is equal to that normal to the boundary and utilizing (116), we obtain at once the stress normal to the boundary. As a starting point for purposes of calculations ($s - s_0$) we may take any point where the periphery of the model in contact with the apparatus becomes a free boundary. Often we can assume without any appreciable error that at such points $\sigma = 0$.

The calculation of stresses along the boundary utilizing the relationship (116) offers a series of important advantages. The most important of these is the fact that we do not utilize the isoclinics and in doing so we remove the basic source of errors, while the calculations are considerably simplified. In those cases where the boundary is a straight line, the calculations become particularly simple. As a rule, the fringe order is higher near the boundary than in the center portion of the model in the study of various processes. Because of this the error in the determination of the fringe order near the boundary will be less, and this in the final analysis will improve the precision of the results. Besides that, the state of stress along the boundary often is a matter of basic interest since it determines the loads exerted against the deforming apparatus.

Among the disadvantages of the calculations by the method of integration along the boundary we must consider the fact that the derivative $\frac{\partial n}{\partial N}$ must be computed according to the values of n at points lying only to one side of the line along which the integration is carried out. It is useful to note from the derivation of formula (116), that it permits us to compute the mean stress by the method of integration along any trajectory of the maximum shearing stress and thus that it may be utilized in all cases in which these

trajectories are known. When it is necessary to compute the stress tensor over the entire field of the specimen the calculations may be carried out by the method of the difference of tangential stresses utilizing as starting points the nearest points on the boundary.

More precise results may be obtained in the following manner. Since the mean stress satisfies Laplace's equation, it may be calculated over the entire field on the basis of the values of stresses at the boundary. In order to do this we may utilize any approximate method of calculation, for instance the grid method.

The mean stress, the maximum shearing stress and the value of the angle θ obtained on the basis of isoclinics, determine completely the state of stress.

CHAPTER V

MODELS FOR STUDY OF PROCESSES OF FABRICATION BY PRESSURE

1. Stamping.

At the present time the stamping process is used widely in the national economy because of its high productivity, reduction of the waste of metal and high quality of the product. This process is successfully employed both in the fabrication of metal parts by pressure and in the fabrication of plastics.

The flow of metal under the conditions of the stamping process presents a complex process of plastic deformation. In a number of cases there occurs during stamping a combination of compression, indentation, and flow. Moreover, under conditions of stamping the process of filling the die is not a stationary one and the rate of deformation varies for various parts of the product.

The study of the relationships governing the flow of metal during stamping is intimately related to the solution of the general problem of stress distributions and deformations under sharply defined conditions of three-dimensional compression.

In order to solve the indicated problem the application of the method of mathematical analysis based on modern mechanical-mathematical concepts of the theory of plasticity proves to be inadequate. The incomplete knowledge of the boundary conditions and an entire series of distinctly specific periods of transition which accompany the stamping process make it difficult to obtain reliable quantitative results. Therefore, it is expedient to employ an

experimental method of studying stresses in order to solve the indicated problem -- the method of photoplasticity.

Let us consider the character of the state of stress in the models undergoing deformation which are prepared from optically sensitive resin and are subjected to deformation in dies of simple and complex form. In Figure 65 there are shown various stages of the stamping of the model in a die of a simple form.

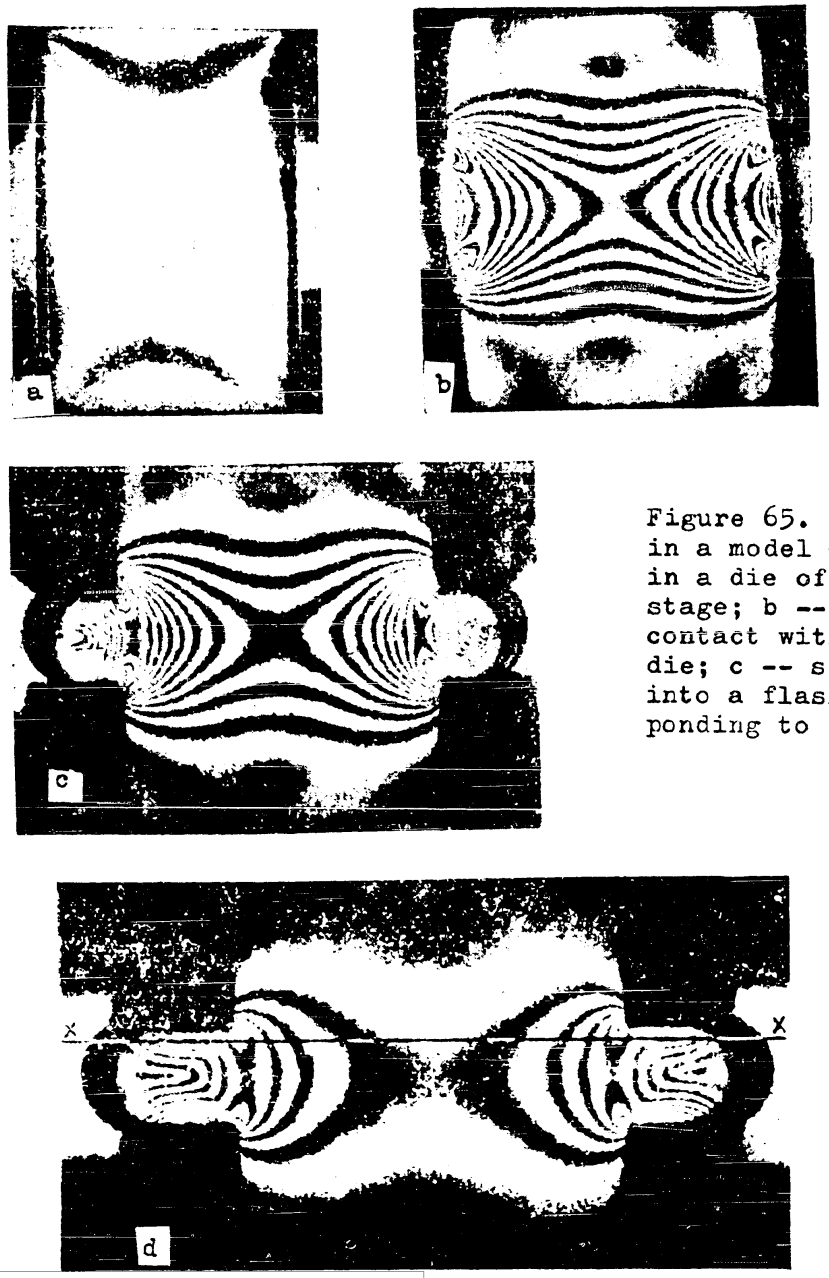

Figure 65. Fringe pattern observed in a model 40 mm thick being deformed in a die of simple form: a -- initial stage; b -- stage corresponding to contact with the side walls of the die; c -- stage corresponding to flow into a flash vent; d -- stage corresponding to filling of the flash vent.

In the initial stage of compression when the contact surfaces are lubricated, we observe a uniform state of stress in the model; this has an optical effect of producing a uniform coloring of the entire field of view of the model. In subsequent loading the uniform coloring changes 2-3 times after which we begin to observe individual fringes which indicate the origin of inhomogeneities in the state of stress of the deformed model. This inhomogeneity in the state of stress appears first at the surface of contact. It is caused by the friction between the material and the model and the surface of the apparatus.

Since the lubricant is forced out of the space between the contact surfaces during the process of compression of the model, the material begins to adhere to the surface of the apparatus. The displacement of the model material along the contact surface of the apparatus is retarded considerably due to the presence of large surface frictional forces. The layer of the material which adheres to the surface of the apparatus retards the adjacent layers and in this manner forms zones of low mobility. This factor (retardation of layers situated near the contact surface of the apparatus) aids in intensifying the spread (broadening) of the middle layers of the model in the direction of least resistance. As a result the model acquires a barrel-like shape.

It can be seen from the examination of the given illustrations that in the initial stage of the stamping process the lines of equal maximum shearing stresses are arranged the same as in the case of a simple compression of a model whose height is considerably greater than its width. As the degree of deformation increases the region of uniform state of stress in the middle portion of the model gradually decreases. The number of fringes gradually increases. The reduction in the height of the model causes an increase of the end surface at the expense of the material extruded at the side surfaces of the model.

The model material flowing sidewise comes in contact with the interior

side walls of the die. As the contact is made with the side surfaces of the die, there occurs a redistribution of stresses in the interior of the model which reveals itself by the change of the fringe pattern (Figure 65b). The new fringes which originate at the places of contact with the side walls along with fringes previously produced form a new fringe pattern. In this instance the highest fringe order is observed at the point of entry into the flash vent. In these places the maximum shearing stresses are found. It is precisely in these places where the flow of the excess material of the model into the opening of the flash vent takes place.

Owing to the adherence of the model material to the contact surfaces of the apparatus and the resistance of the side walls of the die to the flow of the material there is created a more sharply defined three-dimensional state of stress. As a result, at this stage of the stamping process the material begins to flow into the portions of the die which are difficult to fill (corners) and simultaneously into the opening of the flash vent. This is primarily aided by the resistance to the flow of the material into the opening of the flash vent. If the material encounters a greater resistance to flow at the opening into the flash vent than into other portions of the die, then as a result we shall have a more intensive filling of the still incompletely filled portions of the die. As the unoccupied portions of the die are filled, the fringes also disappear. As the entire interior of the die is filled the state of stress in the upper and lower portions of the model becomes more uniform and a uniform coloring is acquired which indicates the presence of a uniform state of stress (Figure 65d).

The dimensions of the flash vent must be such that it offers sufficient resistance to the flow of the material into the vent and that it assures by this the complete filling of the interior of the die for a minimum expenditure of effort. Excessive resistance to the flow of material into the vent above the necessary value will cause an excessive expenditure of energy -- and an

unnecessary increase in the deforming force. Therefore, the regulation of the flow of the material in the die during stamping may be achieved by varying the width of the flash vent and the thickness of the flash ribbon. The values of these quantities (parameters) have a substantial effect on the magnitude of the pressure causing the flow of the material into the interior of the die. We shall observe either complete or incomplete filling of the interior of the die depending upon the relationships of these quantities.

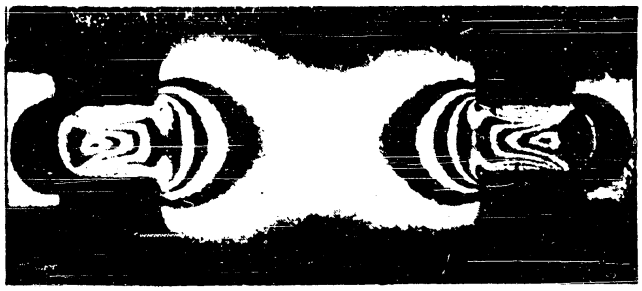

Figure 66.

In the final stage of the stamping process we observe a uniform darkening of the field of view in the upper and lower portions of the model (Figure 66). This points to the presence of a uniform state of stress in these portions of the volume of the model. The middle portion of the model has a uniformly light coloring which indicates that in this portion of the model we have equal maximum shearing stresses of small magnitude. The portions of the model situated near the entry to the flash vent are subjected to the most nonuniform state of stress. In these places we observe concentration of stresses and deformations.

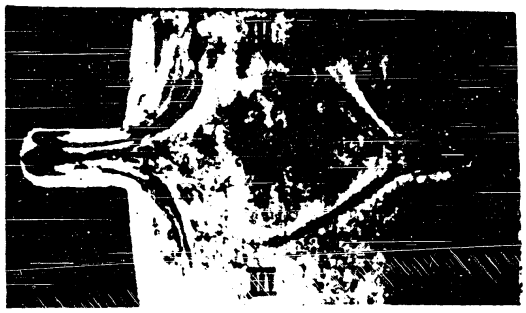

Figure 67.

We may draw the very same conclusion from examination of Figure 67, in which there is shown the distribution of trajectories of tangential stresses (characteristics) throughout the volume of the model obtained by illuminating it in nonpolarized light.

The entire volume of the model in one of the last stages of a stamping process is divided as it were into three zones. The first zone corresponding to the concentrated nonuniform state of stress is situated near the openings of the flash vent. In this zone are situated the most closely spaced trajectories of tangential stresses. The second zone occupies the middle (central) portion of the model. In its external appearance it has a lens-like form. In this zone we observe a more uniform state of stress (Figure 66). The third zone presents itself as an envelope in which is included the lens-like zone of the more uniform state of stress. Plastic deformation is absent in the third zone and there exists in it a uniform and homogeneous state of stress (hydrostatic pressure). In this zone the deviation of the state of stress may be set equal to zero.

We can verify the above by considering systems of isoclinics observed in linearly polarized light. As we rotate the plane of polarization from 0 to 90° we find that the completely darkened regions (isotropic) are the upper and lower portions of the model in which we observe a uniform state of stress (Figure 68).

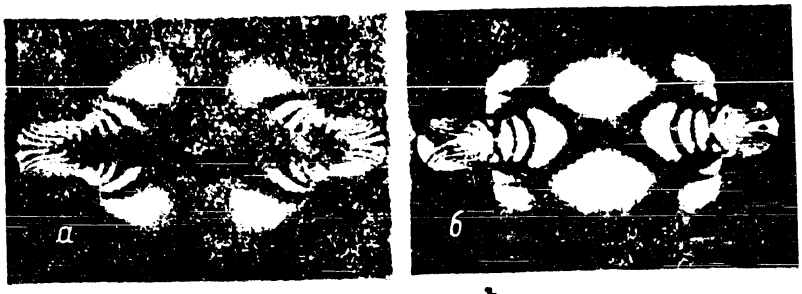

a b

Figure 68. Isoclinics observed at one of the final stages of stamping: a -- 0° isoclinic; b -- 45°.

We find still another confirmation of the results obtained with resin

models from the examination of deformed models of lead having an engraved coordinate grid [29] (Figure 69).

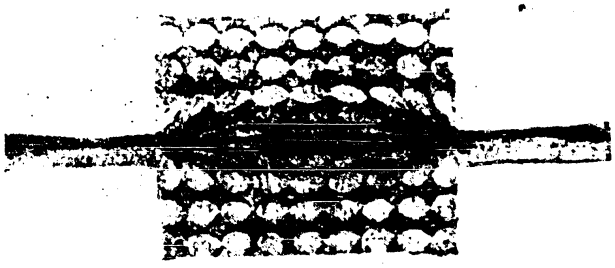

Figure 69. A lead model with a coordinate grid deformed in stamping (from E. S. Bogdanov).

Let us consider the fringe pattern which accompanies the process of stamping for a model in the presence of a slight excess of the amount of material needed to fill the mold, that is, when the model fills the interior of the die almost completely. In this case the fringes are observed only at the entry into the flash vent (first zone). In the second zone the stresses have a small value. This is evident from examination of Figure 70 in which there are shown two stages of the flow of the excess part of the material into the flash vent.

The volume of the model was only sufficient to fill the interior of the die and the flash vent (stamping with a small flash). The field of the model and the fringes are observed to grow lighter only in a limited zone -- near the entry to the flash vent. In the remaining portion of the model the coloring remains uniform which indicates a more homogeneous state of stress. This shows that only those portions of the model which are situated near the entry to the flash vent and the center portion of the model are deformed. The flow into the flash vent is due only to these regions, that is, only the first and the second zones feed the flash.

The above is also confirmed by the system of isoclinics. In Figure 71 there is shown the field of isoclinics at the stage corresponding to filling of the flash vent. The isotropic regions are observed in the upper and lower

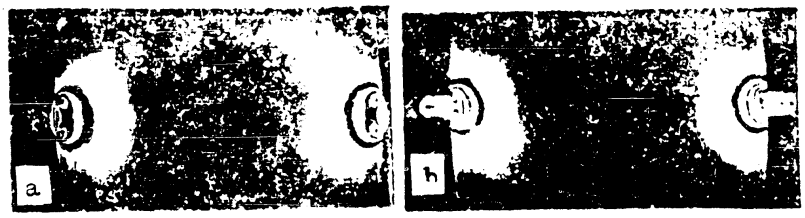

Figure 70. Fringe pattern observed in stamping of a model having a small excess of required material: a -- contact of model material with the edges of the opening of the flash vent; b -- the stage corresponding to complete filling of the flash vent.

portions of the model (third zone). In the middle portion of the model (in the plane of separation of the die) we observe an increase in the light intensity as the angle of the plane of polarization rotates from 30 to 60°, which indicates the presence of maximum shearing stresses of small magnitude.

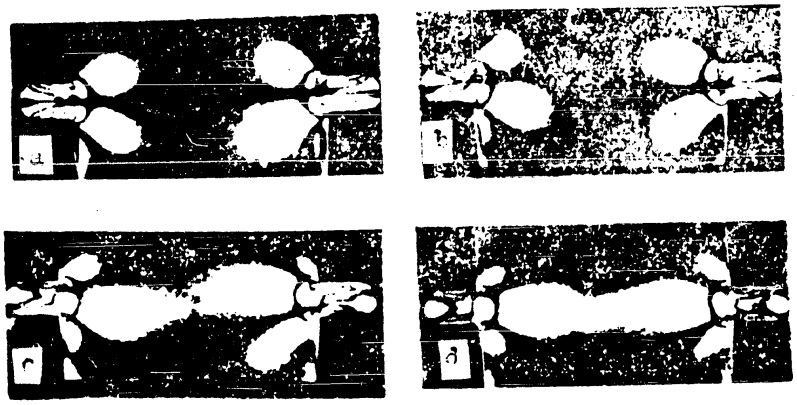

Figure 71. Isoclinics at the stage corresponding to the filling of the flash vent: a -- isoclinic of 0°; b -- 15°; c -- 30°; d -- 45°.

The very same results are obtained when we observe models of lead having an engraved coordinate grid. The distortion of the lines of the coordinate grid (for a small excess of required material) is observed only at the entry into the flash vent (Figure 72). In the remaining portions of the volume of the forging a coordinate grid remains practically unchanged (from E. S. Bogdanov and M. I. Kalachev).

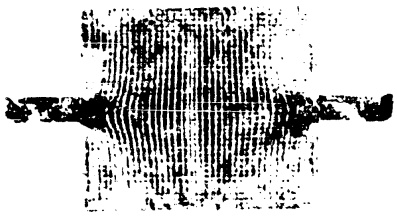

Figure 72.

In the final stage of the stamping process the entire field of the model presents an isotropic region (Figure 73). The rotation of the plane of polarization changes the character of the disposition of the isoclinics only near the entry to the flash vent and within the vent itself. In these places there is concentrated in the final stage of the stamping process a plastic flow and there is observed an inhomogeneous state of stress. In the isotropic region, however, which now covers the entire field of the model, uniform normal stresses are acting while the shearing stresses are equal to zero.

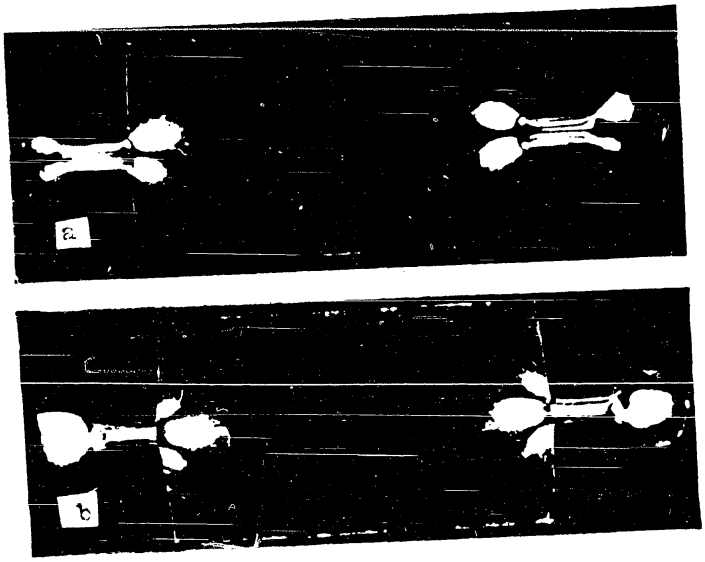

Figure 73. Isoclinics observed at the final stage of the stamping process: a -- 0° isoclinic; b -- 45°.

In Figure 74 there is shown a field of isoclinics obtained for the stage corresponding to the filling of the interior of the die as indicated in Figure

65d. The isoclinics are given for increments of 15° both for the interior of the die and the flash vent.

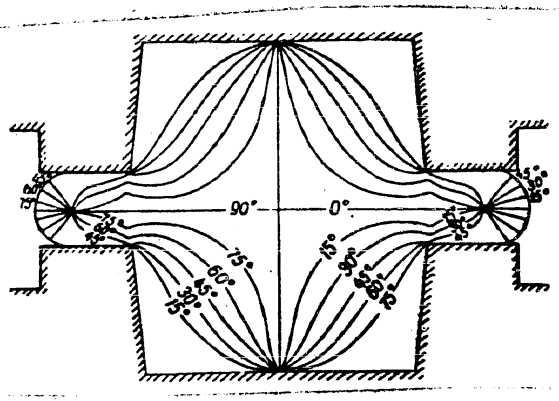

Figure 74.

Since we have the pattern of isoclinics, it is possible to construct a sample grid of trajectories of the principal normal stresses both for the interior of the die and the flash vents (Figure 75). In Figure 76 there are shown magnified views of the isoclinics observed at the flash vent and the trajectories of the principal normal stresses constructed on the basis of these lines.

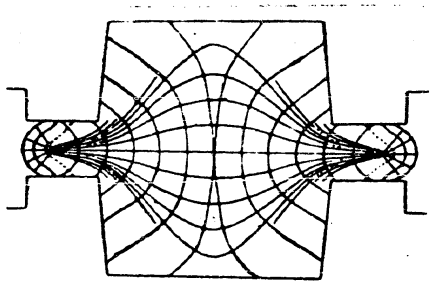

Figure 75. Grid of trajectories of principal normal stresses in die of simple shape during stamping process.

As can be seen from examination of isoclinics and also the trajectories of the principal normal stresses, the most abrupt change in their direction is observed at the entry to the flash vent, that is, in the region of the first zone where concentration of stresses exists.

Thus, the examination of the state of stress in the final stages of the stamping process enables us to draw the following conclusions:

(a) There is observed throughout the volume of the forging an inhomogeneous state of stress during the stamping process;

(b) The intensity of pressure is uniformly distributed over the contact

surface of the main body of the forging;

(c) The pressure at the last stage of the stamping process does not depend upon the form of the forging, but upon the geometry of the flash vent and primarily upon its height.

Let us consider the state of stress of that portion of the model which flows into the vent.

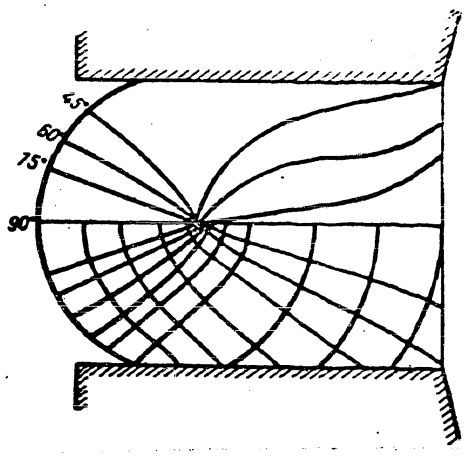

Figure 76.

As the excess material of the model flows into the flash vent there is observed in it a very definite fringe pattern, and therefore a very definite state of stress. The character of the state of stress in the flash vent depends on how completely the interior of the die is filled. If the material enters only the flash vent we observe the fringe pattern shown in Figure 77, while in the presence of other openings in the interior of the die into which the model material may flow, we observe at the flash vent the fringe pattern shown in Figure 78.

As can be seen from Figure 77, as the material flows into the opening of the flash vent, the fringes originate at the corners of the opening. As they are developed further, they go round the corners and show a tendency to line up along the boundaries of the flash vent. In the front part of the flow vent the fringes turn toward the boundary of the vent. In its middle portion there is observed a dark neutral fringe which divides the general fringe pattern into

two symmetrical parts. At the outer end of the vent the neutral fringe becomes wider. Along this fringe, the magnitude of the maximum shearing stresses in the plane of the ray of light is equal to zero. These stresses increase as we proceed from the neutral fringe to the boundary of the flash vent and attain their maximum value at the boundary. The value of the maximum shearing stresses is determined by the order of the fringes, and the order is reckoned from the neutral fringe. As the load is removed, the change in the fringe pattern proceeds in the opposite direction.

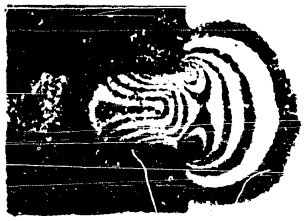

Figure 77.

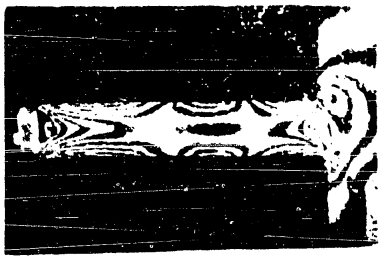

Figure 78.

In the case of Figure 78 the fringes are arranged in the same manner as for a wide model being compressed between two moving plates. At the same time the fringe pattern is symmetrical with respect to a certain vertical plane which we may call a neutral plane. This shows that as the boundaries of the flash vent approach each other, there is a period when the resistance to flow into the flash vent is blocked, and this curtails the flow of the material from the interior of the die into the flash vent.

The instant during the stamping process at which the material ceases to flow from the interior of the die into the flash vent is called by the authors the instant of locking of the material within the die. The conditions of the state of deformation which determine this instant are called the conditions of locking. From this moment the material flows only into the vacant spaces in the interior of the die and thus assures that it becomes completely filled.

The observed neutral plane may be situated at various portions of the flash vent. Its location depends upon the dimensions of the flash vent and

the amount of excess material being fed into it. For greater heights of the flash vent (earlier stage) the neutral plane is nearer its opening. As the height is reduced (other things being equal), the neutral plane is shifted toward the interior, but by a distance not exceeding half of the width of the vent.

The neutral plane in the flash vent is observed only up to the stage when the interior of the die is completely filled. As soon as all its recesses are filled, the fringe pattern at the flash vent changes. The fringes begin to arrange themselves along the boundaries of the vent. This shows that the interior of the die is filled and that the excess of the material flows only through the opening of the flash vent. One fringe pattern is transformed gradually into the other.

The problem of determination of the moment of locking or locating the neutral surface (critical surface in the terminology of I. A. Tarnovsky and O. A. Ganazo) was studied by a number of investigators [29 and 30]. They determined the moment of locking by comparing the amounts of material flowing into a flash vent and into auxiliary recesses. The moment at which the amount of material flowing into the flash vent decreases while the amount flowing into an auxiliary recess increases, was considered the moment of locking. This determination required the performance of a large number of experiments. The location of the neutral plane could not be determined at the same time. The application of the method of photoplasticity furnishes visual data for determining the moment of locking and the location of the neutral surface.

The state of stress in the billet undergoing stamping depends exclusively upon the geometry of the branches of the die. We shall show this in the following examples.

In Figure 79 one can see the character of the origin and distribution of fringes when a model of rectangular form is being deformed in a die having openings in the upper and lower parts. The width of the entry into the

STAT

openings is equal to 8 mm. The height of the flash vent at the surface of contact of the two halves of the die along the plane of separation is equal to 2.6 mm.

Even in the initial stage of the plastic deformation one can determine the sources of the fringes situated near the corners of the openings. As the process develops the fringes join in the middle portion of the model forming a system of lines which is determined by the form of the given deforming apparatus (Figure 79a). In the side portions of the model we observe a uniform coloring which indicates a state of uniform stress caused by the compression of these portions of the model. As the load increases the fringes become more concentrated. A change in the height of the model causes a contact of its sides with the walls of the interior of the die as the process develops. As a result there occurs a redistribution of stresses within the model which fact leads to the change of the fringe pattern (Figure 79b, c). The non-uniformity of stress distribution becomes more pronounced. Due to the greater resistance to flow into the flash vent the flow of the material of the model is channeled into the supplementary openings.

The fringe pattern observed at all stages of the stamping process near the upper opening is a mirror image of the fringe pattern observed at the lower opening. The flow of the model substance into the indicated openings proceeds simultaneously. The amount of the substance which flows into the upper and lower openings of the die is identical. This is valid only in the case where the die is symmetrical with respect to the plane of separation and the openings have the same form and dimensions and the surfaces have the same degree of finish. In the opposite case the observed optical patterns will not coincide completely.

The material flows into the openings from the center portion of the model. At the openings of the flash vents the flow is slight and the material undergoes almost no deformation. This may be seen from examination of

STAT

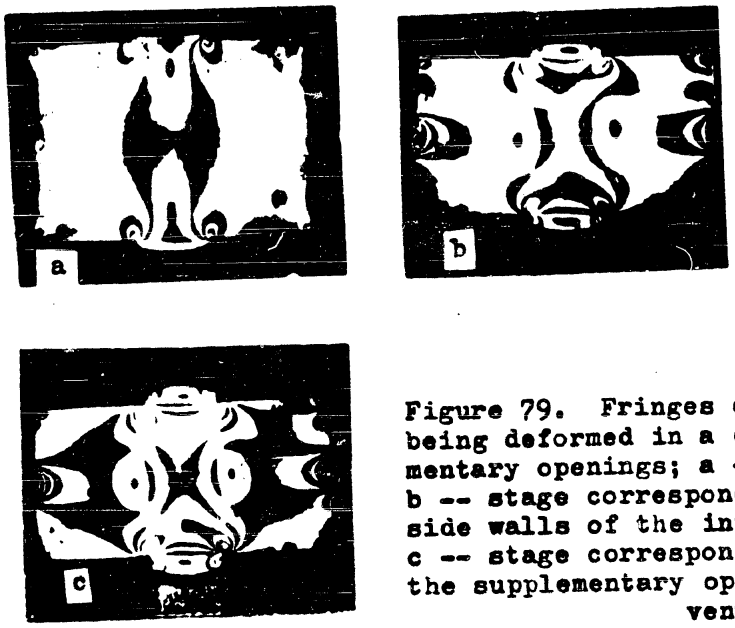

Figure 79. Fringes observed in a model being deformed in a die with two supplementary openings; a -- initial stage; b -- stage corresponding to contact with side walls of the interior of the die; c -- stage corresponding to flow into the supplementary openings and the flash vent.

isoclinics observed for increments of 15° and shown in Figure 80. As the plane of polarization is rotated from 0 to 90° completely darkened regions are observed to the left and right of the zone situated along the axis of the openings. The greatest extent of illumination is observed at the middle portion and the least at the openings of the flash vent. It follows then that the flow of material into the upper and lower openings proceeds from the middle portion of the model.

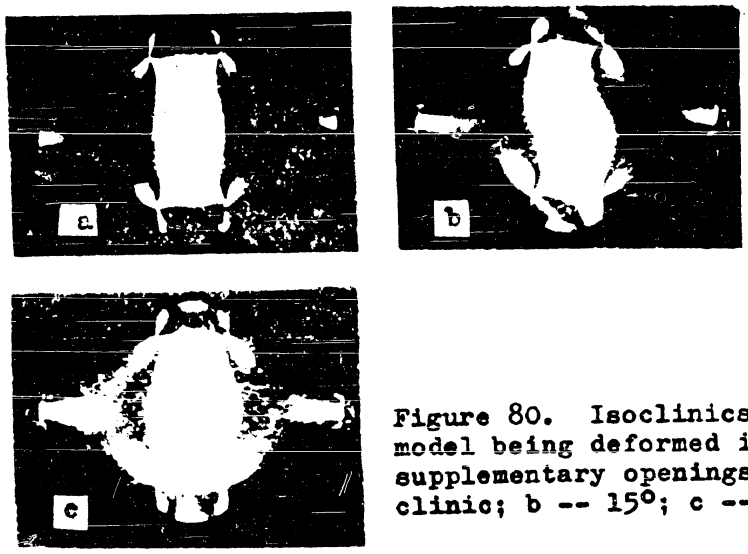

Figure 80. Isoclinics observed in a model being deformed in a die with two supplementary openings: a -- 0° isoclinic; b -- 15°; c -- 45°.

STAT

This is also confirmed by experiments [29] carried out with metal models having a grid of coordinates (Figure 81). The specimen had an initial form shown in Figure 79c. After the test the grid of coordinates was deformed only at the upper and lower openings and at the flash vent.

In the final stage of the stamping process when the openings are completely filled there is developed throughout the volume of the billet a state of uniform stress. The fringes disappear over the entire field of view of the model and are retained only at the flash vent.

Figure 81. A lead model with a grid of coordinates undergoing deformation in a die having two supplementary openings (from E. S. Bogdanov).

In Figure 82 there is shown the character of the origin and distribution of fringes observed in the stamping of a gear-like model (stamping accompanied by indentation).

Even in the initial stage of the plastic deformation fringes develop along the points of the projecting portions of the die (Figure 82a), while the number of fringes increases with an increase in load. We observe two broad, indistinct, dark fringes to the left and right of the middle portion of the model. These are neutral fringes in which the value of the maximum shearing stresses is zero. These fringes form the boundary between the region of compression and the region of tension. The peripheral portions of the model are light. They are subjected to tensile stresses of small magnitude. With further increase in load the tensile stresses attain considerable magnitudes. In Figure 82b can be seen dark fringes of the first order which are situated along the unloaded periphery of the model.

As the load increases the region of uniform coloring in the middle portion of the model decreases. The concentration of fringes in this instance occurs until the sides of the model come in contact with the walls of the

interior of the die. Then a redistribution of stresses within the model takes place and the fringe pattern covering the field of the model changes. In the given case this leads to still greater nonuniformity in the distribution of stresses which becomes intensified as the process develops (Figure 82c). As the interior of the die is filled the state of stress becomes more uniform and the fringes disappear. The field of the model acquires a uniform coloring and the stresses become more uniform. The fringes are preserved only near the openings of the flash vent where the flow of the material still continues.

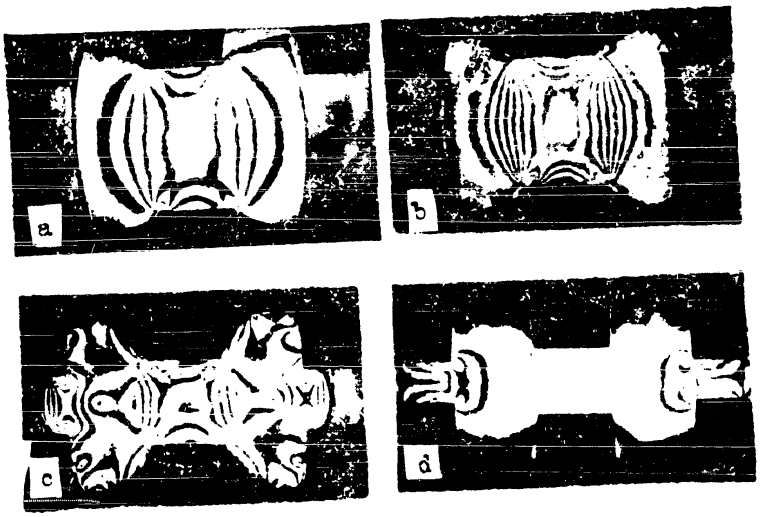

Figure 82. Fringe pattern for a resin model during a stamping process accompanied by indentation: a -- initial stage; b -- appearance of fringes of the first order along the free boundary of the model corresponding to tensile stresses; c -- disposition of fringes at the stage corresponding to flow into a flash vent (nonuniformity of the stress distribution became intensified); d -- final stage of the stamping process.

For a given geometry of the branches of the die certain regions develop in which the shearing stresses are zero. These are isotropic points which are subjected to either a triaxial compression or tension. Formation of such points or distinct regions is observed in dies of a complex form. Such points may be seen in Figure 79 (a, b, c) and 82c (in the given case these are points of triaxial compression).

In all the cases considered for models undergoing stamping in dies of simple and complex form, each configuration of the die gives rise to its own

characteristic state of stress. A complete picture of the stress distribution may be studied at various stages of the plastic process of change of form. In each individual case we may visually observe points of stress concentration at which the wear of the dies is accelerated. This gives to both the technologist and the designer of the dies the needed material for selection of the proper rational form of the billet and the development of the most rational geometry of the interior of the die.

From the above it is apparent that a state of uniform stress develops in the entire volume of the billet in the last stages of its processing independently of the geometry of the billet. The smaller the volume of the forging billet, the more uniform is the deformation of the billet in various stages of its fabrication.

The examination of the isoclinics in the final stage of the stamping process shows that the less uniform state of stress is replaced by a more uniform and homogeneous state of stress (hydrostatic pressure) in the greater part of the volume of the model. The only exceptions are the regions in the vicinity of the entries to the flash vents.

The investigations conducted by the authors show that the primary attention in designing dies should be paid to the geometry of the trough of the flash vent. In the region of the flash vent there is concentrated a plastic flow from the beginning to the end of the stamping process. In these places there occurs a high concentration of stresses and deformations which may cause an accelerated wear of the apparatus.

As can be seen from the experiments, the extent of filling of the interior of the die depends exclusively on the conditions of locking of material in the flash vent. It is determined by the dimensions (parameters) of the flash vent and the conditions of external friction. The conditions which determine the locking of the material in the flash vent determine the required stamping force, the power parameters of the press, and the stability of the die itself.

The picture of the states of stress and deformation in the stamping process obtained by the method of photoplasticity coincides completely with the picture which we obtain on the basis of the study of the state of deformation by the method of a coordinate grid engraved upon metal models. The method of the coordinate grid enables us to establish the character of the distribution of deformations in a metal model undergoing stamping while the method of photoplasticity confirms these results, substantially supplements them, and introduces a certain degree of visual clarity.

Now let us pass to the consideration of the numerical values of normal and shearing stresses during the stamping process.

Since in the present case we are solving a problem of a plane state of stress, we may, therefore, utilize the concept of forces distributed along a line instead of forces distributed over a surface. Therefore, the magnitudes σ_x, σ_y, and τ_{xy} will represent those values of the components of the stress tensor which when acting upon a model 1 cm thick create an optical effect corresponding to reality.

In the experiment we shall obtain at each point of the model the value of τ_{max} and the angle θ formed by the trajectory of the principal normal stress with the axis of x. Having the values of these quantities enables us to determine the components of the stress tensor. Their calculation is carried out by the method described in Chapter IV [see formulae (102), (105), (106)]. The experimental values of the fringe order n and the parameters of the isoclinics θ which define σ_x, σ_y and τ_{xy} at various horizontal sections, are taken from Figures 65d and 74 which correspond to one and the same stage of stamping process and loading.

In Figure 83 are shown distributions of σ_x, σ_y and τ_{xy} for one of the horizontal sections of Figure 65d. From examination of the graph it is clear that the stresses σ_x and σ_y acting within the model are compressive stresses, with $\sigma_x > \sigma_y$ in absolute value. The maximum dispersion between the values

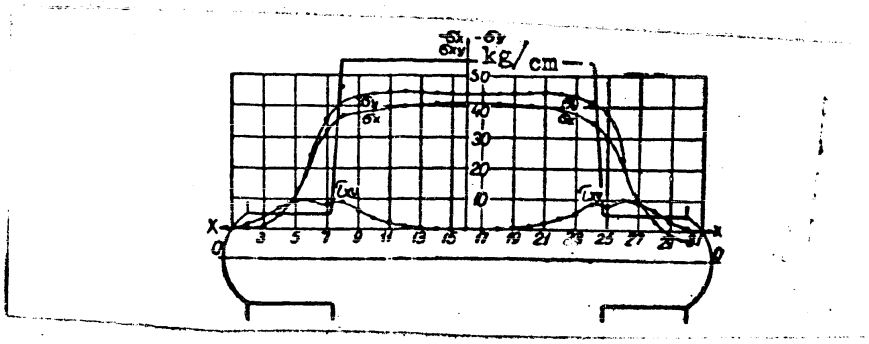

Figure 83. Distribution of σ_x, σ_y and τ_{xy} for the section X-X.

σ_x and σ_y occurs at the entry to the flash vent, that is, in the first zone. In a certain portion of the flash vent $\sigma_x = \sigma_y$, $\tau_{xy} \neq 0$. For the greater part of the horizontal section (second zone) the values of σ_x and σ_y are different, but the difference has almost a constant value. The difference in the numerical values of σ_x and σ_y varies approximately from 5.3 kg/cm in the region of transition from the first zone to the second to 2.8 kg/cm along the vertical axis of symmetry. It is this small difference which determines the almost constant coloring in a greater part of the volume of the second zone.

Thus, it follows from the discussion that the model material within the interior of the die is in a state of nonuniform triaxial compression.

Let us determine the summation of the forces along section X-X (Figure 83). In order to do this let us sum up all the values of σ_y at 30 points of the given section and multiply the value obtained by the length of the interval Δx between the points under consideration. In our case $\Delta x = 0.1$ cm. Summing up the values of σ_y at the section X-X, we obtain a magnitude equal to 895.7 kg. Then the force P = 895.7 x 0.1 = 89.57 89.6 kg. The applied force for the stage of the stamping process indicated in the drawing was 105 kg. Thus, the value of the force P obtained from calculations was less than the value of applied force by 15.4 kg, a difference of about 9 percent.

The observed discrepancy may be explained by the effect of the stresses

acting in the plane of the glass plates which do not reveal themselves optically. Therefore, the optical pattern of the lines of equal maximum shearing stresses observed in Figure 65d corresponds to the fringe pattern for a load of 89.6 kg for a plane state of stress.

Let us determine what factor influences the precision of the determination of σ_x, σ_y and τ_{xy} to the greatest extent. Since we utilize fringes and the parameter of the isoclinics for their determination it is natural that the precision of determination of σ_x, σ_y and τ_{xy} will depend upon how accurately we determine at each point of a given section the fringe orders n and the parameter of the isoclinic θ. However the effect of these quantities may vary.

Let the true value of the difference between the principal normal stresses at a given point of the model be q and the error in its determination be Δ_q. Then

$$q_z = q - \Delta q.$$

In an analogous manner, if θ is the true value of the parameter of an isoclinic and θ_e is the value obtained from an experiment, then

$$\theta_z = \theta - \Delta\theta.$$

The shearing stress determined from experimental data will be

$$\tau_{xyz} = \frac{(q - \Delta q)}{2} \sin(2\theta - 2\Delta\theta),$$

and the true value

$$\tau_{xy} = \frac{q}{2} \sin 2\theta.$$

Let us find an expression for the error in the determination of the shearing stresses:

STAT

$$\Delta\tau_{xy} = \tau_{xy} - \tau_{xy\,\text{изм}} = \frac{q}{2}\sin 2\theta - \frac{q-\Delta q}{2}\sin(2\theta - 2\Delta\theta) =$$

$$= \frac{q}{2}\sin 2\theta - \frac{q-\Delta q}{2}\left[\sin 2\theta \cos 2\Delta\theta - \cos 2\Delta\theta \sin 2\Delta\theta\right].$$

Taking into account the fact that the quantities $\Delta\theta$ and Δq are small, the latter expression may be simplified and then

$$\Delta\tau_{xy} = \frac{\Delta q}{2}\sin 2\theta + q\Delta\theta\cos 2\theta.$$

The relative error in the determination of the tangential stresses will have the following value:

$$\frac{\Delta\tau_{xy}}{\tau_{xy}} = \frac{2\Delta q \cdot \sin 2\theta}{2q \cdot \sin 2\theta} + \frac{2q \cdot \Delta\theta \cdot \cos 2\theta}{q \cdot \sin 2\theta}.$$

Simplifying the latter expression, we finally obtain

$$\frac{\Delta\tau_{xy}}{\tau_{xy}} = \frac{\Delta q}{q} + 2\Delta\theta \operatorname{ctg} 2\theta. \qquad (117)$$

The first term gives the value of the relative error in determination of τ_{xy} which depends upon the precision with which we determine the fringe order at a given point.

The second term defines the relationship of the relative error in the determination of τ_{xy} to the parameter of isoclinic θ and, therefore, to the angle of inclination of the principal normal stresses. From expression (117) it is clear that the second term approaches zero as the parameter of the isoclinic approaches 45°. In this case the relative error in the determination of τ_{xy} will depend exclusively upon the precision of determination of the parameter θ of the isoclinic. This circumstance demonstrates the necessity of determining quite accurately the parameter of isoclinics near the values of angles of 0 and 90° and the necessity of photographing them (or sketching them) every 3-5°. In addition to that, in order to obtain more accurate quantitative results it is necessary to select sections in such a manner as

to reduce significantly the number of points situated near 0 and 90° isoclinics and to exclude the possibility of having either isotropic points or regions upon the selected section.

In Figure 84 there is shown a curve of distribution of normal stresses for one of the vertical sections in the vicinity of the flash vent computed in accordance with equation (108). As can be seen from the graph the values of σ_y along the upper part of the section have a constant value (third zone). As we approach the opening of the flash vent (first zone) the numerical value of σ_y increases and attains its maximum value at the level of the boundary of the flash vent. The least value of this stress exists along the horizontal axis of symmetry.

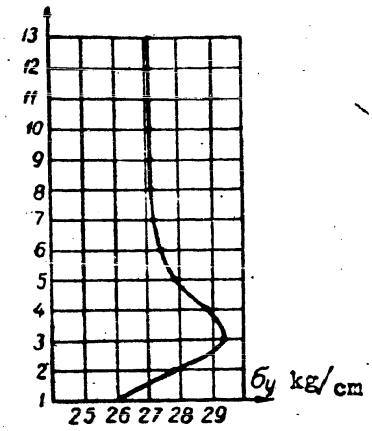

Figure 84. Character of distribution of normal stresses along a vertical section in the vicinity of the flash vent (Figure 65d).

In the combined drawing and Table 85 there are given the numerical values of shearing stresses for one portion of the volume of the die. The values of τ_{xy} are different at all points of the selected sections and the greatest values are observed in the first zone; then they gradually decline in the direction of the second and third zones. A typical curve of distribution of maximum values of τ_{xy} in the volume of the entire model of resin subjected to deformation is shown in Figure 86.

Thus, it follows from the cited example that it is possible in principle to determine at each point of the billet the values of the components of the stress tensor. The precision with which these values can be determined will depend upon the accuracy of determination of n and θ which in turn depend upon the experimental technique. It is important to determine with precision the values n and θ at the initial points along the free boundary. This is

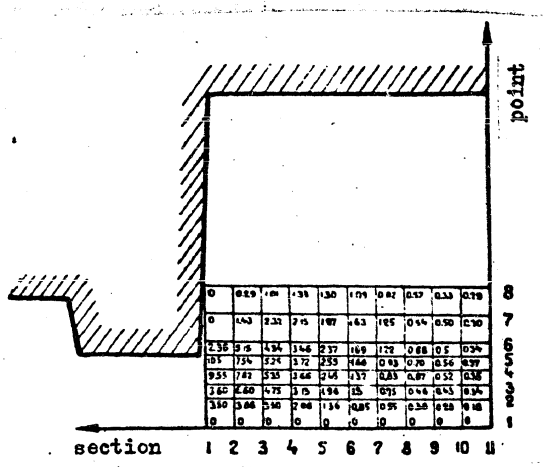

Figure 85. Numerical values of τ_{xy} at points of one portion of the model corresponding to the stage of the stamping process shown in Figure 65d.

rendered difficult because of the appearance of a shadow along the periphery of the curved surface of the flowing portion of the model material. The error in the determination of n and θ along the free boundary will reveal itself in all the calculations of the components of the stress tensors at all interior points of the model. However, this circumstance may be avoided in principle if we utilize an immersion fluid with an index of refraction equal to the index of refraction of the resin from which the model was prepared. Then the boundary of the model will not be darkened and the values n and θ may be determined with precision.

2. Extrusion.

Basically the purpose of modelling the extrusion process is to study the possibility of utilizing the method of photoplasticity for a quantitative determination of stresses.

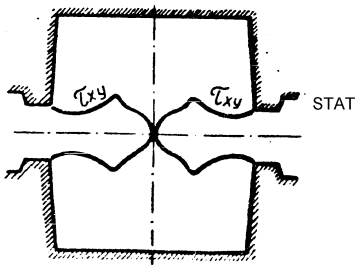

Figure 86. Typical curve showing distribution of maximum values of τ_{xy} in a model undergoing deformation (Figure 65d).

In modelling the extrusion

process the authors utilized a flat container with a rectangular die. The schematic diagram of the process and the basic dimensions of the container are shown in Figure 87. The thickness of the layer in the direction of the incident light exceeded the width of the container by a factor of three, and this assured sufficiently close approximation of the process to a plane one. The experiments were conducted with specimens of resin. The force was applied to the pressure washer by the loading mechanism of the polariscope installation and the load was maintained at a constant value during each individual experiment. The patterns of the fringes and isoclinics were photographed with the light of the yellow line of mercury and the photograph was taken after the fringes had become stable. The process of stabilization of the optical pattern usually took 10-15 seconds.

Figure 88 shows fringe patterns obtained for different forces applied to the pressure washer. As can be seen from the given photographs, as the load is doubled, each previously obtained fringe is replaced by a new one whose order is twice as high, and in the space between each pair of fringes a new one appears. Consequently, the distribution of stresses remains similar with a change in load, and the stress at each point changes in proportion to the applied load. These data confirm the previous assertion that in the case where the viscosity of the entire model is constant the distribution of stresses in it is determined only by the geometric characteristics of the process.

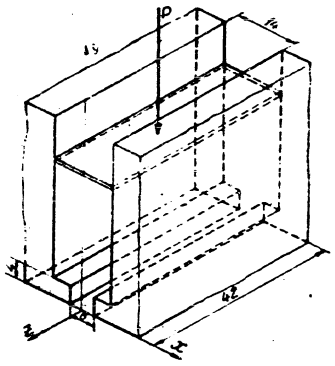

Figure 87. Schematic diagram of the modelling of an extrusion process.

Figure 89 shows fringe patterns obtained at various stages of extrusion with a force of 180 kg applied to the pressure washer. As we examine the photographs we first of all note the fact that the position of the fringes in

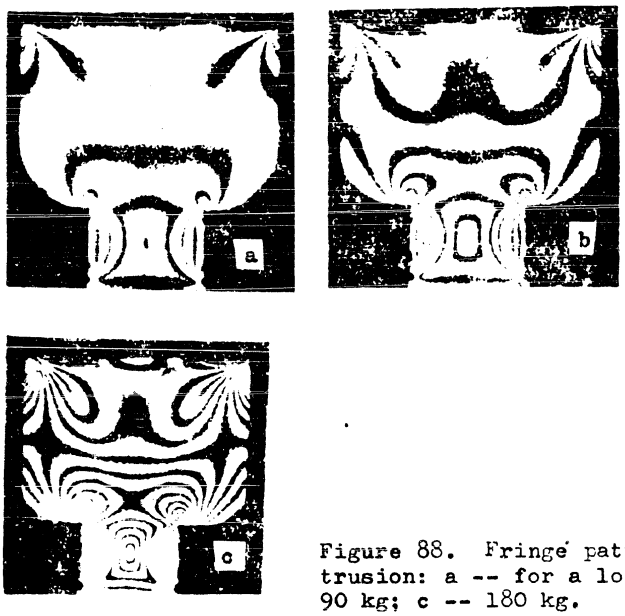

Figure 88. Fringe patterns during extrusion: a -- for a load of 45 kg; b -- 90 kg; c -- 180 kg.

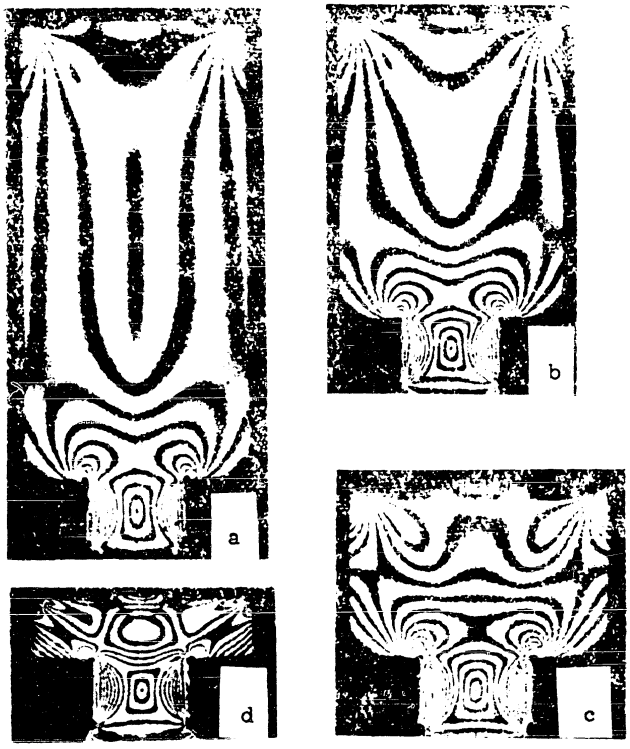

Figure 89. Fringe patterns at various stages of extrusion modelling.

the field of the container exclusive of the region in the vicinity of the die is similar to the distribution of fringes in the field of the channel. This is particularly noticeable in those stages of the process where the height of the column of the material in the container exceeds its width by a factor of two or more. In this case the fringes in the middle portion of the container are disposed parallel to its axis and are uniformly spaced, that is, they are arranged precisely in the same manner as for the case of a plane flow in the channel.

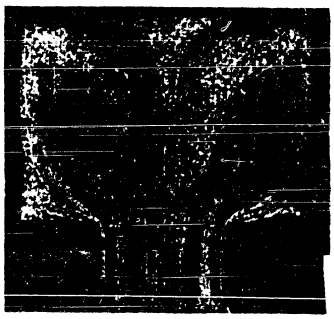

Figure 90. View of a model after its height in the container has been reduced in half by extrusion.

This can be seen from the comparison of Figures 51 and 47. The fringe pattern at the die opening and in its vicinity and also near the pressure washer depends but slightly upon the height of the material in the container. For practical purposes, the pattern only begins to change when the distance between the pressure washer and the die becomes less than the width of the container. The points of concentration of shearing stresses and, consequently, of deformations are the corners formed by the pressure washer and the walls of the container and also the corners at the entry to the die opening. The distribution of stresses near the corners of the pressure washer corresponds to that obtained in the solution of the problem 2 of Section 4, Chapter IV. The photographs reveal the presence of several isotropic lines and points. The STAT following points prove to be isotropic: the point at the center portion of the die opening, the corners formed by the die and the container, and the point upon the axis of symmetry passing through the pressure washer. The fringes which radiate from the corners of the pressure washer and which terminate at some distance from these corners also represent isotropic regions

or fringes of the order zero. In those cases where the height of the column of material in the container exceeds its width by a factor of more than one and one-half, an isotropic line is also observed along the axis of symmetry in the center portion of the container. This line disappears in subsequent stages of the extrusion process.

We may obtain a picture of the lines of flow by examining Figure 90. This photograph was obtained with ordinary light after the height of the specimen in the container was reduced in half by a process of extrusion.

Now let us pass to consideration of quantitative data on the state of stress. We shall cite certain calculations for the stage of pressure which corresponds to the fringe pattern shown in Figure 91.

The isoclinics corresponding to this case are shown in Figure 92.

At first let us compute the state of stress in the horizontal section bb' which passes through the middle of the die. In this cross section there is present an isotropic point. According to the data obtained from the field of isoclinics, at this section $\theta = 45^\circ$ at every point. The value τ_{xy} computed from formula (101) is given in Figure 93.

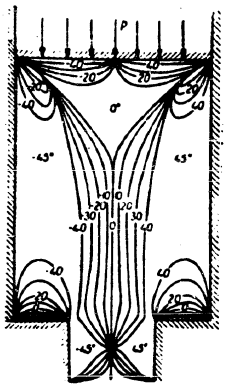

Figure 91. Fringe pattern utilized in the calculations given above.

Figure 92. Field of isoclinics obtained experimentally in modelling an extrusion process.

In order to compute normal stresses let us utilize formula (106) which

we shall rewrite in the form

$$\tau_x(x,y_0) = \tau_x(x_0,y_0) - \tau_0 \int_{x_0}^{x} \left(\sin 2\Theta \frac{\partial n}{\partial y} + \right.$$

$$\left. + 2n\cos 2\Theta \frac{\partial \Theta}{\partial y} \right) dx. \qquad (118)$$

At the points of the section under consideration the tangents to the fringes are parallel to the y axis and, consequently, $\frac{\partial n}{\partial y} = 0$. In view of the fact that at this section $\theta = 45°$, $\cos 2\theta = 0$ and $\sigma_x = \sigma_y$.

Thus, along the section bb' the integral in the formula (118) is equal to zero and $\sigma_x = \sigma_y$ constantly. The value of σ_y may be obtained from the condition of equilibrium of the lower part of the model bounded by the section bb'. This portion of the model is subjected to the action of shearing forces in the direction of the y axis along the side walls of the channel and to the action of normal forces at the section bb' from the direction of the upper portion of the model. The former of the indicated forces are defined by the expression

$$F_1 = 2\tau_0 \int_{y_1}^{y_2} n\,dy.$$

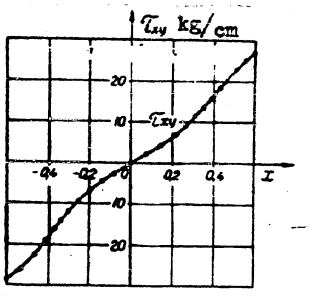

Figure 93. Shearing stresses at the section bb' (Figure 91).

Here the integration is carried out along the walls of the die opening from its outer end to the section under consideration. The value of the integral may be computed on the basis of experimental data by means of numerical integration. The normal force at the section bb' will be given by the following expression in view of the fact that σ_y is constant:

$$F_2 = 2c\sigma_y.$$

where c is half of the width of the die opening.

Since $F_1 + F_2 = 0$, it follows that

$$\sigma_y = \frac{F_1}{2c}.$$

The value σ_y computed in this fashion at the section bb' is equal to 20.6 kg/cm.

Further, it is possible to compute the stresses along the axis of symmetry (y axis). In order to do this, it is expedient to utilize a formula analogous to (118). Taking into account the fact that along the axis of symmetry $\theta = 0$, such a formula has the form

$$\sigma_y = \sigma_y(x_0, y_0) - 2\tau_0 \int_{y_0}^{y} n \frac{\partial \theta}{dx}\, dy.$$

We may take as an initial point (x_0, y_0) the point of intersection of the axis of symmetry with the straight line bb', at which point the state of stress is known from the preceding discussion. The value of σ_y at the axis of symmetry computed by means of numerical integration is shown in the graph of Figure 94.

The same figure also shows the value of σ_x, which in the given case, being the second principal stress, is computed by the formula

$$\sigma_x = \sigma_y - 2\tau_0 n.$$

STAT

Applying the methods described in Chapter IV and utilizing as initial points the points of the axis of symmetry, it is possible to calculate the stresses at various sections parallel to the x axis. The stresses in the plane of the pressure washer (section aa') are shown in Figure 95. In the middle portion of the container the state of stress is close to one defined

by the expression

$$\sigma_x = \sigma_y = f(y).$$

This can be easily demonstrated by substituting the experimental data into formula (118). Of particular interest is the distribution of pressures on the walls of the container (Figure 96).

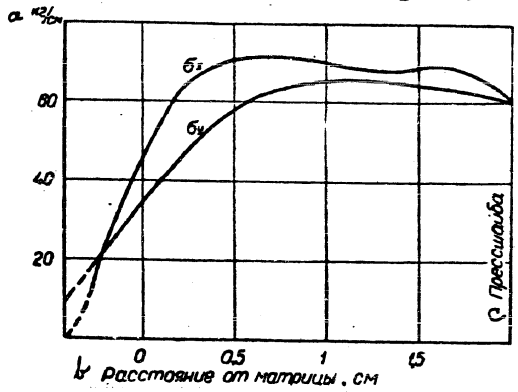

Legend: a) kg/cm
b) distance from die, in cm
c) pressure washer

Figure 94. Stresses along the axis of symmetry.

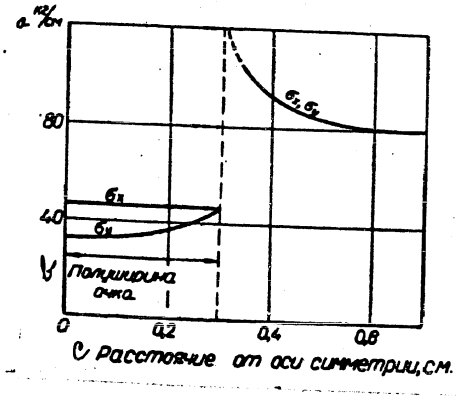

Legend: a) kg/cm
b) half-width of opening
c) Distance from axis of symmetry, in cm

Figure 95.

STAT

In Figure 97 there is shown the quantity σ_y at the boundary between the medium undergoing deformation and the pressure washer. The calculations were carried out by means of numerical integration from the axis of symmetry with formula (118). Since at these points $\theta = 45^\circ$, it follows that

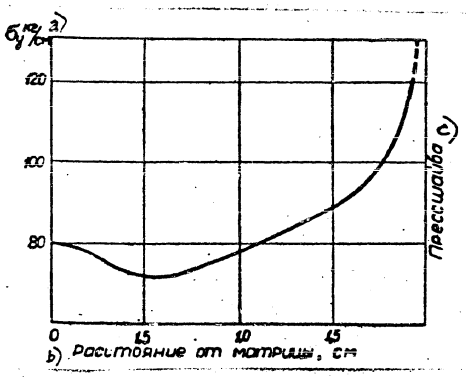

Legend: a) kg/cm
b) Distance from die, in cm
c) Pressure washer

Figure 96. Normal stresses acting on walls of container.

and $$\sigma_y = \sigma_x$$

$$\sigma_x = \sigma_{x(0)} - \tau_0 \int_0^x \frac{\partial n}{\partial y} dx.$$

This method of calculation cannot be used near the corners formed by the pressure washer and the container since the fringes at these regions cannot be obtained by theory.

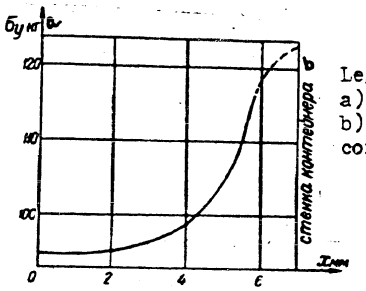

Legend:
a) kg
b) wall of container

Figure 97. Distribution of normal stresses acting upon the pressure washer.

However, as was already shown, the distribution of fringes in these regions is close to the one which follows from the solution of problem 2 dealing with the flow of a viscous medium in a corner. Thus, further calculations and analysis of the state of stress near the corners between the container and the pressure washer may be carried out by utilizing the solutions of this problem.

STAT

It must be noted that it follows from the solution considered that as we approach the vertex of the corner all components of the stresses increase in inverse proportion to the distance from the vertex, that is, they approach

infinity. Moreover, this law of distribution of stresses brings us to the observation that the summation of the forces acting between the model and the pressure washer also approaches infinity. In other words, it follows that the movement of the pressure washer with respect to the container cannot proceed with a finite velocity. This conclusion is refuted by experiments. In actual practice this solution describes the process correctly only within those limits where the coefficient of internal friction may be considered to be constant. As was shown in Chapter IV, the relationship between the shearing stresses and the rates of deformation was not a linear one. As the rate of shearing strain increased the coefficient of internal friction decreased. In addition to that, as the vertex of the corner is approached the temperature of the material increases due to the energy of deformation which increases as a result of the increase of the rate of deformation. (As we know, the energy of deformation per unit of time is proportional to the square of the rate of deformation for the case of viscous flow.) In its turn, the heating of the material lowers its viscosity and this leads to the reduction of the stresses compared with the values given by solution (74).

The presence of heating at the points of concentration of deformation reveals itself in another way. In all the photographs small zones near the corners where the concentration of deformation is particularly large, are dark. The magnitude of these zones, other things being constant, varies depending upon the diaphragm opening of the lens during the photographing. As the lens diaphragm is opened the dimensions of these zones decrease as though they contracted toward the vertex of the corner. This phenomenon can be explained in a logical manner if we take into account the fact that the STAT temperature of the medium in these zones increases toward the vertex of the angle. The medium becomes optically inhomogeneous. Its optical density decreases as we approach the corner. The incident rays of light passing through these zones are deflected in the direction of the gradient of the optical density

and in passing through may miss the objective lens. As the diaphragm opening of the objective is increased the rays having lesser deflection pass through it and the observed magnitude of the dark zone decreases. A typical path of the rays passing through the model at the points of concentration of deformation is shown in Figure 98.

As applied to the case under consideration, the distribution stresses near the corners of the pressure washer is satisfactorily described by formulae (74) with the radii varying within the limits of 0.6 to 3 mm. The absence of data on the state of stress in the immediate vicinity of the corners formed by the pressure washer and the container and on the resistance encountered by the pressure washer in its movement by virtue of the formation of an envelope deprives us of the possibility of comparing the computed force upon the pressure washer with the force applied by the loading mechanism of the machine.

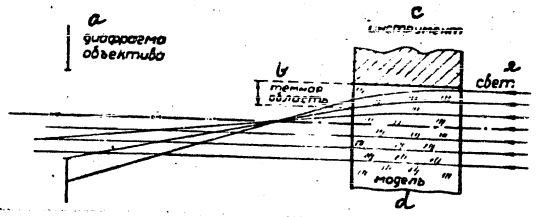

Legend: a) lens diaphragm
b) dark zone
c) instrument
d) model
e) light

Figure 98.

3. Indentation of a Punch.

An analysis of the distribution of stresses caused by indentation of a punch was carried out by means of models of rectangular form prepared from resin and chloric silver. The models were tested in a flat container (STAT Figure 31) and the load was applied in increments of 20, 60 and 100 kg.

As the rigid punch is pressed into the model prepared from an elastic material, we observe a system of fringes in the form of circles which pass through the boundary points of the punch. From the theory of elasticity it is known that the pressure at the surface of contact for the boundary points

must have theoretically infinite values. From examination of Figure 23, it is seen that considerable concentration of stresses is observed precisely at the boundary points. Even after application of a small load to an elastic body, plastic deformation near the corners of the punch must be initiated. This is confirmed by experiments carried out with specimens of mild steel subjected to a concentrated load /8/. In this case we observe a system of slip lines radiating from the corners of the punch. In more brittle bodies, destruction of the material also is initiated at these corners. This phenomenon is observed also for plastic material of the resin type.

First let us consider the fringe pattern observed when the punch is pressed into a model made from resin for various ratios of width to height of specimen, and also for various dimensions of the punch.

The character of the state of stress observed when a punch is pressed into a body depends both upon the dimensions of the models and the dimensions of the indenting instrument. This is revealed by the number and arrangement of the fringes caused by the deformation of the model.

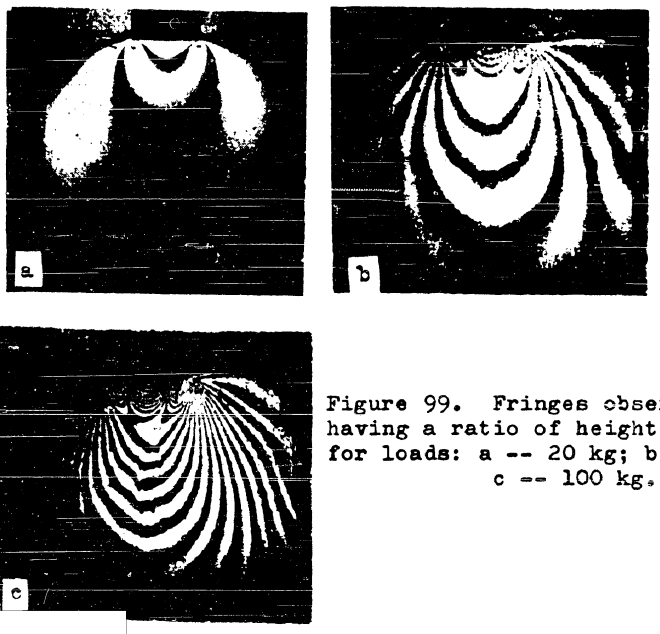

Figure 99. Fringes observed in a model having a ratio of height to width = 1 for loads: a -- 20 kg; b -- 60 kg; c -- 100 kg.

Figures 99, 100, 101 and 102 show fringe patterns observed during the indentation by a punch 10 mm wide into models having ratios of height to width of 1.0, 0.75, 0.5 and 0.25. The width of the model in all these cases was equal to 40 mm.

At the initial moment of application of load there occur at the boundary points of the die fringes having the form of closed curves of oval form. The major axis of these curves ("peacock spots") is directed at an angle of approximately 50-60° to the contact surface of the punch. As these fringes are displaced, those radiating from the corners of the punch merge in the center portion of the model and then diverge. One part of the fringes is shifted toward the punch in the form of arcs convex away from the punch, and a second part is shifted from the locus of merging fringes both to the left and right of the axis of symmetry. The left and right portions of the model, which are not loaded, are not stressed in the initial stage of the loading. These regions are separated in the following stages from the remaining portion of the model by a neutral fringe. After this even these portions of the model are subjected to deformation. The sign of the stresses acting in these regions is different from the sign of the stresses acting in the major part of

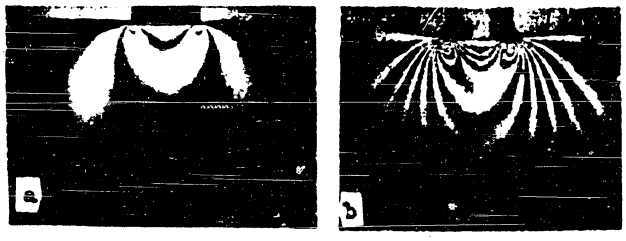

STAT

Figure 100. Fringes observed in a model for a ratio of height to width = 0.75 for a load: a -- 20 kg; b -- 60 kg; c -- 100 kg.

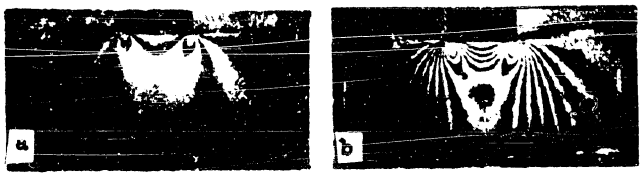

Figure 101. Fringes observed in the model for a ratio of height to width = 0.5 and a load: a -- 20 kg; b -- 60 kg.

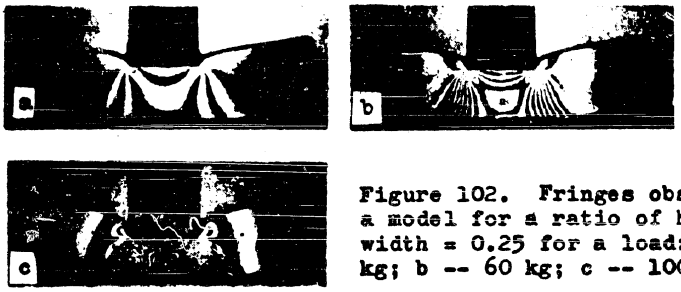

Figure 102. Fringes observed in a model for a ratio of height to width = 0.25 for a load: a -- 20 kg; b -- 60 kg; c -- 100 kg.

the model. An investigation by means of a compensator shows that tensile stresses exist along the free boundary of the model. Thus, there must exist an intermediate region with both tensile and compressive stresses between the free boundary and the central portion of the model where we have only compressive stresses.

As the model is loaded the regions in which tensile stresses are present grow lighter. This indicates that the tensile stresses increase. In Figure 102c the tensile stresses attained considerable magnitude. Fringes of the first order corresponding to these stresses, which only became apparent STAT Figure 102b, are shown to have spread over the entire height of the model in Figure 102c in the form of dark wide fringes embracing the region of nonuniform compression from both sides. From consideration of Figure 102 it is apparent that the number of fringes under the punch differs from the number of fringes in the other portions of the model. The larger the load on the model, the larger is this difference. The order (n) of the fringes under the punch is

always lower than in the remaining portion of the model, with the greater portion of the model having all the fringes from the first to the highest order; however, in the region below the punch we observe fringes ranging from some intermediate order, depending upon the load, to the highest order.

Fringes ranging from the first to the highest order are preserved only in that portion of the model which is bounded by neutral fringes. The material underneath the punch is in a state of triaxial nonuniform compression and the neutral fringe is absent in this region, since regions of tensile stress are absent in it. Therefore, in this region we do not observe any concentration of fringes. As the shearing stress increases here, the difference in the paths increases and we observe corresponding fringes of a certain order. As the difference in the paths increases, the fringe of the first order disappears first, then the second one, etc. As the loading is discontinued or as it is removed, fringes begin to disappear starting with the highest order down to the first order. The disappearance of the last fringe corresponds to complete unloading of the model (that is, to the complete removal of the state of stress). This phenomenon is repeated under repeated applications of load. Table 4 gives the values of the fringe orders at various portions of the indicated models for various loads.

Thus, if in Figure 100a the ratio of the fringes at various portions of the model is equal to 1:1, then in Figure 100b it is equal to 4:5, and in Figure 100c it is equal to 9:12. For a load of 60 kg we observe a difference of one fringe, and for a load of 100 kg the difference is already equal to three fringes. Still greater difference is observed in models whose height is considerably less than the width (40x10x5 model). From the given photographs and Table 4 it follows that the smaller the ratio of height of the model to its width, the smaller is the deformed region of the model. In view of this, the major portion of the model is not deformed (free of any stresses) and has a dark appearance. This can be clearly seen in Figure 102. Since

STAT

for one and the same load the deformed region of the model decreases, it follows that the concentration of stresses in the deformed part increases and this is revealed in a noticeable increase in the number of fringes. Experiment shows that the free portions of the model do not change the form of the deformed portion. The magnitude of the latter depends upon the ratio of the dimensions of the model and the instrument.

While in the initial stage of loading, when we observe only elastic deformations, the fringes are almost of circular form, in the second stage of loading the similarity of the fringes to circles is destroyed. In this stage and the following stages of loading the fringes become ovals elongated in the direction of the applied load.

Table 4

Dimensions of models in mm	Width of Punch in mm	Load in kg					
		20		60		100	
		a*	b**	a	b	a	b
40x40x5	10	1.0	1.0	4.0	5.0	9.0	12.0
40x30x5	10	1.0	1.0	4.0	5.0	9.0	12.0
40x20x5	10	1.0	1.0	4.0	6.0		
40x10x5	10	1.0	2.0	3.0	8.0		

* a -- number of fringes under the punch
** b -- number of fringes in the other portions of the model

In Figure 103 there is shown a fringe pattern for an indentation by a punch 5 mm wide into a model having dimensions of 40x40x5 mm. In the given case the entire discussion presented above for a punch 10 mm wide is completely applicable to this situation as well.

Figure 103. A fringe pattern observed for indentation of a punch 5 mm wide into a resin model.

Figure 104 shows a fringe pattern observed for an indentation of a punch 20 mm wide into a 40x20x5 mm model.

The colored isochromatic pattern of the stress distribution for indentation

of a punch is shown in Figure 105 (see insert between pages 178-179 in text). The presence of a colored isochromatic pattern enables us to determine easily the neutral fringe (fringe of the zero order) which always has a dark color, the order of any isochromatic line (each order is bounded by a green line), and the place of its origin.

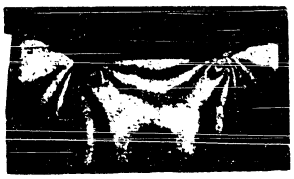

Figure 104. Fringes observed in a model for an indentation by a punch 20 mm wide.

If the model is unloaded and is loaded again after removal of the state of stress, the character of the origin, development and distribution of fringes will be the same as during the first loading of the previously untested model. This may be seen by comparing Figures 106 and 99c obtained from one and the same model. Figure 106 shows the fringe pattern after the model corresponding to the stage of Figure 99c was unloaded, and subsequently loaded again. The fringe patterns in these figures, corresponding to one and the same stage of loading (100 kg), are quite similar. The order of the fringes both in the region under the punch as well as in the remaining portions of the deformed models is one and the same, and the orders are respectively 9.5 and 12.5.

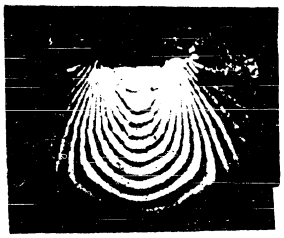

Figure 106. Fringe pattern obtained in the model of Figure 99c after it was unloaded and reloaded at 100 kg.

When we test models of resin we observe occasionally their failure under load. It is characteristic of these models that the cracks which originate at the points of stress concentration develop along lines of equal maximum shearing stresses.

As was shown by L. A. Rapaport [317], under the indentation (dynamic) of

a punch of rectangular form having dimensions of 6.5x4 mm into a specimen of steel of grade 45 in a form of a parallelepiped having dimensions 8x8x6.5, cracks develop in the specimen which coincide with the loci of the maximum localized deformations (Figure 107). The line along which failure occurred is similar in form to the lines obtained in pressing the punch into a plastic material. This may be seen by comparison with Figure 108, which gives a schematic diagram of the arrangement of fringes for a similar model. The line designated by number 5 corresponds to the maximum value of the shearing stress under a given load. Along this line there occurs in crystalline bodies of comparatively fine grain structure, localization of stresses and deformations and failure when stresses of a certain magnitude are attained.

The fringe patterns enable us to construct curves showing distribution of equal maximum shearing stresses. As can be seen from Figure 109, we obtain a sharp increase in the curve at the point of concentration of stresses (a curve with two maxima) at the section which is close to the contact plane of the punch, that is, for the boundary points. The further from the contact plane of the punch is the section under consideration, the less sharply does the character of the distribution change. This curve becomes smoother and finally becomes a curve having one maximum value which is now situated at the center portion of the model.

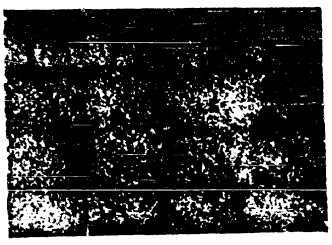

Figure 107. Formation of cracks at an indentation of a punch into a specimen of steel of grade 45 (from L. A. Rapaport).

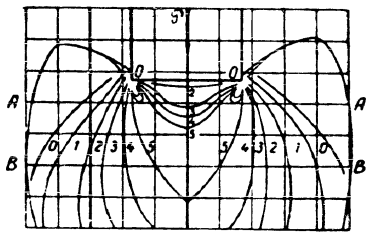

Figure 108. A schematic diagram of distribution of fringes for a punch indenting a model of resin with a ratio of height to width equal to 0.5

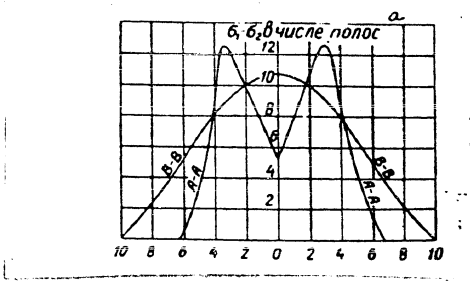

Legend: a) among fringes

Figure 109. Distributions of maximum shearing stresses at sections A-A and B-B for the model shown in Figure 108.

As was already shown, one can obtain by the method of photoplasticity a system of isoclinics which permits us to construct a system of trajectories of normal stresses (isostatics) and a system of trajectories of shearing stresses (characteristics) for models subjected to finite plastic deformations.

The indentation of the punch into a model of resin gives isoclinic lines shown in Figure 110 (see insert between pages 178-179 of text). The entire field of isoclinics obtained with the plane of polarization rotated from 0 to 90° is shown in Figure 111.

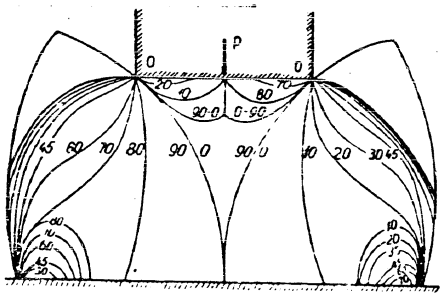

Figure 111.

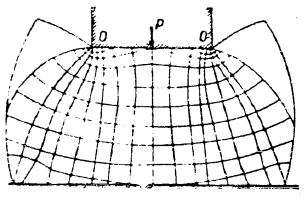

Figure 112. Arrangement of trajectories of principal normal stresses for a resin model indented with a punch.

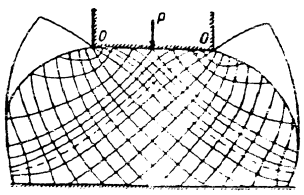

Figure 113. Arrangement of trajectories of shearing stresses (characteristics) for a resin model indented with a punch.

STAT

The grid of the trajectories of principal normal and shearing stresses for the given case is shown in Figures 112 and 113. In Figure 112 we observe an appreciable curvature in the trajectories of the principal normal stresses in the regions situated in the vicinity of the extreme points of the punch.

The effect of friction is also shown in the character of the disposition of trajectories of the shearing stresses.

In the preceding part of the chapter we considered the character of the distribution of stresses for a resin model indented by a punch. Now let us consider the character of the state of stress for a loading of the indicated type in models of a plastic material of crystalline structure -- a model of chloric silver.

In models of chloric silver having a coarse grain structure we observe a disordered motley isochromatic pattern for indentation by a punch (Figure 10b). Each grain is deformed in a different fashion depending upon its strength, location and magnitude, and therefore, the entire field of the model presents a disordered colored mosaic. In this case we do not observe a system of continuous fringes and isoclinics as in the case of an amorphous material.

Figure 114 shows a pattern obtained with a model with a finer grain structure. In this case we also do not observe discrete continuous fringes, but we do observe neutral fringes which bound the deformed region.

Figure 114.

If we reduce the dimensions of the grains, we can obtain sufficiently sharply defined continuous fringes having completely defined form and location. This may be confirmed by the photographs in Figure 115. In Figure 115a we observe in addition to neutral fringes two continuous fringes of regular form. Figures 115b, c, d show an increase in the number of fringes with an increase in load. In Figure 115d we can count up to 11 fringes. Under the die there occurs bulging of the

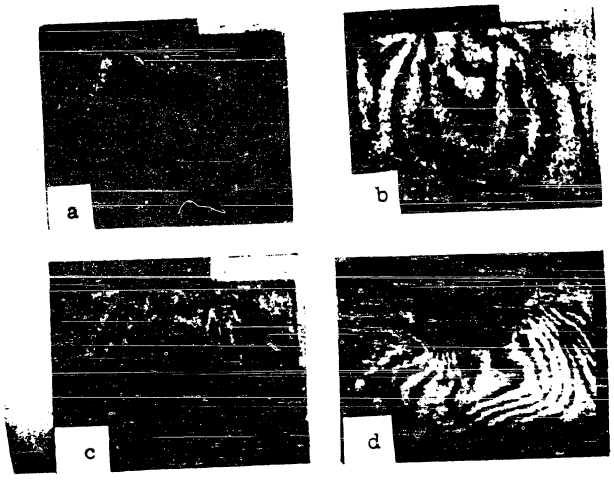

Figure 115. Fringes observed in deforming a model of polycrystalline chloric silver.

material in view of the plastic deformation taking place. As the load is removed not all the fringes disappear. The form of the remaining fringes is the same as under the load.

Still more convincing is the fringe pattern shown in Figure 116. Since the punch did not come in contact with the top surface of the model over its

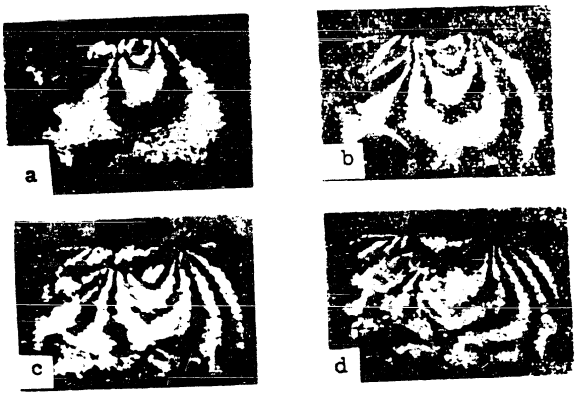

STAT

Figure 116. Fringes observed in deforming a model of polycrystalline chloric silver with a finer grain structure.

entire surface, the fringes shifted somewhat to the right. In Figure 116a there are clearly visible two continuous fringes and a third one located in the general background of the portion of the model being deformed. In Figure 116b, three fringes are already observed and a fourth one is being initiated. In Figure 116c there are already four fringes. In Figure 116d the fringe pattern directly beneath the punch is distorted due to bulging of the material.

When the model was unloaded a part of the fringes disappeared due to removal of the elastic component of the deformation (Figure 117), but two continuous fringes which determine the character of distribution of the residual stresses of the first kind remained on the right hand side after the plastic deformation had taken place. These fringes had the same form and location as were observed in the loaded model.

Figure 118 shows the fringe pattern obtained for a model of considerable dimensions with a ratio of height to width equal to 0.5, and for a punch 10 mm wide. In this case we succeeded in obtaining a system of continuous fringes covering the entire field of the deformed part of the model. In all cases the fringes had an oval form (ellipses) elongated in the direction of applied load.

In the cases considered we observed a pattern of continuous fringes even for a grain size of the order of 0.06-0.03 mm. For still finer grain structure, the pattern must be even more regular.

Figure 117. Residual stresses remaining in deformed model of polycrystalline chloric silver after unloading.

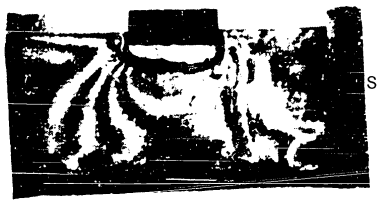

STAT

Figure 118. Fringe pattern obtained for a model of polycrystalline chloric silver with a ratio of height to width equal to 0.5.

Figure 105. An isochromatic pattern observed in a resin model indented by a punch.

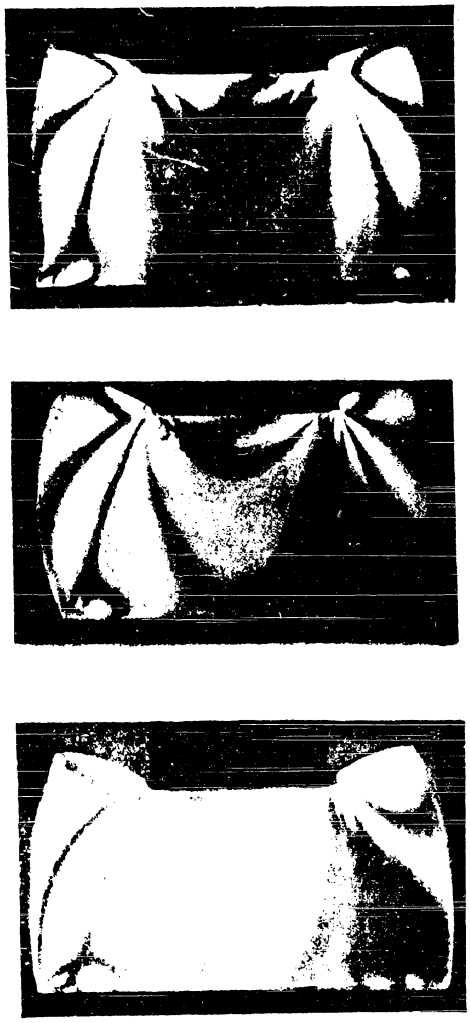

STAT

Figure 110. Isoclinics observed in a resin model indented by a punch: a -- 0° isoclinic; b -- 10°; c -- 20°; d -- 30°; e -- 45°.

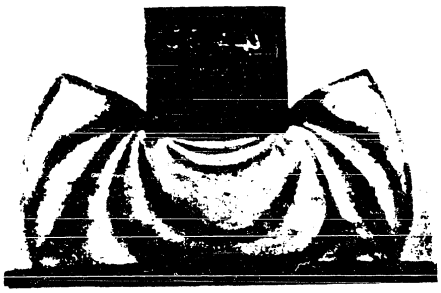

Figure 119. Isochromatic lines observed in a gelatin-glycerine model indented by a punch.

a

b

Figure 120. Isoclinics observed in a gelatin-glycerine model indented by a punch: a -- 0° isoclinic; b -- 60°.

STAT

The observed pattern of continuous fringes of regular form may be interpreted in the following manner.

When a model consisting of uniform grains of constant length of axis is deformed, a sufficiently large number of the grains located in the path of the polarized light must produce a certain averaged optical effect consisting of the optical effects introduced by the individual grains. In spite of the fact that each grain is deformed in an individual fashion, depending upon its individual properties and arrangement (orientation), at each point of the model there will be observed a certain mean optical effect which is independent of the orientation of the individual grains and their properties. The optical effects introduced by individual grains will be summarized by the passing ray and averaged, while their individual properties will be minimized. The optical effect will then depend upon a certain mean value of all the grains in the field of state of stress. In an optical and mechanical sense the model will behave as a solid and homogeneous body. Naturally, this state will be achieved only when a sufficiently large number of grains is present in the path of the ray of light.

As can be seen from the examples considered, a material of crystalline structure consisting of fine grains may yield a macroscopic pattern of stress distribution which coincides sufficiently close with the pattern obtained with models of plastic noncrystalline material.

The authors subjected models of gelatin-glycerine material to indentation by a punch which produced considerable plastic deformations. The arrangement of the fringes and isoclinics for this case is shown in Figures STAT and 120.

However, it is premature to draw any conclusions regarding the state of stress in the given case since the relationships between the observed optical effects for considerable plastic deformations in gelatin-crystalline material are not yet adequately known.

CHAPTER VI

PRACTICAL SIGNIFICANCE AND PROSPECTS OF THE METHOD OF PHOTOPLASTICITY

1. Practical Significance of the Method of Photoplasticity.

The method of photoplasticity even at the present time may be called upon to solve the number of practical problems.

The most important of these problems are:

1. Modelling of geological and geophysical phenomena involving plastic deformations.

In this case, as a rule, the problem of modelling deals with a system of strata which are inhomogeneous in mechanical properties and rheological behavior. We may construct suitable models by combining optically sensitive resins of various viscosities which assure similarity to the strata for selected dimensions of the model.

Similar models may be utilized in certain cases for the study of phenomena observed in mining operations. At the present time the study of problems dealing with pressures encountered in geological formations is carried out by the method of photoelasticity. It is quite expedient also to call upon the method of photoplasticity in solving such problems. STAT

2. Modelling of the technological processes of deforming of plastics.

The application of parts of considerable dimensions made of plastics has recently become quite widespread. Plastics are used for fabrication of boats, parts of small airplanes, and other parts being used in the most varied branches of technology.

However, the technology of production of these plastic parts is still limited by a number of substantial shortcomings. These shortcomings must be eliminated both by perfecting the existing technological processes and also by assuring further progress of this extremely important branch of technology. This technology sometimes utilizes transparent optically sensitive plastics, or plastics whose rheological behavior may be simulated by homogeneous amorphous media which show double refractivity.

Therefore, the data which we obtained in the study of processes of deformation of the homogeneous plastic under conditions of viscous flow may be utilized by the industry for perfecting the existing processes and development of new technological processes for manufacture of parts made of plastic materials.

3. Modelling of technological processes involving deformation of metals (primarily those involving pressure and cutting).

While the plastic deformation of plastics takes place primarily under conditions of viscous flow, the plastic deformation of metals occurs primarily under conditions of plastic flow and in certain cases under conditions of viscous-plastic flow. In addition to that, in dealing with plastic deformation of plastics we have as a rule a homogeneous medium. However, in producing deformation in crystalline bodies the medium is inhomogeneous and at best may be regarded as a conditionally homogeneous medium only for a sufficiently fine grain structure and a random crystallographic orientation.

All this affects the distribution of stresses in viscous and plastic bodies. Therefore, for one and the same method of external loading the STAT distribution of stresses in a viscous body may be substantially different from distribution of stresses in a plastic body. However, in many cases we need not be concerned with the properties of the medium. We can do this in cases when we are interested not in the details of the distribution of stresses in the deformed body and the quantitative aspect of the problem, but in a

qualitative picture of general character. In order to obtain such a picture, it is possible to utilize amorphous homogeneous media instead of crystalline bodies, as was shown by our experiments. Moreover, the clearest qualitative picture giving a general view of distribution of stresses in a deformed body is one yielded by models of amorphous materials which are deformed under conditions of viscous flow. Therefore, in solving by means of models such problems in which the basic task is to obtain a most clearly visible qualitative macro-pattern of distribution of stresses, we must utilize models made of optically sensitive homogeneous amorphous materials undergoing deformation under conditions of viscous flow. As an example we shall cite the following problem.

During a stamping process we observe at times separation of the metal into layers at the points of maximum concentration of deformations. This phenomenon is called "stratification." The stratification splits the forging into two parts and constitutes a defect which cannot be corrected. In order to identify the causes of this phenomenon the authors studied the process of stamping by means of models of optically sensitive resin. The distribution of stresses and deformations in this case are described in a preceding chapter (see Figures 65, 67, 69).

Comparing the photographs showing forgings of the same form, we may draw the conclusion that the concentration of deformations increases with the amount of metal passing into the flash. When the amount of the excess material of the billet reaches a certain value, there occur in the vicinity of the flash vent deformations of intensity which are sufficient to cause failure of the metal. In the vicinity of the imminent failure there occurs a concentration of stresses and deformations and this causes the splitting of the billet.

STAT

In Figure 121 there are shown photographs of macroscopic polished sections of forgings which had a considerable amount of metal in the flash vent. The

macro-polished sections show clearly a dark line which was obtained in the loci of maximum concentration of deformations and which indicates the place of stratification.

Figure 121 Formation of stratification of metal within billet during stamping process: a -- by means of hammer; b -- by means of pressure.

The investigation carried out permits us to draw the following conclusions.

The basic cause of stratification is the presence of excessive volume in the metal billet. The stratification may be eliminated by selecting the proper billet volume.

The distribution of deformations obtained by the method of a coordinate grid engraved on metal models corresponds completely to the distribution of stresses obtained with resin deformed under conditions of viscous flow.

We can solve the following problems related to the processes of forming of metals by using models of resin under pressure:

1. Find the most suitable geometry of the instrument producing deformation.

Figure 122 shows fringes obtained during extrusion of specimens of resin through a die opening with different angles of inclination. The fringe patterns were photographed for a constant value of external load.

Figure 123 shows trajectories of maximum normal stresses obtained by

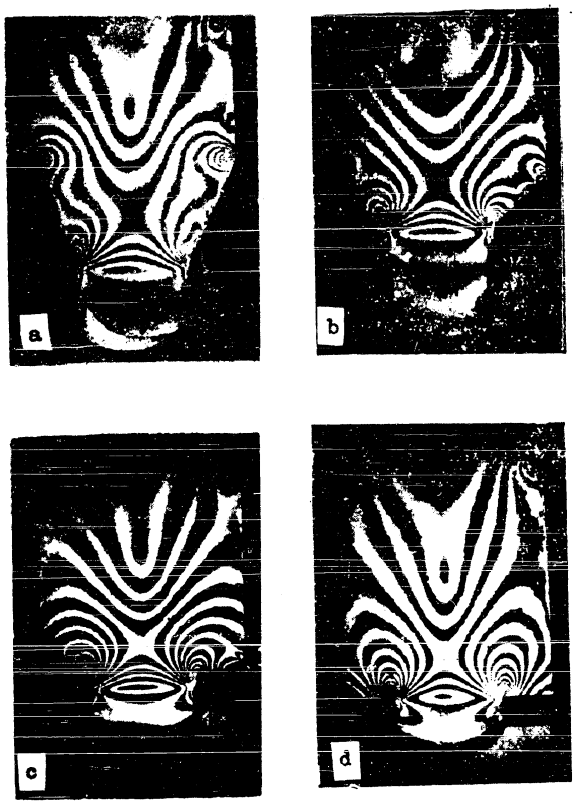

Figure 122. Fringes observed for a flow of resin with an angle of inclination of the die opening of: a -- 25°; b -- 45°; c -- 65°; d -- 90°.

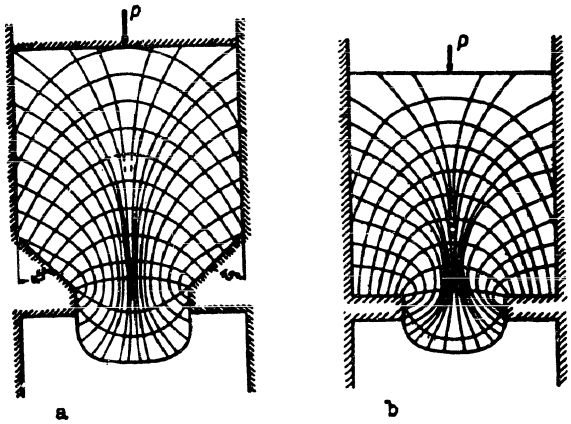

Figure 123. Trajectories of principal normal stresses for an angle of inclination of die opening of: a -- 45°; b -- 90°.

reducing the data in the corresponding photographs of isoclinics.

The examination of this material permits us to conclude that the angle of inclination of the die opening affects materially the distribution of stresses in the material being deformed. (Since quantitative data were not required, these experiments were carried out with thin models.)

2. Determine the zones in which the deformation process is difficult and define the regions of hydrostatic pressure.

3. Determine the places of localized plastic deformation.

4. Determine the places of stress concentration.

5. Formulate a concept of the form and internal boundaries of the regions of origin of the plastic deformation.

6. Obtain a general qualitative picture of the distribution of stresses.

2. Prospects for the Method of Photoplasticity.

The method of photoplasticity may be utilized for the study of the nature of plastic deformation of a substance and the study of the stress distribution under conditions of plastic and visco-plastic flow.

Utilization of the method of photoplasticity for the study of the nature of plastic deformations may aid us in gaining a broader concept of this problem.

We know that it is possible to obtain a well defined pattern of the distribution of stresses in a homogeneous amorphous medium whose elementary particles have a molecular weight of a magnitude measured in hundreds of units, and this will enable us not only to study the mechanism of flow in an amorphous body but to describe it in mathematical terms. This circumstance has a great significance, since studies in recent years have indicated that the amorphous mechanism is applicable to all solid bodies regardless of their nature and constitutes one of the basic mechanisms of plasticity.

Even with substances of mycelian structure we observe a fairly well defined pattern of stress distribution (Figure 19). Among such substances

are, for example, gelatin-glycerine materials. For large rates of loading these substances behave as quite elastic bodies which develop large elastic deformations measured in tens of percent. When large deformations are developed under comparatively high rates of loading, gel fails without showing any noticeable plastic deformations. However, such a failure cannot be called a brittle failure since it proceeds quite "sluggishly" (this is a distinguishable type of failure). The large elastic compliance of these bodies can be explained by the elastic flexibility of its mycelia. In the case of slow loading there is, apparently, sufficient time for an irreversible mutual displacement of the mycelia. This displacement in the present case is precisely the basic mechanism of plastic deformation. Moreover, there is a possibility that for slowly applied forces some permanent changes take place in the form of the mycelia themselves. This supposition appears to be credible but it still requires verification.

The study of deformation of transparent crystals at various temperatures will enable us to understand more fully the characteristics of the amorphous mechanism and to establish its specific features both for crystalline materials and amorphous homogeneous media. As expected, the study of deformations of crystals will enable us to understand more fully the mechanism of slip and other mechanisms characteristic of crystalline bodies. The prospects are particularly favorable for the study of the behavior of the material between grains and the phenomena occurring at the grain boundaries.

The study of the nature of plastic deformations by means of the photoplastic method has in fact been initiated. This fact is convincingly confirmed by the work of S. C. Tzobkallo and B. A. Kuznetzov [19] which was concerned with the study of the nature of plastic deformation of a polycrystalline material by an optical method. The material under study was a polycrystalline chloric silver. The work demonstrated that in the grains the residual stresses of the second kind are nonuniformly distributed and that stresses are localized

near the grain boundaries. Figure 124 shows characteristics curves of the distribution of stresses of the second kind.

However, the distribution of residual stresses has such a character only under a static load. In the case of cyclic loading, the concentration of residual stresses of the second kind near the grain boundaries is reduced. After a large number of loading cycles, the traces of slip indicate large local distortions. The authors have also shown that the distribution of stresses is quite nonuniform in individual grains of the polycrystalline material. Figure 125 shows the distribution of stresses in a grain 1.2 mm long.

V. M. Krasnov and A. V. Stepanov carried out an interesting study by an optical method [22] of the initiation of failure under the action of a concentrated force applied to the surface of a crystal of fluoric casting. Inasmuch as this work was concerned with residual stresses, and also with the origin of cracks, slip and twinning, it must be classified as an investigation in the field of photoplasticity both with respect to its method of attack and formulation of the problem.

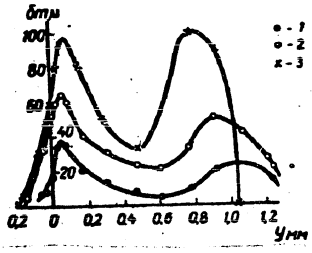

Figure 124. Distribution of residual stresses in the grains of chloric silver along individual sections.

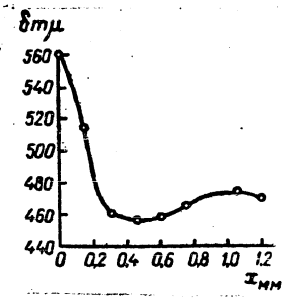

Figure 125. Distribution of stresses in a grain under the action of an external load.

STAT

The facts cited here indicate that the method of optical investigation of stresses in polarized light is already being utilized in the study of the nature of plastic deformation. The possibilities of exploiting the method of photoplasticity will become quite favorable after we solve the problem of distribution of stresses under conditions of plastic flow.

For the case of viscous flow we have the solution of the simplest problem. Its simplicity is due to the fact that the properties of the body do not change during the process of plastic deformation. In the case of plastic flow, however, we encounter a considerably more complex problem. Its complexity is due to the fact that the properties of the body change during the process of plastic deformation. In the case of viscous flow we are dealing with a homogeneous medium, while in the case of plastic flow the medium is either heterogeneous and anisotropic, or quasi-homogeneous (quasi-isotropic).

V. M. Krasnov and A. V. Stepanov made a study of the state of stress in a transparent monocrystal of an alloy of 60 mol.% of bromic and 40 mol.% of iodic thallium under a concentrated load [21]. Crystals of this alloy belong to the cubic system, are optically isotropic, have a relatively high yield point (2 kg/mm^2), and have high photoelastic constants. The pattern of isochromatics obtained for this material under load differs substantially from that usually observed under a load of this type (Figure 126). The isochromatics for the anisotropic medium do not coincide with the curves of maximum shearing stresses as is the case for isotropic bodies, and the anisotropy of the mechanical properties has a character different from that of the anisotropy of the photoelastic properties.

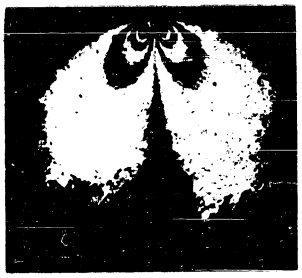

Figure 126. A photograph of a specimen under a concentrated load illuminated by circularly polarized light. The dark lines in the photograph are the isochromatics.

STAT

V. M. Krasnov and A. V. Stepanov showed that in order to determine the state of stress in an anisotropic medium one must have in addition to the isochromatic pattern, the orientation of the axes of the optical ellipsoid in the region under investigation. These investigators developed a corresponding theory which enables us to obtain on the basis of experimental data a complete picture of the state of stress in an

anisotropic medium, and in particular enables us to obtain the curve of maximum shearing stress (see Figure 127).

The problem now arises how to propagate the theoretical concepts of V. M. Krasnov and A. V. Stepanov as they apply to polycrystalline material and how to find reliable methods for quantitative determination of stresses in a quasi-isotropic polycrystalline material on the basis of the macropattern of isochromatics obtained during the plastic deformation of such a polycrystalline material. The solution of this problem along with the problem of determination of the fringe value under the conditions of plastic flow will be the basis for the study of stresses for plastic deformation in bodies which change their properties during the process of deformation (plastic bodies).

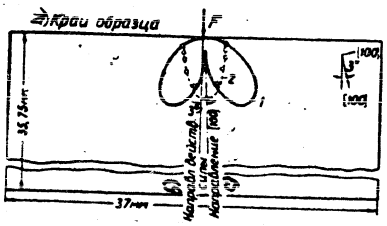

Legend: a) edge of specimen
b) direction of action of force
c) direction [100]

Figure 127. Curve 1 -- isochromatic based on experimental data; 2 -- theoretical curve of equal shearing stresses. The points on curve 2 are experimental data.

Solution of the problem of stress distribution under conditions of plastic flow will enable us to examine a number of most important problems of the theory of fabrication of metal parts by pressure, which problems are concerned with a quantitative determination of stresses for those deformation processes which take place at temperatures corresponding to regain STAT of strength, and even to the state of incomplete loss of strength. The quantitative determination of stresses for the deformation processes in metallic alloys taking place in the presence of incomplete or complete loss of strength is already concerned with the solution of the problem of photoplasticity under conditions of viscous-plastic flow.

The solution of the viscous-plastic problem presents a maximum of difficulties both with respect to experiment and theory. In this case, just as in the case of the viscous problem, the resistance to deformation is affected by the rate of deformation and the level of the mean stress, and at the same time during the deformation process the structure, and sometimes even the properties of the body undergoing deformation, may vary. The plastic problem is simpler, since in this problem neither the rate of deformation nor the mean stress level have any effect on the resistance to deformation. The solution of viscous-plastic problem heads the list of basic problems which must be considered for the complete development of the method of photoplasticity.

STAT

BIBLIOGRAPHY

1. Chernov, D. K. Obobshcheniye po povodu nekotorykh novykh nablyudeniy pri obrabotke stali [Generalizations with respect to some new observations in the working of steel], 1884.

2. Trudy konferentsii po opticheskomu metodu izucheniya napryazheniy [Proceedings of the conference on the optical method of study of stresses], NIIMM LGU, 1937.

3. Stepanov, A. V., "Zhurnal Tekhnicheskoi Fiziki," [Journal of Technical Physics] XX, 1950.

4. Stepanov, A. V., Physikalische Zeitschrift der Sowjetunion [Journal of Physics of the Soviet Union] 8, 25, 1935.

5. Zaytsev, A. K. Opticheskiy metod izucheniya napryazheniy, [Optical method of study of stresses], Promburo, 1927.

6. Gubkin, S. I., Teoriya obrabotki metallov davleniyem [Theory of metal working by means of pressure] , Metallurgizdat, M., 1947.

7. Kobeko, P. P., Amorfnye veshchestva [Amorphous substances], Publisher, AN, SSSR M. - L., 1952.

8. Nadai, A., Plastichnost' i razrusheniye tverdykh tel. Izd. inostrannoy literatury. [Plasticity and failure in solid bodies. Publishers of Foreign Literature] M., 1954.

9. Gogoberidze, D. B. and Kirvalidze, I. D., "Zhurnal Tekhnicheskoi Fiziki," [Journal of Technical Physics], 1951.

10. Gubkin, S. I. and Dobrovolsky, S. I., "DAN SSSR" [Reports of the USSR Academy of Sciences], XXIII, 1, 1950.

11. Gubkin, S. I. and Dobrovolsky, S. I., Ibid., XXXVIII, 5, 1953.

12. Frocht, M., Fotouprogost'. V. I. Gosudarsvennoye izdatel"stvo tekhniko-teoretichnoy literatury [Photoelasticity, V. I., State Publishers of Technical-Theoretical Literature] M., 1948.

13. Feldman, G. I., "Zavodskaya Laboratoria," [The Plant Laboratory], XVII, 2, 1952

14. Prigorovsky, N. I., Preise, A. K., and Slutzker, O. D., "Zavodskyaya Laboratoria," [The Plant Laboratory], XV, 3, 1949.

15. Entsiklopedicheskiy spravochnik "Mashinostroyeniye" [Encyclopedia "Machine Construction" V. I and III, Mashgiz, 1947.

16. Ibid. , V. IV, Mashgiz, 1947.

17. Stepanov, A. V., "Zhurnal Tekhnicheskoi Fiziki", [Journal of Technical Physics], XIX, 2, 1948.

18. Zhitnikov, R. A., Dissertatsiya "Razrabotka opticheskogo metoda issledovaniya usrednennykh napryazhennykh sostoyaniy v melkozernistykh polikristallakh" [Dissertation, "Development of an optical method of investigation of mean stress levels in fine grained polycrystals,"] 1953.

19. Tzobkallo, S. O. and Kuzetzov, B. A., "Zhurnal Tekhnicheskoi Fiziki" [Journal of Technical Physics], XXIII, 1, 1953.

20. Tzobkallo, S. O., "Zhurnal Tekhnicheskoi Fiziki," [Journal of Technical Physics] XIX, 4, 1949.

21. Krasnov, V. M. and Stepanov, A. V., "Zhurnal Eksperimental'noy i Teoreteicheskoi Fiziki," [Journal of Experimental and Theoretical Physics], 25, 1(7), 1953.

22. Krasnov, V. M. and Stepanov, A. V., "Zhurnal Eksperimental'noy i Teoreticheskoi Fiziki," [Journal of Experimental and Theoretical Physics], 23, 2(8), 1952.

23. Sidorenko, Yu. A. "Zavodskaya Laboratoria," [The Plant Laboratory], 6, 1954.

24. Eiring, G., Glasstone, S., and Leidler, K., Teoriya absolyutnykh skorostey reaktsiy [Theory of absolute rates of reactions], M., 1948.

25. Kirpichev, M. V., and Gukhman, A. I., Trudy LOTI, [Proceedings of the LOTI], No. 1, 1931.

26. Volkenstein, M. V., Molekulyarnaya optika. Gosudarstvennoye izdatel'stvo tekhniko-teoreticheskoy literatury [Molecular optics. State publishers of technical theoretical literature,] M., 1951.

27. Landau, L. and Lifshits, E., Mekhanika sploshnykh sred. Gosudarstvennoye izdatel'stvo tekhniko-teoreticheskoy literatury. [Mechanics of solid media. State Publishers of technical-theoretical literature,] M., 1944.

28. Kantorovich, L. V. and Krilov, V. I., Priblizhennye metody vysshego analiza. Gosudarstvennoye izdatel'stvo tekhnikoteoreticheskoy literatury [Approximate methods of advanced analysis. State Publishers of technical- theoretical literature,] M., 1952.

29. Otchet laboratorii obrabotki metallov davleniyem [Report of the laboratory on fabrication of metals by means of pressure,] FTI AN BSSR, 1953.

30. Tarnovskiy, I. A. and Ganago, O. A. Sbornik "Raschet i konstruirovaniye zavodskogo oborudovaniya," ["Design and Construction of Plant Equipment," a Symposium], 48, 1953.

31. Rapaport, L. A., Mikroskopicheskoye issledovaniye sdvigovoy deformatsii polikristallov pri udarnom deformirovanii [Microscopic study of the shearing strain of polycrystalline bodies under impact], 1952.

32. Kochin, N. E., Vektornoye ischisleniye i nachala tenzornogo ischisleniya. [Vector analysis and elements of tensor analysis,] Publishing House of the USSR Academy of Sciences, M., 1951.

STAT

TABLE OF CONTENTS

STAT

STAT